NOVEL THERAPEUTIC STRATEGIES FOR PREVENTION OF POSTRESECTIONAL LIVER FAILURE

TAREK EZZAT ABDEL-AZIZ (MBChB, MS, MRCS)

Hepatopancreaticobiliary Unit

(HPB & Liver Transplantation surgery)

Division of Surgery and Interventional Science

The Royal Free and University College London Medical School

University College London

Presented for the award of the degree of

MD (Doctor of Medicine)

Statement of originality

I, Tarek Ezzat Abdel-Aziz confirm that the work presented in this thesis is my own. Where information has been derived from other sources, I confirm that this has been indicated in the thesis. This work has been carried out at the Institute of Hepatology and the Wolfson laboratory, University College London, London, UK and has not been presented in any other form to any other university. The work presented was carried out under the supervision of Professor. Massimo Malago, Mr. Steven Olde Damink (Division of Hepatopancreaticobiliary Surgery, Royal Free Hospital, University College London) and Dr. Dipok Dhar (UCL Hepatology, University College London Medical School, Royal Free Hospital, University College London, UK

Dedication

…To my wife Sally, for her love, warmth and patience over the last three years,

to my children Maryam and Hussein who brought joy into our lives

Abstract

Background: Sinusoidal obstruction syndrome (SOS) occurs in 50-70% of patients receiving oxaliplatin for hepatic metastasis. Patients suffering from SOS preoperatively are at increased risk of developing postresectional liver failure. To date, there is no ideal therapy to prevent SOS. Moreover, SOS delays liver regeneration following liver resections instigating the possible role of cell therapy. It is essential however to understand the dynamics of the transplanted cells. First, we studied the effect of a flavonoid (monoHER) on prevention of SOS. Second, we studied the role of a dual labeling technique for non-invasive tracking of stem cells *in-vivo*. **Methods:** A monocrotaline (MCT) induced SOS model was used in rats, with/without monoHER pretreatment. We studied hepatocellular damage and matrix metalloproteinase (MMP) expression. The potential inhibition of oxaliplatin-induced cytotoxicity by monoHER was tested *in-vitro*. In the second experiment, liver damage was induced in mice by acetaminophen. Green fluorescence protein (GFP) positive mouse embryonic stem cells (ESCs) were stained with a near infrared dye before transplantation. The distribution of the cells was monitored real-time. Immunohistochemistry was used to identify expression of GFP and albumin. **Results**: MonoHER ameliorated the increase in portal pressure after MCT and prevented hepatocellular damage. The liver damage score was lower in the monoHER group and was associated with less inflammation. Livers of MCT-treated rats had higher expression of MMP-9 when compared to monoHER group. MonoHER had no effect on *in-vitro* proliferation of colorectal cancer cells. In the second experiment, labeled ESCs were easily tracked by non-invasive technique. Within 24-hr of transplantation, homing of almost 90% cells was confirmed in the liver. Constitutively expressed GFP was used to study the cell distribution.

Conclusions: MonoHER prevented MCT induced portal hypertension and hepatic injury in rats. Dual labeling is an effective method for longitudinal monitoring of distribution, survival and engraftment of transplanted cells.

Acknowledgements

It would not have been possible to take this study from the conceptual stages, at which I joined it three years ago, to the position that has been reached today, without the help and support of a great number of individuals. I cannot hope to provide an exhaustive record of the acknowledgments that are due, and take this opportunity to extend my thanks to anybody that I have omitted to mention directly.

I would of course, firstly thank my three supervisors, Professor Massimo Malago, Mr. Steven Olde Damink and Dr Dipok Dhar for their help and guidance throughout the various stages of the project. It has been both a privilege and an inspiration to have been so closely supported.

Without financial support from citadel capital scholarship foundation, and Dr Leslie Borthwick/ Ms.Anita Holme,Hertfordshire UK, this work would not have been completed. This is in addition to the clinical fellowship received by Mr. Steven WM Olde Damink from the Netherlands organization for health research and development (grant 907-06-177) and a Fast Track CRDC grant from University College London.

I would like to express my deepest thanks to Professor Eddie Wisse, Maastricht University for his kind help and sincere guidance in conducting the electron microscopic study and to Prof D. Hochhauser, University College London for supplying the colorectal cancer cell lines.

I would like to thank those working in the Biological Service Unit at both University College London and the Royal Free campus for their support, involvement and their continuous efforts to facilitate performing the required experiments.

Lastly, to my family I am truly indebted. My absence has been accepted with grace on numerous occasions and I have unfailingly been lifted by their smiling faces and laughter on my return home. To my father and mother who have been supportive throughout my career and have always provided me with the most sincere advice. To my darling wife, Sally, and to our children, Maryam and Hussein, I would like to express my eternal gratitude and love.

Table of contents

Contents

Title....1
Statement of originality....2
Dedication....3
Abstract....4
Acknowledgements....6
Table of contents....8
Table of figures....12
List of abbreviations....19
1.Introduction....23
1.1 Background....24
1.2 Postresectional liver failure....25
1.2.1 Chemotherapy induced liver damage....26
1.2.2 Structural and Functional aspects of the Hepatic Sinusoid....28
1.2.3 Pathogenesis of sinusoidal injury during oxaliplatin-based regimen....31
1.2.4 Role of SOS in development of PLF....35
1.2.5 Assessment and Detection of PLF....36
1.2.6 Prevention....39
1.2.7 Treatment....42
1.3 Cell therapy for treatment of PLF....42
1.3.1 Liver regeneration following partial hepatectomy....44
1.3.2 Neoadjuvant chemotherapy and liver regeneration....47
1.3.3 Hepatocyte Transplantation....49
1.3.4 What are stem cells?....51
1.3.5 Clinical applications of stem cells in regenerative medicine....55
1.4 Stem cells and liver disease....56
1.4.1 Embryonic stem cells....56
1.4.2 Bone Marrow Stem Cells (BMSCs)....59
1.5 Cell tracking....62
2.Aims and experimental study design....65
2.1 Section 1....66
2.1.1 Experiment 1....66

2.1.2 Experiment 2.....67
2.2 Section 2.....69
3.Materials and methods.....71
3.1 Animals.....72
3.2 Methods.....72
3.2.1 Measurement of portal pressure.....72
3.2.2 Cell culture.....73
3.2.3 Tracking of the transplanted cells using the *in-vivo* Imaging System (IVIS).....76
3.2.4 Cell proliferation assay.....80
3.2.5 Blood and tissue sampling/handling and storage.....81
3.2.6 Analysis of Protein expression.....82
3.2.7 Electron microscopy (EM).....87
4.Development of a model of sinusoidal obstruction syndrome in rats.....91
4.1 Background.....92
4.2 Results.....94
4.2.1 Portal pressure measurements.....94
4.2.2 Biochemical evidence of monocrotaline induced liver injury.....95
4.2.3 Histological evidence of monocrotaline induced liver damage.....98
4.2.4 Electron microscopic examination of Monocrotaline induced liver damage.....103
4.2.5 Role of Matrix Metalloproteinases in development MCT induced SOS.....107
4.3 Discussion.....110
5.Semi-synthetic flavonoid monoHER prevents development of sinusoidal obstruction syndrome in rats.....116
5.1 Background.....117
5.2 Results.....119
5.2.1 MonoHER reduces the portal pressure in SOS.....119
5.2.2 Liver damage is attenuated by monoHER.....120
5.2.3 MonoHER reduces MMP-9 expression in the liver.....121
5.2.4 Protective effect of monoHER on HUVEC cell line.....130
5.2.5 MonoHER does not interfere with oxaliplatin cytotoxicity.....133
5.3 Discussion.....135
6.Cell therapy and dynamic tracking in an experimental acute liver failure model.....141
6.1 Background.....142

6.2 Results 143
6.2.1 Dual labeling of mouse embryonic stem cells using the near infra red dye DiR 143
6.2.2 MCT-SOS model could not be established in mice 143
6.2.3 Transplantation and *in-vivo* imaging 145
6.2.4 Ex-vivo imaging 146
6.2.5 Engraftment of the transplanted cells in the liver 149
6.2.6 Liver functions 149
6.3 Discussion 154
7.Discussion and future directions 159
Presentations arising from the studies contained in this thesis 168
Publications arising from the studies contained in this thesis 169
References 170
Appendix-1 192
Appendix-2 196
Appendix-3 203

Table of figures

Figure 1 Adopted with permission from Prof. Eddie Wisse (34). A schematic representation of the liver sinusoid showing the alignment of the SECs containing the fenestrae allowing the exchange of solutes with the hepatocytes----------30

Figure 2 Adopted with permission of Prof. Eddie Wisse. TEM x 6000 of normal hepatic sinusoid showing the fenestrae with size between 150-175 nm----------30

Figure 3 Unpublished own group SEM images of liver SECs following oxaliplatin. Disruption of the SEC lining with gaps in the space of Disse can be detected (Top x5000). Exposure of the hepatocyte microvilli could be seen at higher magnification (Bottom x 10000)----------33

Figure 4 Unpublished own group TEM images of liver sinusoids. Normal liver showing intact sinusoids (Top). Following Oxaliplatin chemotherapy there is disruption in the space of Disse with extravasation of the erythrocytes from the sinusoidal lumen into the space (Bottom)---------- 34

Figure 5 Different sources of cellular therapy for postresectional liver failure---------- 43

Figure 6 A schematic representation of the hepatic stem cells which are bipotential cells and may either be directed into a hepatocyte or cholangiocyte lineage. Under certain conditions, Cholangiocytes, which are terminally differentiated cells, may differentiate into hepatocytes and regenerate the liver----------46

Figure 7 Steps of Embryoid body formation from undifferentiated embryonic stem cells. The three most popular methods are illustrated. In all methods, the principle is induction of aggregation of cells into a ball like mass which will lose the undifferentiated state in the absence of LIF and differentiate into ectoderm, mesoderm and endoderm from which hepatocytes arise----------58

Figure 8 Schematic representation of the studied groups at the designated time points. 7 rats from each group were studied at 24, 48 or 72 hours following gavage with either MCT or vector----------66

Figure 9 Schematic presentation of the two studied groups. Pre treatment with monoHER was started 24 hours before the MCT dose and was continued daily at the same time. (n=7) rats were sacrificed from each group at each time point----------68

Figure 10 Experimental animal design. 40 mice were treated with APAP. The animals were then divided into 2 groups Cell therapy group=Group1 with and control group=Group2. During the first 24 hours 19/40 animals died due to the effect of APAP. Animals from both groups were then killed at 72 hours when the fluorescent signal started to decay and at two weeks when the signal could no longer be detected *in-vivo*----------70

Figure 11 IVIS Lumina 2, computer and monitor----------76

Figure 12 IVIS Lumina 2 and XFO-12 fluorescence equipment----------77

Figure 13 Portal pressure measurements in MCT treated rats compared to the control group. MCT administration caused a significant rise in portal pressure measurements when compared to the control group at all designated time points----------94

Figure 14 Serum ALT measurements in both groups. Serum ALT was significantly higher in the MCT group at 48 and 72 hours, however no significant difference could be detected at 24 hours----------96

Figure 15 Serum bilirubin measurements in both groups. Serum bilirubin levels were significantly higher in the MCT group when compared to the control group at 48 and 72 hours however not at 24 hours----------97

Figure 16 Histological examination of the liver in both studied groups at 24 hours. Normal appearance of the liver in the control group with no dilatation of the hepatic sinusoids following gavage with DMSO (left). The effect of MCT on the liver could be seen in the form of sinusoidal dilatation that was extensive all over the liver (right low magnification) and showing the ballooning of the sinusoids and the presence of inflammatory cells within the sinusoidal spaces (right high magnification) Low magnification x100, high magnificationx400----------99

Figure 17 Histological examination of the liver in both studied groups at 48 hours. No liver damage could be detected at 48 hours in the control group (left); however in the MCT group there was severe congestion that was extensive over large areas of the liver (Right low magnification). This was associated with areas of peliosis and beginning of necrosis in some areas of the liver (Right high magnification). Low magnification x100, high magnification x400----------100

Figure 18 Histological examination of the liver in both studied groups at 72 hours. No damage could be detected in the control group at 72 hours (left). The liver in the MCT group shows extensive areas of coagulative necrosis in the centrilobular regions of the liver (right) with damage of the endothelial lining of the central vein and its separation from the basement membrane. (Right high magnification, solid arrow). Low magnification x100, high magnification x400----------101

Figure 19 Histological changes in the liver following oxaliplatin and MCT treatment. A very mild degree of SOS could be seen in the livers of oxaliplatin treated rats at 24 hours when compared to MCT treated rats at 24 hours (A, B). There was no progression of liver injury with time in the oxaliplatin group. At 72 hours oxaliplatin treated rats lacked hepatocellular necrosis and inflammatory cells unlike in the MCT group which progressed from sinusoidal dilatation at 24 hours to frank necrosis at 72 hours (C, D)----------102

Figure 20 Scanning Electron Microscopy images of both control and MCT treated rats at 72 hours following gavage. The sinusoidal endothelial lining is intact in the control group receiving DMSO only with no detachment of the sinusoidal lining or gap formation (Ax2500). In the MCT treated rats, there is detachment of the sinusoidal endothelial lining occluding the blood flow in the sinusoid and congestion with erythrocytes (Bx5000). Dilatation of the fenestrae with formation of large gaps that develop in the sinusoidal lining of MCT treated rats (Cx2500, Dx5000 arrows pointing to gaps in sinusoids)------104

Figure 21 Transmission Electron Microscopy images of the sinusoidal lining in both the control and MCT treated groups. The SEC lining is intact and basement membrane with normal sized fenestrae (Arrow) and abundant glycogen in the control group (A). There is ballooning and detachment of the SEC lining from the basement membrane with an increase in the size of the fenestrae due to gaping of the SECs (Arrow). This is also associated with glycogen depletion (B)----------105

Figure 22 Transmission Electron Microscopy images of the sinusoids in both the control and MCT treated groups. Dilatation of the sinusoid with detachment of the SEC lining from the basement membrane with disruption of the space of Disse could be clearly seen in the MCT group (B). Separation of the SECs which are floating in the sinusoid and obstruct the lumen leading to dilatation and direct contact of erythrocytes with hepatocytes that have lost their SEC lining with loss of hepatocyte microvilli (arrow) (C). The sinusoids appear normal in the control group following DMSO gavage with abundant glycogen compared with the MCT group and intact SEC lining (A)----------106

Figure 23 Difference in expression of MMP-2 and MMP-9 in control and MCT groups at 72 hours. There was no marked difference in MMP-2 and MMP-9 expression in the control group at 72 hours (A, B). In the MCT group however, MMP-9 was markedly expressed when compared to MMP-2 which was similar to the expression in the control group (C, D)----------108

Figure 24 MMP-9 expression at different time points in the livers of the MCT group. A higher expression of MMP-9 could be detected in the MCT group when compared to the control group as early as 24 hours (A, B). Areas of MMP-9 expression included inflammatory cells and walls of the sinusoids (higher magnification C). An increase in the intensity of MMP-9 expression could be seen at 72 hours (E) with strong expression in damaged hepatocytes that show vacuolation (higher magnification F)----------109

Figure 25 Portal pressure measurements in monoHER pre-treated rats compared to MCT rats. Pre-treatment with monoHER significantly reduced the portal pressure at all time points when compared to the MCT group----------119

Figure 26 Representative samples showing morphological appearance of the liver at different time points. The congestion is evident at 24 hours in the MCT group (A), with appearance of punctuate hemorrhagic spots at 48 hours (B) and areas of frank necrosis in a deeply congested liver at 72 hours resembling the blue liver seen in the clinical scenario (C).

Congestion also occurred in the MCT+ monoHER group however was much less severe than in the MCT group and without the development of punctuate hemorrhages or frank necrosis----------122

Figure 27 Serum ALT and bilirubin measurements in the two studied groups. Rats pre-treated with monoHER had significantly reduced serum ALT at 72 hours when compared to MCT treated rats. There was no difference between both groups at 24 or 48 hours. There was no significant difference in bilirubin levels in both groups----------123

Figure 28 Histological examination of the liver in both studied groups at 24 hours. Generalized sinusoidal dilatation could be detected in the MCT group with inflammatory cell infiltration (A, B). The sinusoidal dilatation is less pronounced in the monoHER group with less inflammation (C,D). Low magnification x100, high magnification x40----------124

Figure 29 Histological examination of the liver in both studied groups at 48 hours. Extensive areas of congestion could be seen in both groups (A, C). Inflammation is less severe in the monoHER group (C, D)----------125

Figure 30 Histological examination of the liver in both studied groups at 72 hours. Massive areas of necrosis could be detected in the MCT treated liver (A), with detachment of the endothelial lining of the central vein and presence of subendothelial erythrocytes (B). No necrosis was detected in the monoHER liver at the same time point (C). Congestion was still present however the endothelial lining of the central vein was intact (D)----------126

Figure 31 Semi-quantification of liver damage in studied groups. The overall H&E liver damage severity score (A) and inflammatory cell count /HPF were significantly lower in the MCT+monoHER group only at 72 hours (B)----------127

Figure 32 Semi-quantification of MMP-9 expression in the liver samples of both groups. The MMP-9 expression was significantly higher in the MCT group at 24 and 48 hours-------128

Figure 33 MMP-9 expression in both groups at different time points. The MMP-9 expression in the monoHER group was weaker than in the MCT group at all time points. The most striking difference could be seen at 72 hours where MMP-9 was greater in both extent and intensity in the MCT group----------129

Figure 34 Oxaliplatin effect on HUVEC cell line. Oxaliplatin reduced the viability of HUVEC cells which was dose dependant----------131

Figure 35 MonoHER attenuates the effect of oxaliplatin on HUVEC cells----------132

Figure 36 *In-vitro* analyses of proliferation of colorectal cancer cell lines. MonoHER did not interfere with the dose-dependent cytotoxic effects of oxaliplatin. MonoHER alone had no

effect on viable cell count as measured by optical density in either cell line (OXA=Oxaliplatin,MH=MonoHER)----------134

Figure 37 IVIS images of GFP +ve cultured ESCs without DiR staining (LT) and with DiR staining (RT) showing background fluorescence using the GFP and CY5.5 filters, but not with the ICG filter----------144

Figure 38 Histological appearance of the liver following MCT administration in mice. No sinusoidal dilatation or hepatocellular damage could be detected in mice treated with MCT at 72 hours (A). When the mice were treated with APAP 300 mg/kg, marked hepatic necrosis was evident at 72 hours (B)----------145

Figure 39 Labeling and tracking of the fluorescent ESCs following APAP administration. Images of a pair of mice (cell therapy group-RT) compared with the (control group-LT) using IVIS. At 30 min following transplantation, a strong signal could only be detected from the spleen where the cells were injected. Between 3 and 24 hours following the cell transplantation, signal started to intensify between the spleen and the liver which is most probably the splenic vein owing to its tortuous course. A strong signal was detected over the liver 24 hours post-transplantation which faded out by 72 hour time period. At one week, the signal could not be detected over the liver but still strong was detectable over the spleen which completely disappeared by two weeks----------147

Figure 40 *Ex-vivo* images showing the distribution of fluorescent cells in different organs as detected by the ICG filter of the IVIS. A signal was detected at the site of injection in the spleen however; the highest signal was noticed in the centre of the liver at 72 hours, which faded out after two weeks. A weak fluorescent signal was also detected in the lungs at 72 hours and two weeks but not seen in kidneys at any of the designated time points (A). A graph showing the highest uptake of cells in the liver at all time points with a significant drop at two weeks (B)----------148

Figure 41 ESC liver engraftment following APAP induced damage. GFP +ve cells were present under the liver capsule (A-solid arrow) and around the central veins of the liver at 72 hours as seen under direct fluorescence (A-dashed arrow) with no fluorescence detected in the control group (B). Characteristic pattern of APAP induced liver damage after 72 hours affecting mainly the centrilobular portions of the liver with marked damage of the pericentral hepatocytes in both the cell therapy and control groups although pericentral vacuolation was more evident in the control group (C and D). At 2wks, the GFP +ve cells could be detected using IHC in the hepatic parenchyma and within the sinusoidal lining (E). Localised colonies of GFP +ve cells were also detected in the spleen at 2 weeks (F). After 2 weeks the liver recovered in both groups with the liver sections from the cell therapy group (G) showing less inflammatory cells and congestion than in the control group (H)(Scale bar=200µ)----------151

Figure 42 Serial sections examined for GFP and Albumin expressions. GFP +ve transplanted cells (A) showed very faint albumin expression at the cell periphery of dividing cells at 72

(B), whereas areas stained with anti-GFP antibody (C) were positive for albumin(D) at 2w following cell therapy (Scale bar=100µ)----------152

Figure 43 Serum levels of ALT, Albumin, Bilirubin and Urea are shown. ALT level significantly dropped in both groups at two weeks when compared with the 72 hour time point. When compared with the 72 hours, there was a significant reduction in serum ALT level at two weeks in the ESC treatment group only but not in the control group (A). Albumin level also improved in both groups with level being significantly higher in the cell therapy group when compared with the control group at two weeks (B). The drop in urea levels was not significant in both groups. (C) Bilirubin levels dropped significantly from 72 hours to two weeks with no significant differences between groups at similar time points (D)----------153

Figure 44 Mir126 expression in the three studied groups at different time points. A steady increase with time in the MCT group; however expression was five-fold lower in the MCT+ monoHER group when compared to the MCT group at 72 hours----------162

Figure 45 well-formed EBs in culture using GFP+ C57BL6 mouse embryonic stem cells using the static suspension method (A) Under fluorescence microscopy (B)----------166

Figure 46 The amplification plot following the PCR reaction----------195

Figure 47 Primary cell culture of ligated bile duct epithelial cells showing organization of the cells at different time points. At day 10 the cells form a structure resembling a bile duct with a lumen and surrounded by polyhedral and rounded cells with another layer of fibroblasts and mesenchymal cells----------200

Figure 48 A primary cell culture of bile duct epithelial cells with some cells of variable morphology expressing CD 133----------201

List of abbreviations

APAP: Acetaminophen

ALF: Acute liver failure

ALT: Alanine aminotransferase

ASCs: Adult stem cells

AST: Aspartate aminotransferase

APRI: AST to platelet ratio index

BDL: Bile duct ligation

BM: Bone marrow

BMSCs: Bone marrow stem cells

CCD: Charge coupled device

CASH: Chemotherapy associated steatohepatitis

CECs: Circulating endothelial cells

CRC: Colorectal cancer

CLM: Colorectal liver metastasis

DAB: 3,3' –diaminobenzidine tetrahydrocholride

DiR: 1, 1-dioctadecyl-3,3,3,3-tetramethylindotricarbocyanine iodide

DMSO: Dimethyl sulfoxide

EM: Electron microscopy

EBs: Embryoid bodies

EGCs: Embryonic germ cells

ESCs: Embryonic stem cells

FBS: Fetal bovine serum

5 FU: 5-Flurouracil

GFP: Green fluorescent protein

HSCs: Haematopoietic stem cells

H&E: Haematoxylin and eosin

HGF: Hepatocyte growth factor

HT: Hepatocyte transplantation

HUVEC: Human umbilical vein endothelial cell

HA: Hyaluronic acid

ICC: Immunocytochemistry

IHC: Immunohistochemistry

ICG: Indocyanin green

iPS: Induced pluripotent stem cells

ID1: Inhibitor of DNA Binding 1

i.p: Intraperitoneal

IVIS: Invivo imaging system

LIF: Leukemia inhibitory factor

LT: Liver transplantation

MMP: Matrix-metalloproteinase

MSCs: Mesenchymal stem cells

MIR: Micro RNA

MCT: Monocrotaline

MCT-P: Monocrotaline pyrrole

MonoHER: 7-monohydroxyethylrutoside

MTS: 3-(4,5-dimethylthiazol-2-yl)-5-(3-carboxy-methoxyphenyl)-2-(4-sulfophenyl)-2H-tetrazolium

NIR: Near infra red

NO: Nitric oxide

NRH: Nodular regenerative hyperplasia

PBS: Phosphate buffer solution

PMN: Polymorphonuclear

PP: Portal pressure

PVE: Portal vein embolization

PLF: Postresectional liver failure

SEM: Scanning electron microscopy

SECs: Sinusoidal endothelial cells

SOS: Sinusoidal obstruction syndrome

sTM: Soluble thrombomodulin

SDF-1: Stromal derived factor-1

SC: Subcutaneous

TEM: Transmission electron microscopy

VCAM: Vascular cell adhesion molecule

VEGF: Vascular endothelial growth factor

vWF: Von willebrand factor

1-Introduction

1.1 Background

Liver failure, which may either present in an acute or chronic form, is a growing health problem ranking as one of the leading causes of death worldwide. The etiology and presentation of liver failure differs according to age. In children, the leading identifiable cause of acute liver failure (ALF) is acetaminophen (APAP) induced hepatic toxicity followed by metabolic and autoimmune liver disease (1). Although APAP is the most common cause of ALF in adults in the UK, acute viral hepatitis is the leading cause worldwide (2).

In children, biliary atresia is the most common cause of chronic liver disease with excellent survival rates following liver transplantation (LT) (3). Liver cirrhosis however, remains the most common cause of end stage liver disease in adults with its two main etiologies; alcohol consumption and viral hepatitis C. The only established long-term successful treatment for these conditions is LT with long waiting lists of patients to be transplanted (4). Patients with liver tumours are not treated with LT but with liver resections and have excellent postoperative recovery; however liver failure may occur in about 2-5% of patients following liver resections with considerable mortality (5). LT maybe used in critical situations to rescue the liver following postresectional liver failure (PLF) and has shown better survival rates than with any other method of treatment (6). There has been an ethical argument however, whether to put patients with PLF on a priority list for receiving an organ compared with other indications of ALF. Also, patients with PLF have very high mortality rates when compared to the other indications of LT. For these reasons, PLF represents a complex and challenging problem to most liver surgeons.

1.2 Postresectional liver failure

Liver resection remains the gold standard of treatment for both primary and secondary liver tumours with the most common indications for liver resection being colorectal liver metastasis (CLM) (7), followed by hepatocellular carcinoma and cholangiocarcinoma (8).

In the United Kingdom, colorectal cancer (CRC) is the third most common cancer after breast and lung with about 40,000 newly diagnosed cases and 16,000 deaths per annum (Cancer Research UK, 2008). CLM occurs in at least 30% of patients with CRC and accounts for more than two thirds of deaths (9), (10). Advances in chemotherapeutic drugs and changes in the resectability criteria have improved survival in patients after resection of CLM (11). In England, the liver resection population access rate was 1.82 and 2.95/100,000 general population in 2000-1 and 2004-5, respectively, with a 62% increase during the 5-year study period (12). The incidence of short-term postoperative complications on the other hand has increased with the more aggressive approaches and more specifically the occurrence of PLF (13).

PLF is a dreadful complication following major hepatic resections occurring once the remnant liver volume falls below a critical threshold. It presents a spectrum that ranges from mild liver dysfunction to ALF. A similar problem occurs in patients following LT due to size mismatch between recipients and the graft resulting in a small-for-size syndrome (14). Several definitions for PLF exist; however the best quantitative definition with specificity of 96.6% is the 50-50 criteria, which describes PLF as prothrombin time <50% and serum bilirubin > 50% µmol on postoperative day 5. Serum bilirubin is preferred because prothrombin time may be

altered by administration of fresh frozen plasma and a peak bilirubin of 7.0 mg/dl has been considered a specific cut-off value for PLF related deaths (15),(16)

To prevent PLF, the acceptable remnant liver volume following a resection should be at least 25% (17). However this may change if the remaining liver parenchyma is dysfunctional, where the required remnant volume of liver parenchyma would range from 30-40 % in patients with chemotherapy induced liver damage to 40-50 % in case of cirrhosis. When the remnant liver volume falls below this critical threshold, liver failure develops.

1.2.1 Chemotherapy induced liver damage

Until recently palliative chemotherapy was the main line of treatment for patients with unresectable CLMs with very few patients surviving for 5 years due to low tumour response rates (18). The revolution in chemotherapy regimens with the introduction of 5-Flurouracil (5-FU), Oxaliplatin and Irinotecan has converted non-resectable liver metastases into resectable ones allowing a 10-30% increase in patients eligible for curative surgery with a 30-35% survival at 5-years (19), (10). Moreover, these powerful modern neoadjuvant chemotherapy protocols have allowed a reversal of the alternative approach with chemotherapy first, followed by liver resection and then resection of the CRC. This allows early treatment of the CLM which are the main cause of death in these patients. Also, it has the advantage of patient stratification into responders who have a good prognosis and non-responders in which aggressive treatment should be avoided and would benefit from palliative treatment (20). There have been debates regarding the timing of surgery following neoadjuvant chemotherapy and the consensus is that surgery should be

performed once the CLM become resectable. This is due to the toxic effect of neoadjuvant chemotherapy on the normal hepatic parenchyma with an increase in development of PLF in these patients. Also, there is a risk of disappearance of small hepatic lesions with high impact chemotherapy. These lesions are difficult to treat and may lead to recurrence in the future (21) (20).

Irinotecan

Irinotecan inhibits topoisomerase I, resulting in single strand DNA breaks and inhibition of DNA synthesis. When used in combination with 5-FU and Leucovorin it leads to both an improved response rate and survival in patients with metastatic CRC (22). Unfortunately, Irinotecan-based regimens are associated with the development of chemotherapy associated steatohepatitis (CASH) in patients with CLM, independent of their body mass index (23). Simple steatotic hepatitis can develop into steatohepatitis after exposure to oxidative stress and reactive oxygen species. Irinotecan indeed induces oxidative stress leading to the development of CASH and is associated with increased 90-day mortality after liver surgery for CLM (23).

Oxaliplatin

Oxaliplatin is a third generation platinum containing antineoplastic agent which has a spectrum of activity that is different from first and second generation platinum compounds. Oxaliplatin has been shown to be effective against colon, breast and gastric cancers, in addition to sarcomas and renal cell carcinomas with the concentration and duration of exposure being important factors for its cytotoxicity (24), (25). Oxaliplatin exerts its activity by causing intra- and interstrand cross links

with DNA within 2 hours of its administration. This blocks DNA replication and transcription leading to apoptotic cell death (26).

Oxaliplatin is associated with an improvement in disease free survival when used as an adjuvant in stage II or III CRC in combination with 5-FU and leucovorin (27). Oxaliplatin based regimen are highly effective but induce histologically proven sinusoidal injury in 50%-75% of patients with CLMs treated with oxaliplatin based chemotherapy prior to liver resection (28**).** The sinusoidal injury seen is characterized by damage to sinusoidal endothelial cells (SECs), hepatocellular atrophy, disruption of the sinusoidal membrane, sinusoidal dilatation, collagenization of the space of Disse, centrilobular or perisinusoidal fibrosis and resembles the injury observed in patients who have undergone myeloablative conditioning therapy before hematopoietic stem cell (HSC) transplantation (8, 9). This type of injury is described as the sinusoidal obstruction syndrome (SOS), formerly known as veno-occlusive disease. However, up until now, no reliable methods have been developed for the detection of endothelial injury during oxaliplatin-based chemotherapy and prior to liver resection.

Patients with oxaliplatin induced SOS present with increased bilirubin level, hepatomegaly, right upper quadrant pain and weight gain or development of ascites (29). Patients with histologically proven sinusoidal injury who have undergone major hepatectomy have a higher risk of post-resectional morbidity and longer hospital stay (30).

1.2.2 Structural and Functional aspects of the Hepatic Sinusoid

The hepatic sinusoids represent the principal site where blood regulation and solute exchange takes place between the blood and the space of Disse in the liver. The SECs which constitute the sinusoidal lining start to form between the 4^{th} and 6^{th}

week of gestation. Initially they do not contain fenestrae and acquire the fenestrated architecture between the 10^{th} and 17^{th} week of gestation (31). The main afferent supply to the sinusoid is through small branches of the portal vein with a less consistent contribution from the arterial system. Following the exchange of blood and solutes, blood drains into the central venules (32). This transvascular exchange allowing better hepatocyte oxygenation and adequate clearance of toxic metabolites and chylomicron remnants is possible due to the unique structure of the SECs containing fenestrae measuring about 170 nm in diameter within their cytoplasm. This permits access of the solutes into the space of Disse where the hepatic microvilli project (33) (Fig.1 and 2).

Ultrastructural studies have shown that the fenestrae are dynamic structures supported by actin cytoskeletal filaments under paracrine control of vascular endothelial growth factor (VEGF) released from the hepatocytes and the stellate cells (35). Kupffer cells are resident macrophages that are anchored to the sinusoidal wall through interdigitations between the endothelial cells. They represent an important component of the sinusoidal lining and are responsible for clearance of macromolecules as well as toxic substances in the portal flow (32).

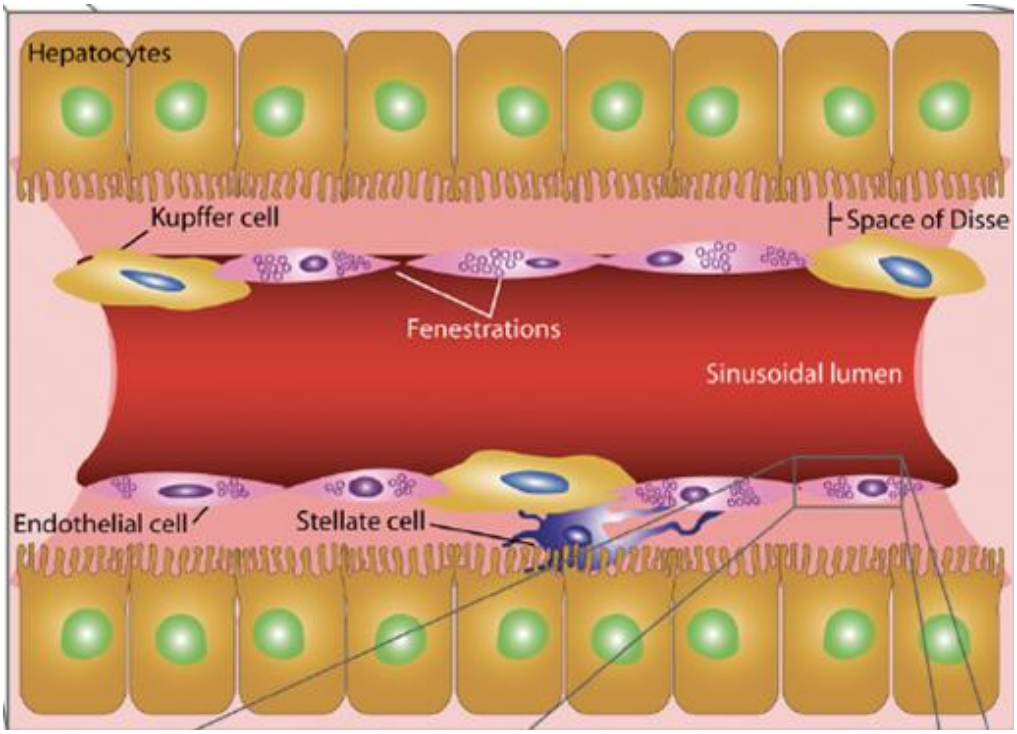

Figure 1 Adopted with permission from Prof. Eddie Wisse (34). A schematic representation of the liver sinusoid showing the alignment of the SECs containing the fenestrae allowing the exchange of solutes with the hepatocytes.

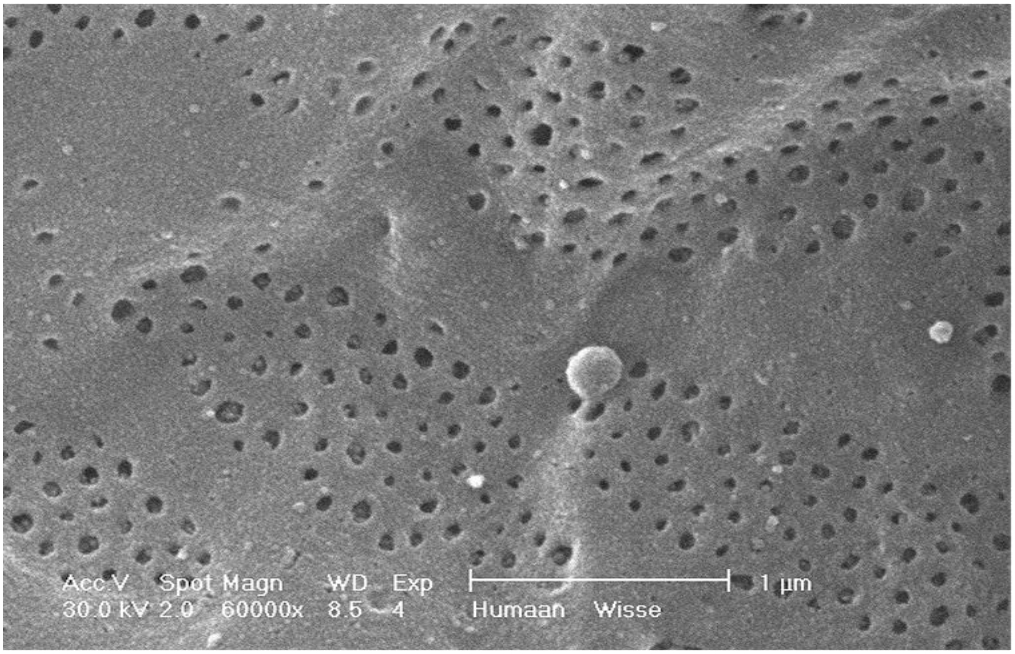

Figure 2 Adopted with permission from Prof. Eddie Wisse. TEM x 6000 of normal hepatic sinusoid showing the fenestrae with size between 150-175 nm.

1.2.3 Pathogenesis of sinusoidal injury during oxaliplatin-based regimen

Microvascular injury to SECs is a key factor in the development of SOS. Drugs implicated in the development of SOS (e.g. oxaliplatin, azathioprine) deplete SEC glutathione and seem to be selectively toxic to SEC as depletion of hepatocyte glutathione has not been shown to occur (36). This is most probably due to a greater glutathione defensive capacity in hepatocytes with a higher turnover when compared to SECs, in addition to exposure of the circulating toxic metabolite at a much higher concentration than the hepatocytes (37). The resulting hepatocellular injury therefore seems to be more related to the SEC-induced microvascular events leading to hepatocyte ischemia rather than a direct hepatotoxic effect. The depletion of SEC glutathione has not yet been proven *in-vivo* or *in-vitro* for oxaliplatin, but several articles have already shown that one of the two main metabolites of oxaliplatin; the heavy metal DACH platin, reacts to and is detoxified by glutathione through adduct formation. It has been shown that high glutathione levels prevent injury induced by platinum-containing chemotherapeutics and that a decrease in glutathione concentrations induce cytotoxicity. SEC glutathione depletion is followed by toxicity to SECs (38).

SOS is characterized by swelling and rounding up of SECs, sinusoidal injury including loss of SEC fenestration, formation of gaps between SECs (Fig.3). Red blood cells and inflammatory cells eventually penetrate beneath the swollen SECs into the space of Disse (Fig.4). In addition, swollen SECs block the sinusoidal lumen with redirection of blood flow into the space of Disse leading to complete dissection

of the sinusoidal lining wall. Kupffer cells, SECs and stellate cells embolize into the sinusoid and block sinusoidal flow (39).

Also, nitric oxide (NO) plays a critical role in the pathogenesis of SOS. NO production is reduced due to Kupffer cell depletion (initially) and SEC injury. Due to the loss of NO, NO mediated inhibition of matrix-metalloproteinase-9 (MMP-9) synthesis declines and active MMP-9 separates SECs from the underlying basement membrane which leads to a further decrease in NO synthesis (40).

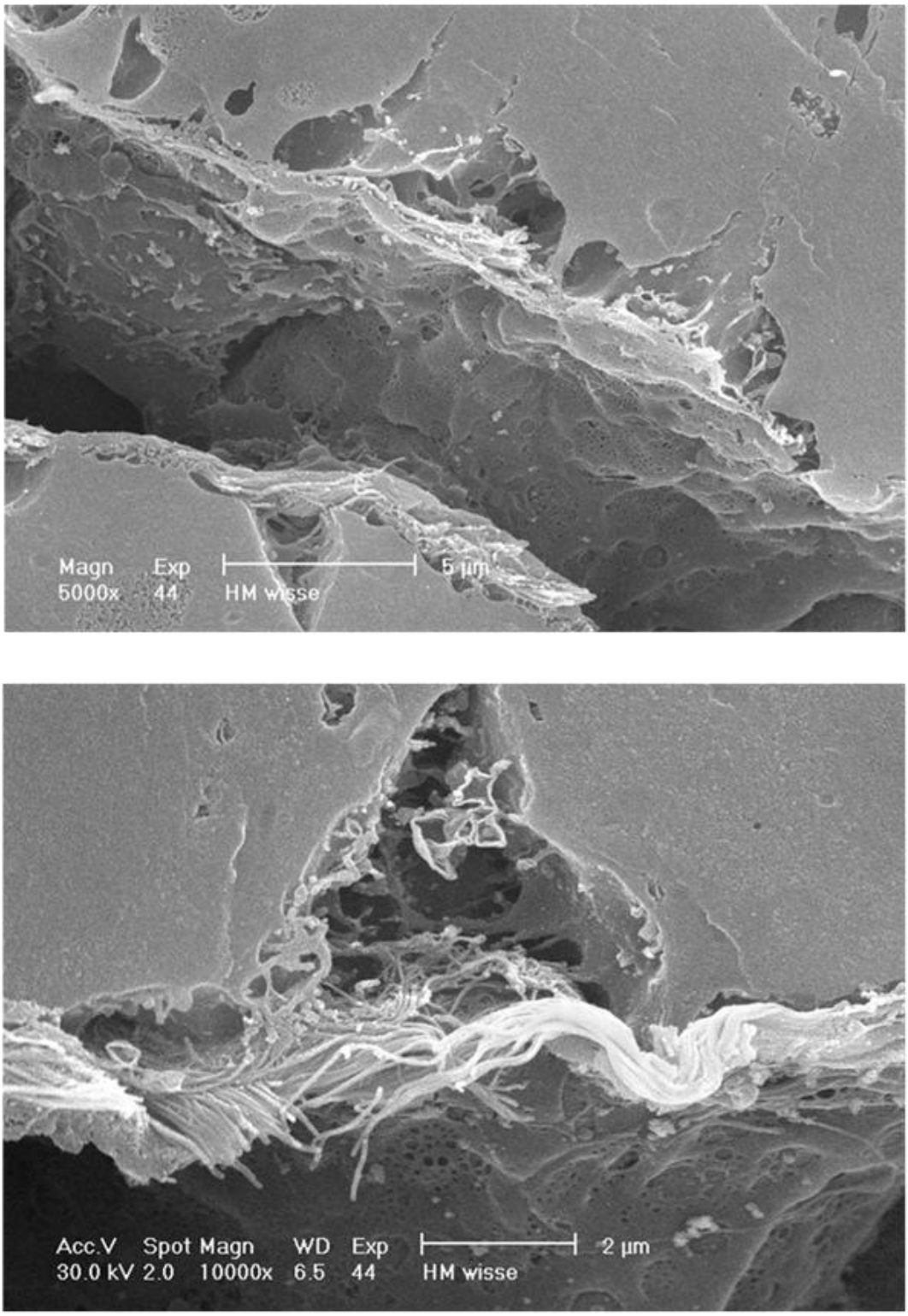

Figure 3 Unpublished own group SEM images of liver SECs. This patient had a liver resection following 6 cycles of oxaliplatin based neoadjuvant chemotherapy. Disruption of the SEC lining with gaps in the space of Disse can be detected (Top x5000). Exposure of the hepatocyte microvilli could be seen at higher magnification (Bottomx10000)

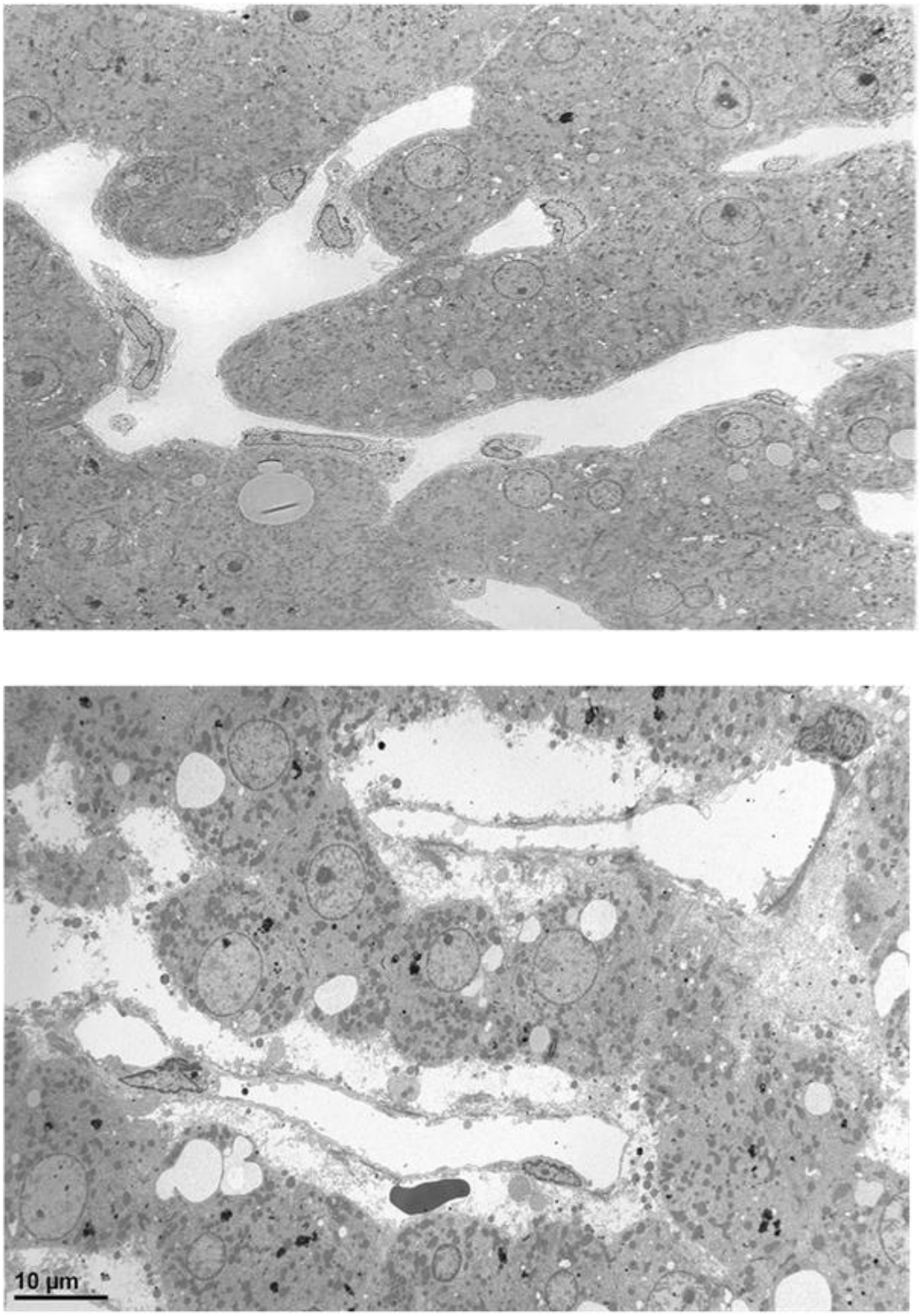

Figure 4 Unpublished own group TEM images of liver sinusoids. Normal liver showing intact sinusoids (Top). Following oxaliplatin chemotherapy there is disruption in the space of Disse with extravasation of the erythrocytes from the sinusoidal lumen into the space (Bottom).

1.2.4 Role of SOS in development of PLF

Several reports have shown that oxaliplatin-induced SOS is associated with an increased risk of PLF following major hepatic resections for CLMs. Karoui et al (21) compared two groups of patients with CLMs who had similar demographics and preoperative liver functions. Both groups were subjected to major hepatectomy with total vascular exclusion and the pathological examination of the non-tumorous liver revealed presence of SOS without steatohepatitis. There was a statistical significant increase in the incidence of PLF in patients who had received prolonged oxaliplatin based chemotherapy (21). Similarly, Nakano et al (30) showed that patients who developed oxaliplatin-induced SOS had higher preoperative aspartate aminotransferase (AST) and alkaline phosphatase levels with impaired functional liver reserve in the form of significantly higher values of indocyanin green (ICG)-R15 when compared to patients with no SOS. Also, there was a significant association between SOS and PLF in patients undergoing major hepatic resections, and those with higher bilirubin levels and longer hospital stay. The authors concluded that a major hepatectomy should be delayed if SOS is diagnosed or even suspected preoperatively and if delay is not possible then other strategic options should be considered including portal vein embolization (PVE) or a two-stage hepatectomy (30). Although Nakano et al suggested a time interval between the last chemotherapy session and the operation; it still remains questionable whether or not SOS is a reversible condition. Indeed, Rubbia-Brandt et al showed that pathological evidence of SOS in the liver exists even after discontinuation of the chemotherapy (28). Soubrane et al (41) also reported that 74% of patients who received oxaliplatin within 4 months of the hepatectomy had impairment of the functional liver reserve when compared to the control group. Moreover, patients with severe SOS lesions

often developed ascites with possible mortality. (41). A recent report showed that patients who develop oxaliplatin-induced high-grade SOS not only have a higher incidence of PLF but also develop earlier intra-hepatic recurrences with a negative impact on survival (42).

1.2.5 Assessment and Detection of PLF

Estimation of the function of the remaining liver volume is an essential preoperative step in planning for a successful liver resection and is most commonly assessed by CT scan. However, the function of the remaining liver may be compromised by cirrhosis, fibrosis or chemotherapy induced damage, and therefore functional studies are needed. ICG is a substrate whose extraction depends on both the functioning hepatocyte mass and the hepatic blood flow. A safe resection would be considered when the ICG retention is 14% at 15 minutes (43). There are several scoring systems to predict PLF in patients with cirrhosis; most widely used is the Child-Pugh scoring system depending on the presence or absence of ascites, encephalopathy, and measurement of albumin, bilirubin and prothrombin time (44). An early diagnosis of SOS while patients are on chemotherapy or during the preoperative work up would be very beneficial to patients avoiding postoperative morbidity and mortality.

Detection of endothelial damage

Sinusoidal endothelial damage is the key feature of SOS of the liver following neoadjuvant chemotherapy treatment for CLM. A number of circulating markers for

endothelial function and activation of the coagulation cascade have been discovered in recent years:

- Hyaluronic acid (HA) is a marker of endothelial function; It is a high-molecular weight polysaccharide, synthesized by mesenchymal cells throughout the body. It comes from peripheral tissues via the lymph into the circulation. Plasma HA is almost exclusively (85-90%) metabolized by liver SECs (45). HA uptake in SECs is achieved by means of receptor mediated endocytosis followed by degradation by lysosomal hyaluronidase, β-glucoronidase and β-N-acetyl-glucosaminidase. The waste products are glucuronic acid and N-acetylglucosamide. The plasma half life of HA is 2-5 minutes. Because the elimination capacity of HA is 10-times that needed for normal endogenous production, the serum HA levels are not influenced by increased input but depend predominantly on the scavenging function of SECs. Whether increased serum levels of HA are caused by increased production or decreased clearance capacity of the hepatic sinusoids, can be evaluated by means of a hyaluronan loading test (46) or [^{11}C] hyaluronan positron emission tomography (47). Increased levels of HA might be seen during SOS because of decreased SEC function or increased vascular damage due to shunting of portal blood. HA has already been used in patients undergoing myeloablative conditioning therapy before HSC transplantation to detect the presence of SOS (48). Mean peak serum HA level was significantly higher in patients who had a diagnosis of SOS compared to those who did not, 1173 ± 982 ng/mL versus 445 ± 736 ng/mL ($p=0.01$). Serum levels increased in time in patients with severe SOS.

- Von Willebrand Factor (vWF) is an endothelial ligand for platelet glycoprotein and is endothelium-specific. It has an important role in mediating adhesions of platelets to the endothelium. When endothelial cells are damaged, vWF is released from Weibel-Palade bodies. vWF antigen can be measured in citrated plasma. Increased vWF levels are expected during and after oxaliplatin based chemotherapy resulting in sinusoidal damage (49).
- Soluble Thrombomodulin (sTM) is a molecule specifically expressed by endothelial cells, a protein C cofactor with anticoagulant capacities. sTM can be released from damaged endothelial cells and measured in citrated plasma by means of an enzyme-linked binding assay. Increased sTM levels were observed in patients with multiple complications after bone marrow (BM) transplantation (50).

CD146 positive circulating endothelial cells (CECs) are detached from their endothelial alignment and indicate severe endothelial damage. The necrotic CECs might cause an inflammatory reaction once phagocytosed by activated macrophages or bound to toll-like receptors. CECs can be detected by means of immune-magnetic isolation using anti-CD146 antibodies (51).

The AST to platelet ration index (APRI) and the FIB-4 which combines standard biochemical values and age are two scoring systems that were originally used to predict development of liver fibrosis in hepatitis C patients (52), (53). Recently, these scoring systems have been used to predict high grade sinusoidal lesions following oxaliplatin chemotherapy with a sensitivity and specificity of 87% and 69% respectively (41). The advantages of these scoring systems are that they are inexpensive and the parameters used for calculation are part of the standard liver investigations required preoperatively. More invasive investigations for preoperative

diagnosis of SOS have been suggested including preoperative diagnostic laparoscopy for detection of a blue liver. Also a preoperative liver biopsy has been suggested for diagnosis of SOS. Limitations are that a minimum of 25mm of liver tissue is required to provide accurate information using a semiquantitative score. This in addition to the variability of distribution of liver lesions in SOS makes a preoperative liver biopsy a less reliable diagnostic measure (54).

1.2.6 Prevention

The mainstay of management of PLF should be a preventive one.

Preoperative

Identifying problematic patients who are likely to develop PLF in the future is key in prevention of PLF. Preoperative correction of the patients' co-morbidities is very important in prevention of PLF including special attention to the nutritional status. Parenteral nutrition provides adequate caloric intake and nitrogen support. Enteral nutrition on the other hand prevents gastrointestinal atrophy and preserves normal gut flora. No statistically significant differences could be detected between enteral and parenteral nutrition, however patients with enteral nutrition show better postoperative immune competence (55). There have been debates regarding the routine performance of percutaneous transhepatic drainage in all patients with jaundice as it has shown no benefit in patients with obstructive jaundice resulting from tumours (56). Recently, in a cohort of patients with tumours in the head of pancreas, it has been shown that preoperative biliary drainage is associated with a higher complication rate when compared to early surgery (57).

Oxaliplatin-induced SOS has a negative impact on postoperative recovery of liver function and is associated with an increased incidence of PLF. Several factors that if taken into consideration during the planning of the neoadjuvant chemotherapy might reduce the risk of SOS related PLF. The most important factor seems to be the number of chemotherapy cycles before the operation. Karoui et al (21) correlated the development of PLF with the number of chemotherapy cycles, where patients receiving a median number of five cycles had fewer postoperative complications than patients receiving a median number of 12 cycles. A recent report showed that more than nine cycles of oxaliplatin based chemotherapy was not associated with improvement in the pathological response and was considered an independent prognostic factor with patients having a four-fold risk of developing SOS and PLF when compared to patients receiving less than nine cycles (58). Soubrane et al showed that although the number of chemotherapy cycles might correlate with the development of SOS, this could not accurately predict the severity of SOS lesions and that a short interval period between the end of chemotherapy and operation time was a more important factor associated with high grade SOS lesions and PLF (41). If postponing surgery is not possible or there is fear that delaying surgery might be associated with cancer progression then preoperative PVE could be done to augment the volume of future remnant liver and thus circumvent PLF.

Preoperative PVE is an effective measure to induce hypertrophy of the contralateral lobe of the liver. The gain in the residual volume ranges between 4 and 21 ml/day with a parallel improvement of liver functions, and an average of 4-6 weeks is required before the operation to achieve adequate liver hypertrophy (59). This procedure has led to an increase in the percentage of patients undergoing extended hepatectomies with fewer complications and a shorter hospital stay. This technique

however is not always successful and may result in an increase in the size of the existing tumour (60), (61).

Intraoperative and postoperative

Intra and postoperative hypotension also plays a role in prolonging the hepatic ischemia and this may result from either blood loss or sepsis; which has a suppressive effect on kupffer cell function (62). Neoadjuvant based oxaliplatin chemotherapy regimens have been associated with more intraoperative blood loss and packed red cell transfusions when compared to the control group. This has been hypothesised to be related to increased splenic sequestration of platelets leading to thrombocytopenia (63), (64).

Several measures have been described to reduce excessive intraoperative blood loss including total vascular occlusion or lowering the central venous pressure (65). Patients who were subjected to ischemic preconditioning through intermittent vascular occlusion were associated with less morbidity when compared to continuous vascular occlusion. There was no difference between both groups in term of mortality or development of liver failure (66). Ischemic Preconditioning involves intermittent clamping of the hepatic pedicle for a short period (5-10) minutes followed by reperfusion (5-10) minutes. This renders the liver more tolerant to subsequent prolonged episodes of ischemia and has been shown to decrease the severity of liver necrosis through several mechanisms including the upregulation of cytokine TNF and IL-6 with downregulation of TGF-β (67).

1.2.7 Treatment

Due to the low incidence of PLF, there is great difficulty in conducting a randomized controlled trial that would evaluate the effect of different treatment modalities in these patients (5). Patients with PLF should be treated in the ITU with intensive monitoring and support of the vital body functions. Due to the strong association between sepsis and PLF, antibiotics should be administered empirically in the setting of PLF and later adjusted according to the results of the cultures taken (17). Several measures for liver support have been documented and could be divided into cell-free liver support systems and bioartificial livers. The former include plasma exchange (68) and the molecular adsorbent recirculating system (69), none of which seem to provide definitive treatment for PLF as they cannot replace the synthetic and metabolic functions of the failing liver.

Bioartificial devices have been designed in the recent years to support functions of metabolic organs. They are basically extracorporeal bioreactors loaded with different cell types (70). The cells used in the liver model are either human or porcine hepatocytes (71). However more research needs to be conducted focusing on developing an ideal bioreactor which should resemble both the normal hepatic tissue structure and function (72). A more promising future management might be the application of stem cells or hepatocytes in the treatment of PLF.

1.3 Cell therapy for treatment of PLF

Cell based therapy is considered a new therapeutic tool that has shown great potential in the recent years and is expected to avoid whole-organ transplantation in

the future. The target of cell therapy is to replace the defective cells in order to substitute organ function through transplantation of cells (73). In case of larger tissue defects, cells alone would not be able to replace the function and tissue engineering is required to load cells on to 3-D biodegradable scaffolding system to support their growth and function (74). There are several sources of cells which can be used in prevention and treatment of PLF (Fig.5).

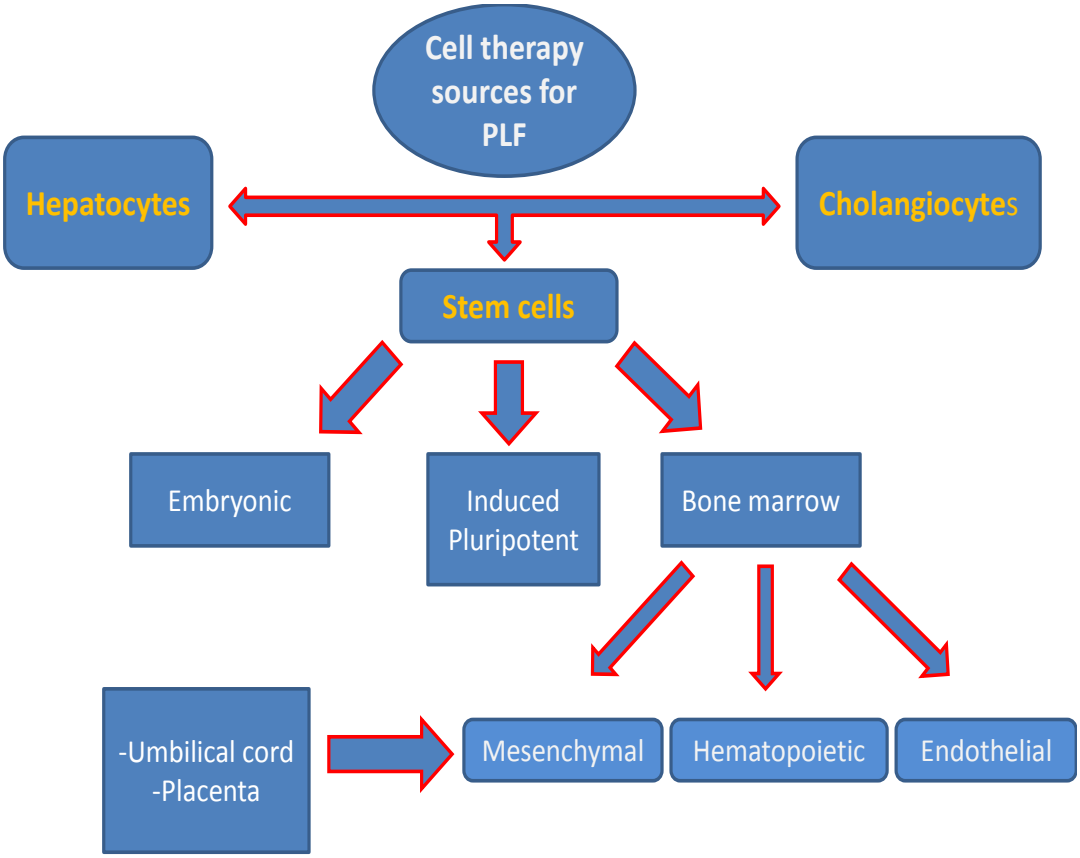

Figure 5 Different sources of cellular therapy for postresectional liver failure.

1.3.1 Liver regeneration following partial hepatectomy

The ideal way of increasing the functioning residual liver volume following major hepatic resections would be through increasing the number of functioning hepatocytes. Replenishing the lost hepatocyte mass might occur through either stimulation of the endogenous hepatocyte population or through an exogenous supply of hepatocytes or cells with the potential to differentiate into hepatocytes.

The liver has an enormous ability to regenerate dependant primarily on the proliferation capacity of hepatocytes. The hepatocytes are in a quiescent state in the intact liver and are non-responsive to growth factors. Following partial hepatectomy or hepatocyte loss, the hepatocytes are sensitized by TNF released from the non-parenchymal cells which release a cascade of growth factors (75). Hepatocyte growth factor (HGF), epidermal growth factor and transforming growth factor-α are the primary mitogenic growth factors that initiate a powerful regenerative drive leading to rapid hepatic regeneration through proliferation of the hepatocytes. This occurs in coordination with proliferation of non-parenchymal cells and the support of the extracellular matrix (76).

Liver regeneration following partial hepatectomy requires two rounds of hepatocyte replication to restore the liver volume. The duration for complete restoration of the liver volume after a partial hepatectomy ranges from 5-7 days in rats and from 8-15 days in humans (77). Hepatocytes have been shown to have their highest DNA synthesis 24 hours following the hepatectomy; followed by Kupffer cells at 48 hours and endothelial cells at 96 hours (78).

With more extensive liver resections, the regenerative drive of hepatocytes is insufficient (79) and regeneration then depends on the stimulation of a second

compartment comprised of hepatic progenitor cells as described by Faber (80), (81). These are bipotential cells with the ability to differentiate into either hepatocytes or biliary epithelial cells (82). It is important to mention however that this only occurs when liver resection is associated with a background of chemical injury which is the situation following oxaliplatin chemotherapy and not following liver resection per se (83). These oval cells reside in four possible 3-dimensional niches, most important of which are the canals of Hering representing the small peripheral branches of the biliary tree (84). The interaction between the cells in these niches with hormones and growth factors adds to their flexibility and regenerative capacity (85). These oval cells have been postulated to be the progenitors of hepatic stem cells because they share cell surface markers with HSCs such as c-kit, Sca-1, Thy-1, and CD-34 (86). This may be clearly understood when looking at the common embryological origin, where hepatocytes, biliary epithelium and the pancreas originate from the endoderm of the foregut (87). Biliary epithelial cells appear capable of changing their phenotype and giving rise to hepatocyte-like cells, moreover gallbladder epithelial cells have been successfully engrafted in mouse recipient liver with similar morphological features and expression to hepatocytes (88). Whether this is due to the presence of bipotential stem cells or terminal transdifferentiation is yet to be investigated (Fig.6).

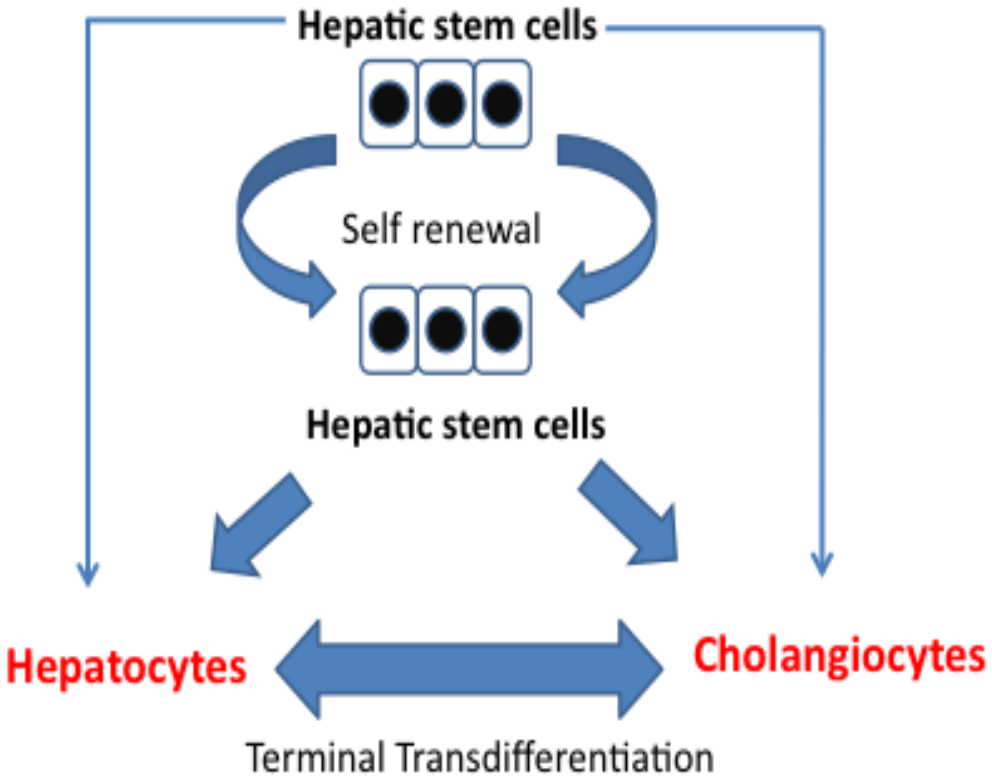

Figure 6 A schematic representation of the hepatic stem cells which are bipotential cells and may either be directed into a hepatocyte or cholangiocyte lineage. Under certain conditions, cholangiocytes, which are terminally differentiated cells, may differentiate into hepatocytes and regenerate the liver.

1.3.2 Neoadjuvant chemotherapy and liver regeneration

Hewes et al showed that hepatocytes from livers of patients who received neoadjuvant chemotherapy retained normal biochemical functions, however the authors did not show that SOS had occurred in the livers of the 12 patients who received oxaliplatin preoperatively, moreover the period between the last chemotherapy cycle received and the operation might have allowed recovery of the hepatocyte function (89). It has been shown more recently that liver regeneration was significantly impaired in an experimental model of SOS. Following partial hepatectomy with underlying SOS there was less increase in HGF mRNA levels with no evidence of hepatocyte proliferation following Ki67 staining which was strongly positive in the control group with no SOS (90). In a recent study comparing liver regeneration in patients with and without oxaliplatin induced SOS following partial hepatectomy and PVE, there was a significant reduction in liver hypertrophy in patients with SOS which was considered an independent factor associated with lower functional liver reserve and higher incidence of PLF (91). The mechanism through which SOS inhibits hepatocyte proliferation is still not completely understood.

Oxaliplatin induced SOS is associated with splenomegaly and persistent thrombocytopenia mainly through splenic platelet sequestration and to a lesser extent through an immune-mediated mechanism (64). Platelets were shown to have a significant role in liver regeneration through a serotonin-mediated mechanism (92). Also, in order to initiate hepatocyte proliferation, platelets accumulate in the sinusoidal spaces in the acute phase following partial hepatectomy with translocation into the space of Disse where they maintain close contact with hepatocytes (93). Therefore, in addition to thrombocytopenia which has a negative impact on liver regeneration, the disruption in the sinusoidal architecture in SOS would limit the

selective contact of platelets with hepatocytes and hence inductive signals for early hepatocyte proliferation.

The importance of SECs in liver regeneration has been recently investigated. The presence of SECs in culture media was essential for the inductive proliferative effect of VEGF on hepatocytes *in-vitro.* This is due to activation of VEGFR-1 on SECs leading to a release of HGF and other paracrine factors that stimulate hepatocyte proliferation. This VEGF-mediated HGF effect is specific to the liver SECs as it has not shown to occur in other vascular endothelial cell beds (94). Another more recent study investigated the role of VEGFR-2 and VEGFR-3 in SEC modulation and liver regeneration. It was shown that in the liver; VEGF-2 and VEGF-3 receptors were specific to SECs and were not expressed in any other liver cells (95). Inhibitor of DNA Binding 1 (IDI) factor is a transcription factor specific to endothelial progenitor cells and is beneficial in tracking endothelial cells in different vascular beds (96). Defective liver regeneration has been observed in ID1-deficient mice through decreased expression of SEC-mediated derived growth factors. Moreover ID1 upregulation occurred following partial hepatectomy driven liver regeneration through activation of the VEGF2 pathway. This leads to restoration of the liver mass in a biphasic mode where hepatocyte regeneration starts in close proximity to SECs in absence of vessel formation in days 1-3 following PH. As the liver mass increases, there is a demand for increased blood supply with a proliferative burst in SECs which starts at day four and returns to normal at day eight. These findings did not occur in the absence of the VEGF2-Id1 mediated pathways in mice leading to abnormal liver functions and delayed liver regeneration following partial hepatectomy highlighting the role of SECs in liver regeneration following liver resections (95).

1.3.3 Hepatocyte Transplantation (HT)

The first HT was performed in an attempt to treat Crigler-Najjar syndrome in rats which are congenitally unable to conjugate bilirubin (97). More studies showed that HT is most successful in treating congenital metabolic diseases of the liver in children and in adults than other liver diseases (98). This might be explained by the low number of cells required to correct the underlying metabolic error, where replacement of 2-5% of the liver mass would improve the function dramatically (99). The main sources of hepatocytes are livers that were judged inadequate for transplantation (100). Other sources include fetal hepatocytes which show higher proliferation and engraftment rates than adult hepatocytes (101). Hepatocytes that were transplanted immediately seemed to provide better results than those that were cryopreserved, thawed and then transplanted (102). The quality of the transplanted cells is essential for efficient engraftment and is a major limiting factor for successful transplantation (103). Following injection there are three major steps that are required for liver repopulation which are deposition of hepatocytes into the hepatic sinusoids, traversing the sinusoidal endothelial cells which represent a physiological barrier to engraftment followed by integration into the liver parenchyma. Loss of cell viability in any of these steps would stimulate the phagocytic system to clear the non-viable cells (104).

The cells are most often delivered by an intraportal infusion directly into the liver; however, cells also survive and retain their function when injected into the spleen which may be considered the best extra-hepatic organ for HT in animal models. Other sites include the thymus which has a good connective tissue network and adequate nutrient supply (105) and the peritoneal cavity for its large capacity and easy accessibility (99).

An important indication for HT is treatment of ALF which requires only temporary support until the liver regains its metabolic functions (106). The use of HT seems to be more effective with ALF than with chronic liver diseases because of the normal liver architecture and the better regenerative capacity of hepatocytes.

Hepatocyte like cells known as NeoHeps that are derived from terminally differentiated peripheral blood monocytes also seem to be very effective in treating experimental ALF (107). There are very few clinical trials published, none of which provide evidence to show that patients who received HT for ALF showed better survival (102).

In addition to limited availability, other problems in HT exist in that mature hepatocytes tend to de-differentiate *in-vitro* and that multiple transplantation procedures would be required to achieve meaningful liver repopulation (108). This problem may be bypassed through transplantation of immortalized hepatocytes based on the use of a clonal cell line that could be grown in culture and exhibit the characteristics of differentiated nontransformed hepatocytes. Such cells could potentially provide an unlimited supply of well-characterized, pathogen-free liver cells (109). However, it is also thought that important interactions occur between hepatocytes and other cells in the body and this is difficult to replicate in standard culture conditions. Attempts at developing sophisticated culture systems may help solve this problem (110).

Currently, HT cannot present a reliable alternative to LT but might be able to bridge a period needed for regeneration or to stretch the waiting time for a suitable liver donation (111). Proper randomized clinical trials are needed to identify the appropriate number of cells required for a successful recovery from liver failure, and

the rate of engraftment of these cells. Stem cells on the other hand present an interesting therapeutic promise owing to their pluripotency and unlimited supply.

1.3.4 What are Stem cells?

Stem cells were first described by Becker in 1963 when he discovered that a macroscopic splenic colony developed from only one cell when transplanted into heavily irradiated mice (112). Stem cells are undifferentiated primal cells common to all multi-cellular organisms possessing two important properties, which are self-renewal and unlimited progeny. When a stem cell divides, it gives rise to an asymmetrical progeny; one cell being a new stem cell with similar self-renewal properties and another more differentiated cell type lacking the tissue regenerating ability.

The division of stem cells is not restricted to one tissue type. The concept of plasticity where stem cells from one tissue may give rise to cell types of a completely different tissue has very important clinical implications both in the field of tissue regeneration and in cancer biology.

According to the stages of mammalian development stem cells can be divided into:

1) Totipotent cells that are produced from fusion of an oocyte and a sperm and are considered the ultimate stem cells as they can differentiate into all different types of human tissue.

2) Pluripotent stem cells which are descendants of totipotent cells and can differentiate into cells derived from the three major germ layers (113).

3) Multipotent stem cells can produce only cells of a closely related family of cells e.g. HSCs can differentiate into red blood cells, white blood cells, platelets (114).

There have been several debates on how to measure pluripotency and how to define it. The gold standard would be the ability of the cells to functionally replace all cell types in the developing organism by introduction of these cells into the blastocyst (115).

From the clinical point of view, it might be more relevant to classify stem cells into three categories:

1) Embryonic germ cells (EGC)

2) Embryonic stem cells (ESC)

3) Adult stem cells (ASC)

Embryonic germ cells

EGCs are stem cells that are derived from the primordial germ cells which occur in the gonadal ridge, and which normally develop into mature gametes (eggs and sperm) (116). EGCs have less proliferative capacity *in-vitro* than ESCs which has limited its experimental use (117).

Embryonic / Induced Pluripotent Stem cell derived hepatocytes

ESCs were first described more than two decades ago, when they were isolated from the inner cell mass of the developing murine blastocyst and grown in the laboratory

(118). ESCs have since been shown to be totipotent cells that can differentiate into cells of all lineages, including the germ line and trophoblasts (119). The potential clinical application of ESCs is confronted however, with many practical and ethical concerns (120). Equivalent to the ESCs in gene expression are the induced pluripotent stem cells (iPS) which have been generated from adult mouse fibroblast cells by retroviral transduction of four transcription factors initially and then only three (121). Furthermore, iPS cells have been generated from primary hepatocytes and gastric epithelial cells in mice (122). Recently, iPS cells have also been derived from human skin (123). IPS cells involve a reversal of the developmental process removing most epigenetic marks laid down during development resulting in a pluripotent cell that must be differentiated into mature cells for therapeutic applications (124). A pancreatic exocrine cell may be converted to a beta cell or an endocrine progenitor that produces all pancreatic endocrine cell types (124), or reprogramming a postnatal astroglia in the nervous system into a neuron or into a neural stem cell (125). However, the application of iPS cells in the clinic may also be a question of debate due to involvement of genetic manipulation that may lead to tumour formation in patients (115).

Adult bone marrow derived hepatocytes

There are less ethical issues with using ASCs, which are undifferentiated cells, found throughout the body to replenish dying cells and regenerate damaged tissue. ASCs are stable cells and very rarely switch from one cell type to another, the occurrence of which may have serious consequences like metaplasia and cancer (126). There are several advantages in using ASCs in organ regeneration as they are

immunocompatible as long as they are from autologous tissue, readily available and pose no ethical considerations.

The most readily available source of ASCs is the BM which contains 3 stem cell subpopulations, which are the Mesenchymal stem cells (MSCs), HSCs and endothelial progenitor cells (127). MSCs are clonogenic, non-hematopoietic cells that are capable of differentiating into multiple mesoderm-type cell lineages (128). They constitute about 0.01%-0.001% of bone marrow cells with the number being highest in neonates and decreasing with advancing age (129). When stimulated by specific signals, these cells can be released from their niche in the bone marrow into the circulation and recruited to the target tissues where they undergo *in situ* differentiation and integration and contribute to tissue regeneration and healing (130).

Because of their extensive differentiation potential, MSCs were among the first stem cell types to be introduced in the clinic (131).

Mechanism of action of MSCs

Two possible mechanisms might explain the conversion of MSCs into more mature, well differentiated cell types. Why a MSC chooses one path over another is not entirely understood but may be related to the ploidies of the cells constituting the organ receiving the stem cells. For organs containing cells of different ploidies which tend to form heterokaryons in severe organ injury like liver, pancreas and muscle, the external stem cells seem to fuse with the native cells and this has been evidenced by the expression of both donor and host genes in organs like the liver

(132). This may not be true, however in other organs like skin and lung, where terminal transdifferentiation seems to be a more likely mechanism (133).

MSCs are not immortal and there is a limit to the time in which they can be cultured *in-vitro*, but this problem has been addressed by transducing them with the human telomerase reverse transcriptase gene in order to extend their life span and provide a large number of cells for therapeutic applications (134). Also, other sources of MSCs have been explored including the human placenta (135), and umbilical cord (136). Adipose derived stem cells are equally capable of differentiation when compared to BM MSCs; moreover they are abundant in many easily accessible sites which can be obtained under a local anaesthetic in a procedure similar to liposuction which is a relatively non painful procedure (137).

1.3.5 Clinical applications of stem cells in regenerative medicine

Due to the inability to harvest or expand stem cells from most adult organs especially heart, liver and brain, the majority of human stem cell trials have focused on clinical applications of MSCs, HSCs or both, which can be easily obtained in sufficient numbers from peripheral blood, BM, umbilical cord blood and placenta (138). In the past few years, extensive research has been carried out on treating spinal cord injuries using different types of stem cells. BM derived stem cells were transdifferentiated into neural tissue and resulted in functional improvement when transplanted into injured spinal cords of paraplegic animals (139). There are some clinical trials that are running but sufficient data is still lacking.

Recent stem cell research points to the potential of cell therapy as a future treatment strategy for heart failure. Cell types used include multipotent progenitor cells, skeletal myoblasts, smooth muscle cells, fetal and embryonic cardiomyocytes, and both BM stromal and HSCs. A recent clinical trial suggests that transplanted BM derived progenitor cells injected into patients following acute myocardial infarction improved the cardiac function (140).

The introduction of islet cell transplantation in contrast to whole organ transplantation in treating diabetes mellitus has the benefit of being minimally invasive, however the success rate of the approach is limited, and a very high percent of the patients would still require insulin after one year (141), and furthermore, advances are hampered by the shortage in cadaveric donor material. Stem cells derived from the BM or reprogramming of the adult pancreatic cells into pancreatic progenitor cells which may be directed to secrete insulin may be possible through expression of certain transcriptional factors (142).

1.4 Stem cells and liver disease

Stem cells have been shown to improve liver functions and survival in liver diseases and present an interesting alternative or adjunct to LT and HT.

1.4.1 Embryonic stem cells

Differentiating ESCs into cells with hepatocyte properties that are metabolically active and immunologically inert is a major goal in the field of tissue regeneration.

When ESCs were injected in their undifferentiated state into mice, they resulted in teratomas that killed the animals (143). In addition, ESC derived hepatocytes were associated with improved survival when compared to undifferentiated ESCs in treating mice from ALF (144). From here, came the need to develop an *in-vitro* ESC differentiating system that would provide an unlimited source of functional hepatocytes without an increased risk of developing tumours.

There are several methods for inducing differentiation of undifferentiated ESCs. Embryoid bodies (EBs) which resemble embryos in the early stages of development are formed when the culture conditions are changed to allow the ESCs to form three-dimensional spherical structures (Fig.7), however, to induce differentiation, the leukemia inhibitory factor (LIF) which is essential to maintain the undifferentiated state needs to be taken out of the culture medium (145). ESCs that were cultured for more than 12 days, were capable of expressing both albumin and urea without the need for any additional growth factors at any stage of maturation, in addition, when cells were cultured for more than 9 days, they were not associated with teratoma formation when transplanted through the portal vein of mice (146). Other studies suggest that the addition of certain growth factors like Fibroblast growth factor, HGF and Oncostatin-M at different time points improve differentiation of ESCs into hepatocytes (147) and when transplanted, they significantly suppressed the onset of fibrosis and improved the survival rate among the recipient mice (148). Transplantation of undifferentiated ESCs also proved to be useful in treating CCL4 induced fibrosis in mice without resulting in tumour formation (149). Developing co-culture systems where ESCs are cultured with liver cells may present an alternative to adding exogenous growth factors. This has been established using hepatocytes (150) as hepatocytes secrete activin, which has been shown to induce endodermal

differentiation (151). However, activin alone cannot induce hepatocyte differentiation and in a more recent study it was used in combination with sodium butyrate and HGF for complete maturation of ESCs into hepatocytes (152).

Unfortunately, there have been no clinical trials using human ESCs to treat liver diseases in patients because utilization of human ESCs is still under ethical debates.

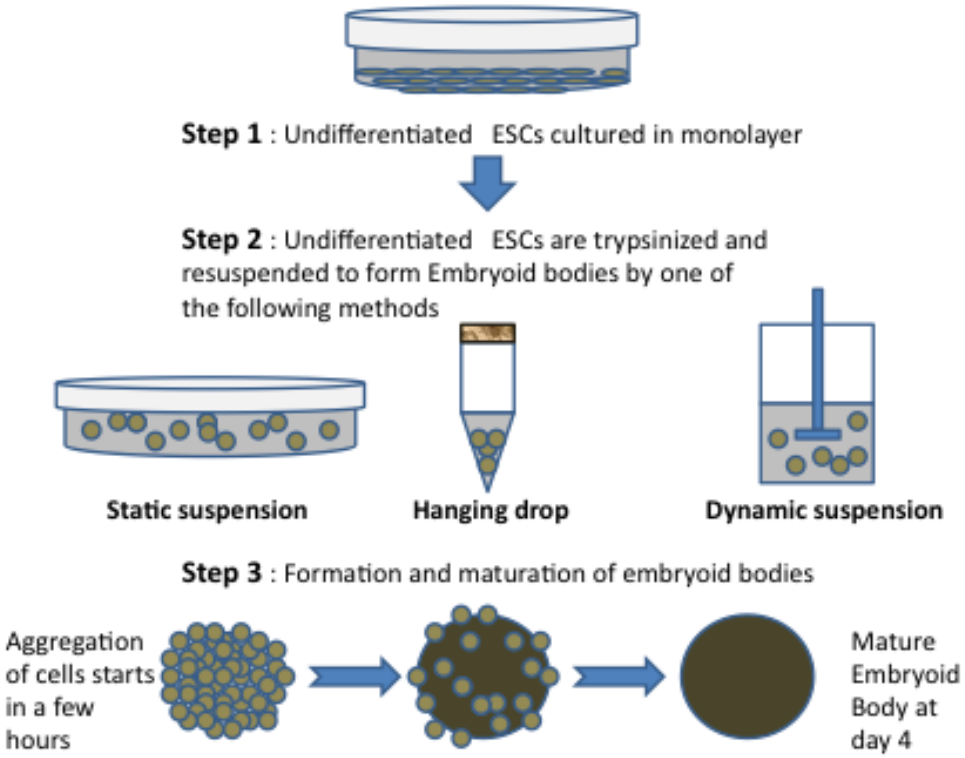

Figure 7 Steps of embryoid body formation from undifferentiated embryonic stem cells. The three most popular methods are illustrated. In all methods, the principle is induction of aggregation of cells into a ball like mass which will lose the undifferentiated state in the absence of LIF and differentiate into ectoderm, mesoderm and endoderm from which hepatocytes arise.

1.4.2 Bone Marrow Stem Cells (BMSCs)

Intensive research is being conducted to evaluate the efficacy of using MSCs as an alternative cell source to HT in treatment of liver disease. MSCs for transplantation ideally would be derived from the patient himself as this would avoid the problem of immunorejection. It has been shown, however, that even if BM derived MSCs were to be transplanted between different people, an exaggerated immunogenic response would not be elicited (153). This may be due to the lack of MHC molecules on MSCs (154), moreover, MSCs may exert an immunoregulatory effect through their inhibition of T-cell proliferation (155).

Experimental data

Several animal experiments have been conducted to understand the mechanism of action of BMSCs. Induced liver damage was an essential factor for cell recruitment and propagation in all experiments. In an experimental murine model, infusion of MSCs following lethally induced ALF restored metabolic functions of the liver through differentiation into hepatocytes (156). The reduced cell requirement and the rapidity of rescue from ALF suggested a paracrine proliferative effect of MSCs on the endogenous hepatocytes rather than direct differentiation into hepatocytes. The paracrine effects of MSCs have also been studied in different organs where they exerted protective effect on the heart (157) and kidney (158). Also, systemic infusion of soluble factors secreted from MSCs provided a survival benefit and prevented the release of liver injury biomarkers (159). Another more recent study showed that transfer of the genetic material from MSCs to resident hepatocytes following 70% hepatectomy in rats improved hepatocyte proliferation and suppressed apoptosis both *in-vitro* and *in-vivo* (160).

MSCs have also been used for improving liver regeneration in liver-transplanted rats with small for size syndrome. It has been proven that the addition of HGF promotes cell uptake in the recipient grafts with production of albumin, improved liver function and survival (161). Both HGF and Stromal Derived Factor-1 (SDF-1) have been shown to play an important role in recruiting and homing of MSCs to damaged liver tissue (162). SDF-1 is a potent chemokine that binds to its CXC receptor 4 on HSCs. Expression of this receptor is higher in BM HSCs when compared to peripheral blood HSCs and elevation of the plasma levels of SDF-1 was found to be responsible for mobilization of stem cells from the BM to peripheral blood down an SDF-1 gradient (163). In another study resident HSCs and CD-90+ BMSCs have been indentified in liver sections of rats where a small for size LT was conducted in an attempt to understand its effect on mobilizing stem cell populations. This also proves that both the liver and the MSCs contribute to liver regeneration (164).

Another theory is the mobilization of endothelial progenitors, which may be due to the increased serum level of VEGF following the vascular damage associated with LT. In animals, it has been shown that circulating $CD133^{+}$ and CD34+ cells are known to contribute to neo-angiogenesis after tissue ischemia and organ regeneration in animal models (165). There is definitely a correlation between the type of injury and the mobilization of different cell populations to rescue the liver. Whereas ischemia reperfusion liver damage associated with LT induced the extensive mobilization of several subsets of hematopoietic and endothelial BM stem cells, liver resection regardless of extent was a weaker stimulus to recruit significant numbers of BM cells despite the increase of the serum level of hematopoietic cytokine (166). SECs that are damaged in the setting of Oxaliplatin neoadjuvant chemotherapy originate from the BM and are key in liver regeneration (167), (95). A recent report

highlighted the role of BMSCs in SEC replacement following SOS in rats. It was shown that MCT not only damages the SECs in the liver but also suppresses the SEC progenitors in the BM leading to defective replacement. In addition, infusion of BM-derived $CD133^{+}$ replaced a considerable portion of the liver SECs with improvement in both structural and functional hepatic elements (168).

Clinical data

The stimuli for stem cell mobilization from the BM and the resulting population of progenitor cells seem to be an important key in designing future therapies. Granulocyte colony stimulating factor and certain chemotherapy protocols have resulted in a significant mobilization of progenitor cells that were used for BM transplantation (169). The same principles have been applied in trials to treat patients with chronic liver diseases. In one study, CD34+ cells were derived from the peripheral blood of nine patients with alcoholic liver cirrhosis. These cells were expanded *in-vitro* and injected into the hepatic arteries of the patients resulting in significant improvement of the Child-Pugh score (170). This might not be possible however in liver resections for malignant tumours as granulocyte colony stimulating factor might enhance tumour growth and increase the risk of splenic rupture which might add to the mortality of PLF patients (167). It is of interest that liver donors showed a great increase of the circulating CD 133+ cell population 12 hours after a partial hepatectomy when compared to one day prior to the procedure. The origin of these cells is not known, but might be the liver itself because no increase was noted in other surgical procedures. Moreover, these cells have the capacity to differentiate into hepatocytes *in-vitro* (171).

There have been only two clinical studies which were performed to assess the use of HSCs for PLF prevention. These studies were conducted on a small number of patients who were expected to undergo major hepatic resections for cancer. The infusion of the CD 133+ cells was combined with PVE which was important to induce a strong proliferative stimulus and to promote the uptake and engraftment of the cells. CD 133+ cells were derived from the BM and highly enriched *in-vitro* then injected into the left lobe of the liver through the portal branches with subsequent PVE of the right liver segments to expand the left hepatic segments. CT volumetric scans showed an increase in the proliferation rate of the left lobe when compared to the control group (172), (173). The main advantage of combining CD133+ cells with PVE would be to reduce the waiting time between PVE and the operation in patients with rapidly progressing tumours and to increase the liver reserve in patients with small left lateral liver segments.

1.5 Cell tracking

There is a lack of understanding of how stem cells behave *in-vivo* following transplantation with limited information on their capacity to migrate, engraft and differentiate in damaged tissue. Most studies were dependant on metabolic tests as indicators of successful organ regeneration and repair. It is essential, however to track the *in-vivo* fate of transplanted cells in addition to their functional capacity in order properly plan and optimize stem cell delivery techniques.

Stem cell tracking in humans is faced with several challenges due to safety and technical considerations. The most successful human cell tracking technique is using the magnetic resonance imaging for tracking cells labeled with iron oxide (174).

Advantages of this method include high resolution and good anatomical localization however, in the liver due to large endogenous iron stores; it may not be possible to accurately localize transplanted cells due to iron overload whether spontaneous or induced. This has been shown to be a barrier in pancreatic-islet cell tracking which home to the liver (175). Another disadvantage is the engulfment of the iron oxide particle by resident macrophages following cell death with limiting ability to distinguish between viable and non-viable cells (176).

Another promising modality is positron emission tomography imaging of cells radio labeled with glucose. It is a sensitive method with easy monitoring of biodistribution and cell quantification; however has a very short half-life which would not allow long term imaging (177).

Experimental animal imaging is far ahead when compared to clinical imaging. The introduction of green fluorescent protein (GFP) as a cell marker in 1994 allowed both direct and indirect visualization of transplanted cells in tissue using fluorescent microscopes and anti-GFP antibodies respectively (178). A major problem in *in-vivo* cell tracking using fluorescent markers is the background autoflourescence. This is due to light absorption by hemoglobin and melanin pigments interfering with adequate cell localization (179). GFP has an emission/excitation wavelength of 490/510 nm which is lower than the ideal optical window for precise cell visualization which is considered between 650-700 nm (179). This has lead to development of fluorescent dyes towards the near infra red (NIR) spectrum (650-900) nm where tissue has minimal interference with transmitted signal allowing accurate imaging of deep tissue (180).

Although optical imaging using fluorescent dyes is not yet permitted for clinical use, ICG which is FDA-approved and emits in the near infra red (NIR) spectrum has been used to label ESC derived cardiomyocytes *in-vitro* with no interference with cell function (181). This carries great hope for future application of optical imaging in clinical trials with accurate localization allowing proper assessment of cell engraftment in damaged organs and hence successful therapy.

2-Aims and experimental study design

The knowledge presented in the introduction formed the basis of the studies described in this thesis. From the overview of the literature it can be concluded that there are numerous possible research questions unanswered regarding the etiology, prevention and treatment of PLF. I decided to focus on two major topics during my research period. 1. The role of a novel semisynthetic flavonoid in prevention of sinusoidal obstruction syndrome which is a significant risk factor in PLF development. 2. The role of cell therapy in repopulating the liver in an ALF model. This is through developing an accurate cell tracking method with the possibility of both early and delayed monitoring. The two research topics will be described in separate sections in this thesis.

Research hypothesis:

1- Pre-treatment with the flavonoid monoHER would lead to a reduction in the portal pressure measurements when compared to the control group. This would be associated with improvement in both liver functions and the overall liver damage severity score.

2-A novel dual labeling fluorescence technique would allow real-time cell tracking with a view to differentiation and cell fate.

2.1 Section 1

2.1.1 Experiment 1

AIM

To establish a model of SOS in rats resembling the disease occurrence in patients following oxaliplatin administration.

Experimental design

The set-up of the experiment is depicted in Fig.8. Male Sprague-Dawley rats were divided into two groups (n=21). A model for SOS using a single gavage of monocrotaline (MCT) (MCT, Sigma Aldrich, St. Louis, MO) was used. Rats were gavaged with 160 mg/kg MCT in 0.5 mL dimethyl sulfoxide (DMSO) (182) and rats in the sham group received 0.5 ml DMSO only. After gavage, rats had free access to food and water. Rats were sacrificed 1, 2, 3 days after MCT gavage.

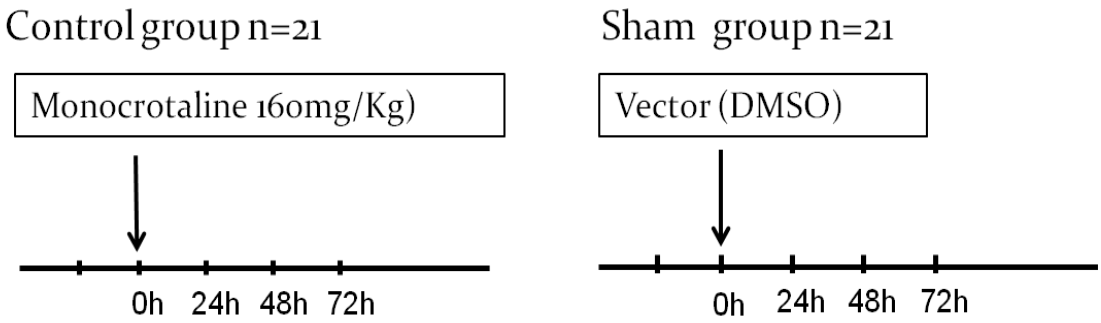

Figure 8 Schematic representation of the studied groups at the designated time points. 7 rats from each group were studied at 24, 48 or 72 hours following gavage with either MCT or vector.

2.1.2 Experiment 2

AIM

1- To evaluate the protective effect of a novel semi-synthetic flavonoid (monoHER) on development of SOS following MCT administration in rats.
2- To study the effect of monoHER and possible interactions with oxaliplatin/MCT in human CRC cell lines.

Experimental design

The set-up of the experiment is depicted in Fig.9. The animals were divided into two groups (n=21). A reproducible rat model for SOS using a single gavage of (MCT, Sigma Aldrich, St. Louis, MO) was used. Rats were gavaged with 160 mg/kg MCT in 0.5 mL dimethyl sulfoxide (DMSO) (182), rats had free access to food and water.

7-monohydroxyethylrutoside (monoHER) was kindly provided by the Department of Pharmacology and Toxicology, Maastricht University Medical Centre. The required amount of monoHER was dissolved in distilled water 36mM NaOH (pH 7.8-8). The experimental animals received monoHER 500 mg/kg i.p., starting 1 day before MCT treatment and continuing once daily up until sacrifice. Sham animals received sodium hydroxide intraperitoneally (i.p), in equivalent volume. Rats were sacrificed 1, 2, 3 days after MCT gavage.

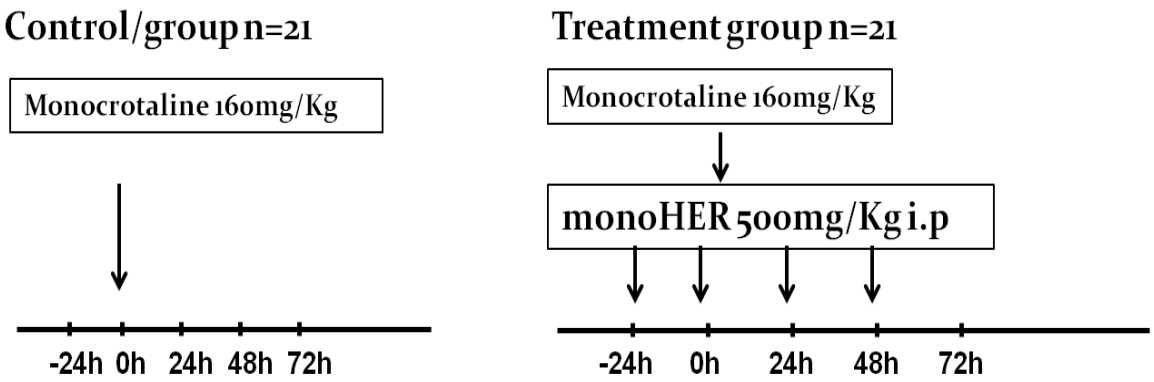

Figure 9 Schematic presentation of the two studied groups. Pretreatment with monoHER was started 24 hours before the MCT dose and was continued daily at the same time. (n=7) rats were sacrificed from each group at each time point.

2.2 Section 2

AIM

To develop a tracking system for monitoring transplanted cells and their distribution in an ALF model.

Experimental design

Forty male C57/BL6 mice (Charles River laboratories) at 5-6 weeks of age with an average weight between 20-25g were used for this study. The animals were allocated into 2 groups. Group 1 (n=20) with cell therapy and group 2 (n=20) with vehicle only. All animals received a single dose of APAP 300mg/Kg administered i.p (183). To ensure adequate dissolution, APAP was sonicated over night in a water bath at 42°C and the temperature was maintained till injection time. APAP administration was preceded by a subcutaneous injection (SC) of 10% dextrose in order to prevent mortality from severe hypoglycaemia (184). The SC injection of dextrose 10% was repeated every 6 hours during the first day of the experiment. At selected time points, the animals were killed by exsanguination (Fig.10). Time points were selected to have an optimal evaluation of ESC cell homing in organs using *ex-vivo* imaging and for immunohistochemistry (IHC) studies.

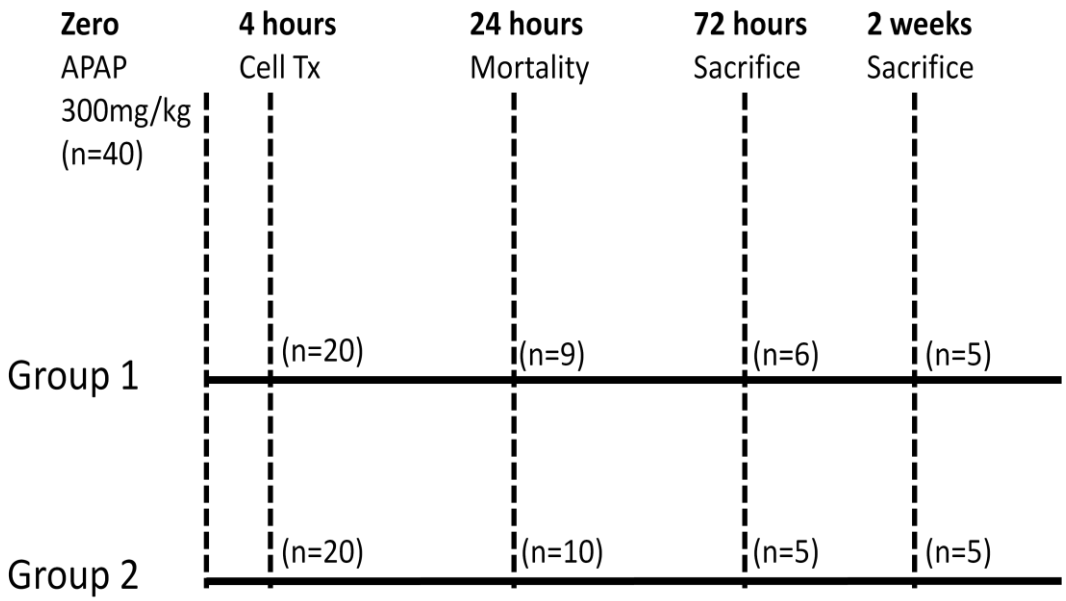

Figure 10 Experimental animal design. 40 mice were treated with APAP. The animals were then divided into 2 groups, cell therapy group= group 1 and control group= group 2. During the first 24 hours, 19/40 animals died due to the effect of APAP. Animals from both groups were then killed at 72 hours when the fluorescent signal started to decay and at two weeks when the signal could no longer be detected *in-vivo*.

3-Materials and methods

3.1 Animals

All animal experiments were conducted according to Home Office guidelines under the UK Animals and Scientific Procedures Act 1986. All animals were housed in the respective unit and given free access to standard rodent chow and water, serially weighed, with a light/dark cycle of 12 h (the dark phase extended from 1900 to 0700 h), at a temperature of 22–23 °C and approximately 50% relative humidity.

Male Sprague–Dawley rats (Charles-Rivers, UK), weighing 230–280 g, were obtained from the Comparative Biology Unit at University College London. Male C57BL/6 mice, weighing 20-25 g, were obtained from the Biological Services Unit at the Royal Free Hospital, University College London.

3.2 Methods

3.2.1 Measurement of portal pressure

Rats were anesthetized with inhalation of isoflurane (4% induction, 2.5% maintenance) and oxygen. The animals were placed in supine position and body temperature was maintained at 37°C using a heating pad. The abdomen was opened through a midline laparotomy and the portal vein was punctured and cannulated with a 25G needle without disturbing the surrounding structures. Portal pressure (PP) was continuously monitored and recorded using a pressure transducer, a pressure amplifier and a computer equipped with a data recording and analysis system (BIOPAC systems, Norfolk, UK). The average pressure over a five minute period was considered as the final PP.

3.2.2 Cell culture

Embryonic stem cells

Preparation of Coated Plates

T-75 flasks (VWR, UK) were coated with enough 10 mL 0.1% gelatin solution (Millipore, Co Durham, UK) to cover the whole surface and left at room temperature to dry after aspirating the excess solution. The minimum incubation period was 30 minutes.

Thawing of Cells

The vial of Milli Trace Constitutive GFP Reporter Mouse ESCs (1×10^6) was removed from liquid nitrogen and incubated in a 37°C water bath to thaw the cells. The cells were closely monitored until only a small ice crystal remained as maximum cell viability is dependent on the rapid and complete thawing of frozen cells. Also, important was not to vortex the cells to avoid cell killing. As soon as the cells were completely thawed, the outside of the vial was disinfected with 70% ethanol. Inside a laminar flow hood; a 1 mL pipette was used to transfer the cells to a sterile 15 ml conical tube. Care was taken not to introduce air bubbles. A 10 mL pipette was used to slowly add 9 ml of pre-warmed complete ESC media with 15% fetal bovine serum (FBS) and LIF (Millipore. ES-101-B) to the 15 ml conical tube in a dropwise fashion so as not to expose the cells to osmotic shock which might decrease the cell viability. The cell suspension was then gently mixed by slowly pipetting up and down twice. The tube was then centrifuged at 300 g for 3 minutes to pellet the cells. The supernatant was decanted to discard the DMSO cryopreservative. The cells were then resuspended in 10 ml of fresh ESC Media

containing 0.5 μg/mL puromycin was always added fresh and a concentration of 0.5 μ*g/mL* was obtained by adding 1μL of puromycin stock to 10 mL of ESC media. Cells were then plated in gelatin coated T 75 flask and incubated at 37°C and 5% CO2 in a humidified incubator.

On the next day, the medium was exchanged once and then every other day. When the cells were approximately 80% confluent, they were dissociated with Accutase cell dissociation solution (Millipore, Co Durham, UK) and passaged or alternatively frozen for later use.

Subculturing

The medium was carefully removed from the gelatin-coated T 75 tissue culture flask containing the confluent layer of ESCs. This was followed by applying 3-5 mL of Accutase solution to detach the cells (Millipore, Co Durham, UK). The flask was then incubated at 37°C for three minutes during which the flask was frequently checked for detachment of the cells. Complete detachment of the cells was confirmed by gentle tapping with the palm of the hand. Five mL of FBS containing media was added to the plate to neutralize the effect of Accutase. The dissociated cells were transferred to a 15 mL conical tube for centrifugation at 300 g for three minutes to pellet the cells. After discarding the supernatant, 1 mL of fresh medium containing puromycin was added and the cells were resuspended thoroughly and this was assisted by repeated gentle pipetting.

Cell viability and counting

Trypan blue was used to assess the cell viability. This dye cannot traverse the cell membrane of live cells as it is a bis-azo dye that is negatively charged at physiological pH. It can however pass through the cell membrane of dead cells staining them blue when inspected under microscope allowing determination of cell viability. For counting the cells, a haemocytometer chamber was used with a cover-slide. A mixture of 50 µl Trypan blue and 50 µl cell suspension was pipetted under the cover-slide and viewed under the inverted microscope. The total number of cells in four corner $1mm^2$ squares with a total volume of 10^{-4} cm^3 was counted. The average number of cells per square was then multiplied by 10^4 and the dilution factor to give the number of cells in 1 ml. The cells were then plated at a density of (4×10^5) and the remaining cells were frozen using freezing medium and stored in liquid nitrogen for future use.

Maintenance of undifferentiated state of ESCs

Undifferentiated C57/BL6 ESCs constitutively expressing GFP (Millipore, Co Durham, UK) were maintained in the undifferentiated state by using millitrace mouse ESC expansion medium (Millipore, Co Durham, UK) supplemented with 15% FBS and LIF. Puromycin was added to the media (0.5µg/ml) for selective growth of GFP-positive cells. Cells were cultured on 0.1% gelatine coated T-75 cell culture flasks till 80% confluence. The undifferentiated state of the ESCs was confirmed by alkaline phosphatase expression in more than 90% of the ESC colonies. Cell fixation was performed with 4% paraformaldehyde for 2 minutes

followed by incubation with a mixture of fast red violet, naphthol AS-BI phosphate solution and water in a 2:1:1 ratio in a dark room for 15 minutes.

3.2.3 Tracking of the transplanted cells using the *in-vivo* Imaging System (IVIS)

The IVIS® Lumina 2 (Caliper life sciences, Cheshire, UK) consisted of a charge coupled device (CCD) camera, an imaging chamber, the XFO-12 fluorescence equipment, and a preconfigured computer (Fig.11).

Figure 11 IVIS Lumina 2, computer and monitor.

In-vivo imaging allowed cell monitoring within small animals. The cells were tagged with fluorescent particles which emitted light following their excitation. The emitted light was detected by the CCD camera maintained in a cooled state to minimize electronic background and maximize sensitivity, working in a range of 400-950 nm wavelength (Fig.12).

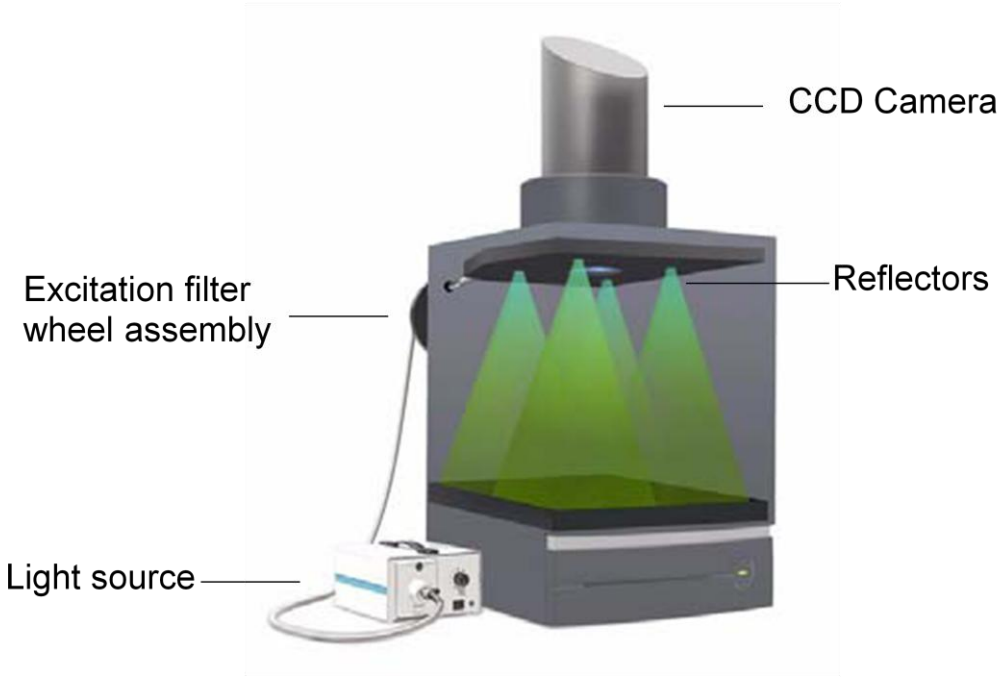

Figure 12 IVIS Lumina 2 and XFO-12 fluorescence equipment.

When the GFP +ve cells were used for *in-vivo* imaging, there was a considerable amount of autoflourescence which made it very difficult to identify the biodistribution of the transplanted cells. Autoflourescence is a fluorescent signal originating from substances other than the fluorophore of interest. The level of autoflourescence limits detection for fluorescent cells. Autoflourescence is primarily biological from the animal tissue with a smaller component arising from the

instruments. The GFP wave length is below that of haemoglobin and other animal proteins interfering with *in-vivo* cell tracking.

In order to eliminate the background fluorescent effect another dye was used to label the cells. This dye emits light in the NIR wavelength, which is much higher than the animal autoflourescence and therefore, made it possible to precisely track the transplanted cells in mice.

Dual labeling protocol

In order to achieve *in-vivo* tracking of the GFP expressing ESCs, the cells were labeled with the fluorescent lipophilic tracer 1, 1-dioctadecyl-3,3,3,3-tetramethylindotricarbocyanine iodide (DiR) (Invitrogen Ltd, UK). The excitation/ emission spectrum of DiR is in the NIR range (excitation 750 nm and emission 782 nm). After preparation of the stock solution, 5ml of cell-labeling solution was directly applied to 1ml cell suspension, mixed and incubated at 37°C for 20 minutes. The labeled suspension was centrifuged at 1500 rpm for 5 minutes and the cell pellet was resuspended in warm fresh media. This procedure was repeated twice to ensure complete removal of any unbound dye.

Cell preparation and transplantation

Following labeling with DiR, $5x10^6$ cells were used for injection in a single mouse, which is equivalent to approximately 7.5-8% of the mouse liver hepatocytes (185). The cells were suspended in 100µl of sterile Phosphate Buffer Solution (PBS) drawn

into a 1 ml syringe and kept on ice till the transplantation. Cell transplantation was performed 4 hours following treatment with APAP in mice. Under adequate anaesthesia and strict aseptic technique, a one cm incision was made in the left flank of the abdomen and the spleen was delivered outside the incision. The cells were injected into the spleen over a period of 5-minutes to prevent any loss of the cells due to the overflow. Following injection the needle was removed and fibrin glue was applied to the injection site to prevent bleeding and cell loss. After confirming haemostasis, the spleen was replaced back into the abdominal cavity and the abdominal wall was closed in single layer. The same procedure was performed for the control group with PBS only.

Tracking of the transplanted cells

The mice were anesthetized with inhaled isoflurane and placed into the IVIS chamber (Caliper life sciences, Cheshire, UK) and sequential images were acquired using the CCD camera at 30 minutes post transplantation, then at 3, 12, 24, 48 and 72 hours, and after one and two week intervals. Following sacrifice of the animals in groups at predetermined time periods, the spleen, liver, lung and kidney were retrieved and placed inside the IVIS and images were acquired. Data of the regions of interest of the illuminated cells were acquired to quantify the cell uptake in different organs. Three fluorescence filters (GFP, CY5.5 and ICG) were used to identify the filter with the least background autoflourescence. Data analysis was performed using the Living Image™ Software 3.0 (Caliper life sciences, Cheshire, UK).

GFP fluorescence

A Nikon fluorescence microscope (E501) was used for direct detection of GFP+ cells using the fluorescein isothiocyanate filter on frozen tissue sections.

3.2.4 Cell proliferation assay

Cell counting is possible using the haemocytometer; however for large scale cell quantification we required a more accurate method in order to measure the effect of monoHer on the cytotoxicity of oxaliplatin and MCT. The potential inhibition of the cytotoxic effect of oxaliplatin by monoHER was tested *in-vitro* in two different CRC cell lines (LoVo and LS174T, a gift from Prof D. Hochhauser, Cancer Research Institute, UCL). This is in addition to studying the protective effect of monoHer on human umbilical vein endothelial cell (HUVEC) lines. We used the CellTitre 96 Aqueous One Solution Reagent (Promega, Southampton, UK). It is an indirect colorimetric method involving the bioreduction of the 3-(4,5-dimethylthiazol-2-yl)-5-(3-carboxy-methoxyphenyl)-2-(4-sulfophenyl)-2H-tetrazolium inner salt compound (MTS) by cells into a coloured formazan product which is soluble in tissue culture medium. This conversion is presumably accomplished by NADPH or NADH produced by dehydrogenase enzymes in metabolically active cells. The quantity of formazan product as measured by the spectrophotometer at 490nm absorbance is directly proportional to the number of living cells in cell culture wells.

Procedure

1- The CellTiter 96® Aqueous One Solution Reagent (Promega, Southampton, UK) containing MTS and an electron coupling reagent (phenazine ethosulphate) was thawed.

2- Briefly, 2000 cells/well in a 96 well plate were incubated with increasing concentrations of (1) oxaliplatin 50-100-200 μM, (2) MCT 2-4-8 mM and (3) monoHER 25-50-100 mM or a combination of two of those. Following incubation for 48 hr, 20μl of CellTitre 96 Aqueous One Solution Reagent was added in each well and incubated for another 2 hr at 37°C in a humidified CO_2 incubator. The optical density was measured at 490 nm by means of LT-4000MS spectrophotometer (East Sussex, UK).

3.2.5 Blood and tissue sampling/handling and storage

Following the sacrifice of the animals at the designated time points, blood samples were taken from the abdominal aorta and liver tissue was cut from the median lobe at sacrifice. A part of the liver tissue was preserved immediately in liquid nitrogen and the remaining portion in 10% neutral formalin for downstream applications. Blood samples were drawn in pre-chilled tubes for EDTA-plasma, heparin-plasma and serum collection then centrifuged. Samples were stored at -80ºC until determination. Serum ALT was measured as a marker of liver damage using COBAS integra 400 biochemistry analyzer (Roche, New York, USA).

3.2.6 Analysis of Protein expression

IHC was used to examine protein expression in histological sections. Several steps were undertaken for routine histology/IHC: fixation, embedding, sectioning and staining.

Fixation with a variety of chemicals allowed tissue to be stabilized and preserved for future examination. A solution of formaldehyde (formalin) was routinely used, which was buffered and osmotically balanced to minimize shrinkage, swelling and cellular damage. Embedding converted tissues into a solid form to allow sectioning into thin slices for staining and IHC. As most cells are essentially transparent with little or no intrinsic pigment haematoxylin and eosin (H&E) staining was used to outline the morphological appearances and IHC for protein expression that were examined under a microscope.

Haematoxylin and eosin

Apart from a primary dye to identify the structure of interest, it is a common practice to counter-stain with a secondary dye to give a contrasting colour to the nucleus. H&E is based on this principle. Haematoxylin is a basic stain with purple colour and stains cell nuclei and ribosomes, while eosin is an acidic stain which stains collagen fibers, red blood cells, muscle filaments and mitochondria. The combination of these two dyes allows morphological features of tissue samples to be examined in detail under the microscope.

Histopathological examination was performed in a blinded fashion by two researchers. A conference microscope was used to reach a consensus regarding the

grading of tissue injury The degree of liver damage was quantified using a modification of the scoring system described by Rubbia-Brandt et al (186), including sinusoidal dilatation (scores; 0,1,2,3), perisinusoidal haemorrhage (scores; 0,1), peliosis (scores; 0,1), hepatocellular necrosis (scores; 0,1,2,3) and inflammatory cell infiltration (scores; 0,1,2,3).

Mononuclear inflammatory cells were counted in three most densely populated areas in high power fields (x400) and the average number of cells was considered as the number of cells per high power field.

Immunohistochemistry

The Principle:

IHC is an established method used in clinical diagnosis and research allowing localization and visualization of tissue and cell antigens. The principle involves attaching the primary antibody to the tissue antigen to be localized. The bound antibody is then detected by a variety of methods.

Some antigenic sites become inactive during the formalin fixation and heat treatment during the paraffin-embedding process. This occurs due to cross-linking between lipoprotein membranes and extracellular material with fixatives forming a barrier preventing antibodies from binding the antigens. It is important therefore to unmask the antigen through an antigen retrieval step to maximize the antigen-antibody reaction. The two most important factors for effective antigen retrieval are the heating conditions and the pH.

Non specific staining is also common in IHC and inhibition of the non-specific peroxidases is essential to avoid false positive results. Therefore blocking of the endogenous active peroxidases highly expressed in the liver before adding the peroxides labeled antibody would eliminate any possibility of background staining due to tissue peroxidases. This could be achieved by adding hydrogen peroxide to deplete the endogenous peroxidases.

Following this step, the primary antibody is applied which might be either monoclonal or polyclonal. Monoclonal antibodies are derived from a clone of single cells whereas polyclonal antibodies consist of several antibodies generated *in-vivo* following treatment with the antigen. The advantage of monoclonal antibodies is that they are more specific however less robust and more expensive than polyclonal antibodies.

This is followed by incubation with the secondary antibody and development of the brown colour using 3,3' –diaminobenzidine tetrahydrocholride (DAB).

The procedure:

1-Three to five μm sections of tissue were cut and paraffin was removed by putting the slides in the oven for one hour to preheat and then four changes of fresh xylene each for 5 minutes.

2- Sections were rehydrated by using:

- One change of absolute ethyl alcohol, each for 5 minutes.
- One change of 90% ethyl alcohol, each for 5 minutes.

- One change of 80% ethyl alcohol, each for 5 minutes.
- One change of 70% ethyl alcohol, for 5 minutes.

3-The slides were washed in PBS for 5 minutes

4-For antigen retrieval:

a) Plastic container was filled with sufficient citrate buffer (pH 6) (Dako, Cambridgeshire, UK) and placed in a microwave oven to bring the solution to boiling.

b) The slides were placed in the antigen retrieval solution and placed in microwave oven to boil for 10 minutes at 800W.

c) Container was removed from the oven and allowed to cool for 20-30 minutes to reach the room temperature.

5- Slides were placed in PBS for 2 minutes three times.

6-Excess liquid was removed by careful tapping off the edge of each slide on paper towels. It was important to dry the slides around sections using gauze pad without drying sections themselves.

7-Endogenous peroxidase activity was blocked for 30 min with 3% hydrogen peroxide.

8- Slides were placed in PBS and washed for 2 minutes x three times.

9-Excess liquid was removed by careful tapping off the edge of each slide with tissue paper.

10-The sections were incubated at 4°C overnight with primary antibodies; polyclonal rabbit anti-GFP (1:10, Millipore), and anti-albumin antibody (1:1000, Abcam).

11- The slides were washed with PBS Tween twenty (0.05%) three times each 2 minutes.

12-The secondary antibodies were added and incubated for 30 minutes.

13-The slides were washed with PBS Tween twenty (0.05%) three times each 2 minutes.

14-The DAB solution was prepared by mixing up 1 ml of substrate solution (Substrate in DAKO kit) with 20µL of buffer (Buffer for DAB and chromagen in DAKO kit) (Dako, Cambridgeshire, UK). The solution was mixed well and applied to the sections.

15-The slides were washed with tap water for 5 minutes.

16-Nuclear counter staining was done using Mayer's Haematoxylin (Sigma, UK) for 1-3 minutes.

17- The slides were washed with tap water for 20 minutes to remove excess haematoxylin.

18- After removing the excessive water, the cover glass slips were mounted with Aqueous mounting media (Dako, Cambridgeshire, UK) using a pair of forceps onto the tissue slides. Proper care was taken not to entrap any air bubbles between the cover glass and the tissue sections. The slides were left to dry for 30 minutes and then visualized under the microscope.

3.2.7 Electron microscopy (EM)

EM allows obtaining images at a much higher resolution than those obtained by light microscopes. EMs use beams of electrons to examine specimens and the interaction of the electrons with the specimen gives information on morphology of the specimens. The EM consists of an electron source, an anode, magnetic lenses, apertures, specimen stage and image recording system all of which operate in a high vacuum.

Preparation of the specimen for EM

Perfusion fixation of total liver in situ

Following anesthetizing the animal and opening the abdominal cavity the intestines were moved to the left side of the abdominal cavity and covered with saline soaked surgical gauze. The hepatic artery was ligated at the hilum with a 7-0 silk and divided. The portal vein was then exposed and a 23 gauge needle connected with a catheter and syringe was used to puncture the portal vein for perfusion. Perfusion was done with glutaraldehyde and the vena cava was incised to allow the infused fluid to escape. Hereafter the liver would change its consistency to firm or hard and its colour to yellow. The perfusion was completed in 5 minutes and small pieces of well perfused liver lobes were placed in the fixative solution. A razor blade was subsequently used to cut 1-mm slices of liver tissue without putting any pressure on the tissue while cutting. Tissue slices were covered with glutaraldehyde all the time and several strips were cut for transmission electron microscopy (TEM) (1 mm × 1

mm × 1 mm) blocks or (1mm × 1 mm × 5 mm) strips for scanning electron microscopy (SEM). The samples were then processed for EM examination.

Procedure for EM

PROCESSING TISSUE FOR SCANNING ELECTRON MICROSCOPY

The Procedure:

The samples were fixed in 1.5% glutaraldehyde for a minimum of 2 hours, then washed with several changes of PBS (Oxoid, Basingstoke, UK) and postfixed using 1% osmium tetroxide/1.5% potassium ferricyanide for 12 hours.

Samples were washed with distilled water and dehydrated through graded acetone (30%, 50%, 70%, 90% and 100%, HPLC grade 2 x 15 minutes each). After dehydration the specimens were transferred to tetramethylsilane for 5 minutes and then allowed to air dry.

They were then attached to aluminium stubs with double sided sticky tabs (TAAB, Berkshire, UK) or carbon dag and then coated with gold using an SC500 sputter coater (EMScope, UK) before being examined and photographed using a Philips 501 SEM **(**FEI UK Limited, Cambridge, UK**).**

Preparation of tissue for transmission electron microscopy

The Procedure:

Tissue was fixed in 1.5% paraformaldehyde/1.5% glutaraldehyde in phosphate buffer, washed with phosphate buffered saline (Oxoid, Basingstoke, UK) and postfixed using 1% osmium tetroxide / 1.5% potassium ferricyanide, washed with distilled water and dehydrated using graded alcohols 30%, 50%, 2 x 70% and 3 x 100%, followed by infiltration with 50% alcohol / 50% Lemix (TAAB, Berkshire, UK) epoxy resin mixture overnight. The next day tissue was infiltrated with 100% Lemix resin for a minimum of 6 hours, followed by a second day of infiltration with 100% resin then polymerised at 70^{o} C overnight.

Sections were cut on a Reichert-Jung ultracut E microtome (Reichert, NY, USA) and collected on 300HS, 3.05mm copper grids (Gilder, Manchester, UK). The sections were stained with saturated uranyl acetate in 50% ethanol (TAAB, Berkshire, UK) and Reynold's lead citrate. Sections were viewed and photographed using a Philips 201 TEM **(**FEI UK Limited, Cambridge, UK**).**

Reagents for EM

Glutaraldehyde (20mls 20% paraformaldehyde (VWR, Dorset, UK) + 16mls 25% glutaraldehyde (TAAB, Berkshire, UK) + 59mls PBS (Oxoid, Basingstoke, UK).

Osmium tetroxide 1% osmium tetroxide (VWR, Dorset, UK) + 1.5% potassium ferricyanide (VWR, Dorset, UK) in PBS (Oxoid, Basingstoke, UK).

Toluidene blue stain 1% toluidine blue (Raymond Lamb, East Sussex, UK) with 0.2% pyronine (Raymond Lamb, East Sussex, UK) in 1% sodium tetraborate (VWR, Dorset, UK).

*Reynolds lead citrate (*Dissolve 1.33g lead nitrate (VWR, Dorset, UK) in 15mls distilled water and 1.76g sodium citrate (VWR, Dorset, UK) in 15mls distilled water,

mixed solutions were dissolved and the resulting precipitate mixed with 8 ml of 1M sodium hydroxide (VWR, Dorset, UK), made up to final volume of 50ml.

*Lemix epoxy resin (*Lemix A (25mls) + Lemix B (55mls) + Lemix D (20mls). Poured into plastic resin bottle and added 2 ml of BDMA, and mixed well.

4-Development of a model of sinusoidal obstruction syndrome in rats

4.1 Background

The treatment of CLM has been completely revolutionized by the introduction of oxaliplatin and irinotecan based chemotherapy. They play an integral role in downstaging advanced liver tumours rendering them more amenable to surgical resection. Moreover, these neoadjuvant chemotherapeutic agents also keep the systemic disease under control and identify the patient groups who would not benefit from surgery based on the progression of the disease during chemotherapy (187).

Although these drugs have become the standard of care in this setting; oxaliplatin has been strongly associated with the development of sinusoidal injury in the non-neoplastic liver. This well recognized side effect of oxaliplatin was first described by Rubbia-Brandt when 78% of post-chemotherapy hepatectomy specimens receiving oxaliplatin were found to demonstrate pathological evidence of striking sinusoidal damage (188).

The sinusoidal changes occurring in the liver following oxaliplatin chemotherapy are pathologically similar to the SOS which is a well known complication of myeloablative therapy in patients receiving HSC transplantation for conditions like aplastic anaemia and inborn errors of metabolism (189).

Patients who develop SOS due to oxaliplatin present clinically with manifestations of portal hypertension including hepatomegaly, ascites, splenomegaly and increased bilirubin levels. Portal hypertension can result in opening of the porto-systemic collaterals to decompress the portal system leading to haemorrhoidal and oesophageal varices which may rupture and cause fatal haemorrhages. Also the blood transfusion requirements for these patients during liver resections were higher when compared to patients receiving other regimens or no chemotherapy with a

higher postoperative complication rate and a prolonged hospital stay (64), (190), (191).

In order to study the pathological effects of SOS and explore the possible therapeutic options to treat this serious overlooked condition it was essential to establish a reliable and reproducible animal model. Although oxaliplatin produces deleterious effects in human liver, similar effects could not be reproduced in rats. MCT is a pyrrolizidine alkaloid toxin that is known to induce hepatic and cardiopulmonary toxicities. It produces hepatic fibrosis and sinusoidal dilatation following ingestion due to its conversion to the active metabolite monocrotaline pyrrole (MCT-P) through the cytochrome P450 system (192). It has been extensively studied in the development of an animal model of pulmonary hypertension through its primary effect on the vascular bed (193). Also, Deleve et al used MCT to induce an animal model of liver sinusoidal injury similar to that occurring following HSC transplantation (182).

In the present study we investigated the effect of MCT in inducing SOS in rat liver with special emphasis on measuring the functional endpoint of PP changes in the animals that received MCT compared to the control group. This was the primary end point as elevation of PP is central in the pathogenesis of oxaliplatin induced SOS. Secondary endpoints included measurement of liver transaminases reflecting the degree of liver damage and examination of the histological sections of the liver both with light and EM. IHC was performed to study the expression of MMP. MMPs are endopeptidases that degrade collagen IV in the extracellular matrix of the basement membrane, and specifically MMP-2 and 9 are reported to be upregulated following SEC damage (194).

4.2 Results

4.2.1 Portal pressure measurements

Rats treated with MCT had significantly higher PP measurements when compared to the control group at all studied time points. The PP measurements were significantly higher in rats receiving MCT as early as 24 hours (9.37±0.99 vs. 6.50±0.70) mmHg MCT vs. control respectively (p=0.0001). The PP measurements in the MCT group also remained significantly higher than in the control group at 48 hours (10.19±1.30 vs. 7.46±1.09) mmHg (p=0.005) and at 72 hours (11.36±2.97 vs. 6.63±0.51) mmHg (p=0.016) MCT vs. control respectively (Fig.13).

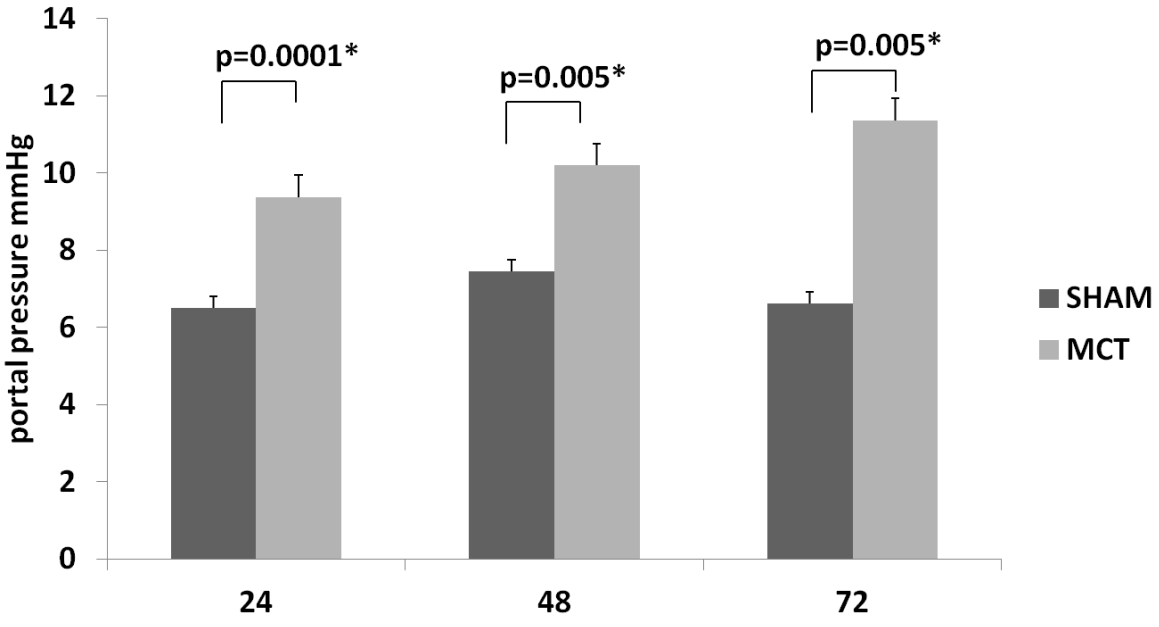

Figure 13 Portal pressure measurements in MCT treated rats compared to the control group. MCT administration caused a significant rise in portal pressure measurements when compared to the control group at all designated time points.

4.2.2 Biochemical evidence of monocrotaline induced liver injury

No mortality occurred in either group, however in the MCT treated rats there was blood-tinged ascitic fluid in the abdominal cavity which was not present in the control group at the time of sacrifice.

Serum ALT levels were significantly higher in MCT treated rats when compared to the control rats at 48 hours and 72 hours reflecting the toxic effect MCT on hepatocytes (48h: 253.35±171.70 IU/L vs. 42.20±3.08 IU/L p=0.034, 72h: 311.91±163.64 IU/L vs. 46.17±4.34 IU/L p=0.002) MCT vs. control respectively. There was no significant difference between both groups at 24 hours (24h: 79.80±47.27 IU/L vs. 42.57± 6.89 IU/L p=0.109) MCT vs. control respectively (Fig.14).

Also, there were significant differences in serum bilirubin levels when compared between both groups at 48 and 72 hour following gavage (48h: 1.96± 0.28 vs. 1.01± 0.55 p=0.016, 72h: 5.37±2.70 vs. 1.16±0.35 p=0.01) MCT vs. control respectively, however, no significant differences could be detected at 24 hours (24h: 2.00± 0.69 vs. 1.27± 0.15 Mmol/L p=0.054) MCT vs. control respectively (Fig.15).

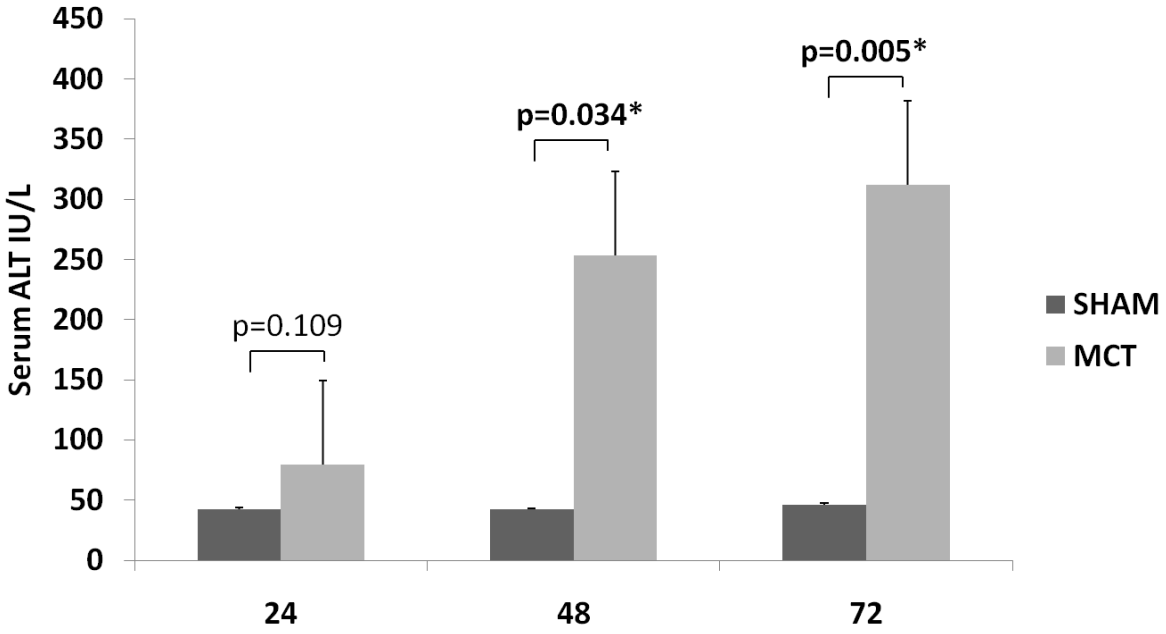

Figure 14 Serum ALT measurements in both groups. Serum ALT was significantly higher in the MCT group at 48 and 72 hours, however no significant difference could be detected at 24 hours.

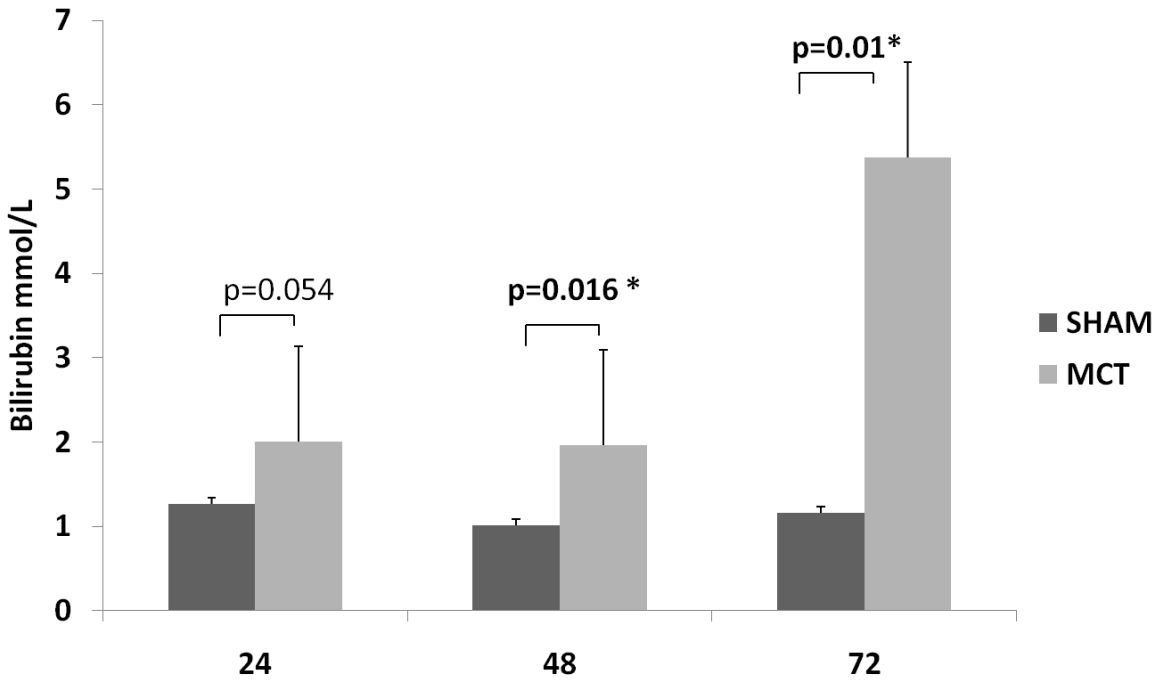

Figure 15 Serum bilirubin measurements in both groups. Serum bilirubin levels were significantly higher in the MCT group when compared to the control group at 48 and 72 hours but not at 24 hours.

4.2.3 Histological evidence of monocrotaline induced liver damage

Light microscopic examination revealed normal large polygonal hepatocytes with prominent round nuclei and eosinophilic cytoplasm, and well spaced hepatic sinusoids arranged in-between the hepatic cords. The histology of the control group was consistent at different time points.

In the MCT group, extensive sinusoidal dilatation with separation of the hepatic cords could be detected as early as 24 hours following MCT gavage. This was associated with inflammatory cell infiltration which was much denser than in the control group (Fig.16). At 48 hours, severe congestion was evident in the MCT treated group with inflammatory cells within the sinusoids (Fig.17). Massive areas of hepatic necrosis associated with inflammatory cell infiltration were evident at 72 hours predominantly in the centrilobular regions of the liver with detachment of the endothelial lining of the central vein (Fig.18).

However, treatment with Oxaliplatin did not produce any significant histological changes that were consistent with SOS when compared to the MCT group at of the time points (Fig.19).

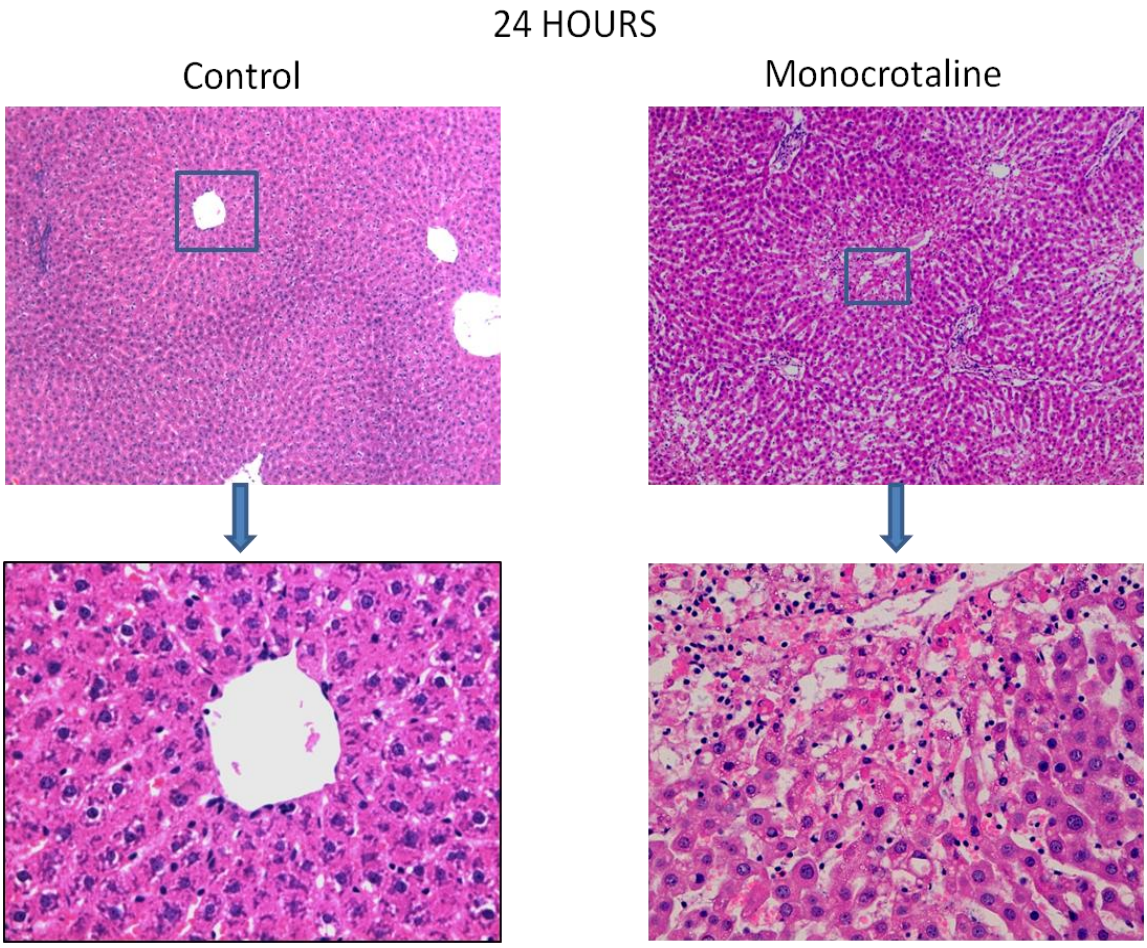

Figure 16 Histological examination of the liver in both studied groups at 24 hours. Normal appearance of the liver in the control group with no dilatation of the hepatic sinusoids following gavage with DMSO (left). The effect of MCT on the liver could be seen in the form of sinusoidal dilatation that was extensive all over the liver (right low magnification) and showing the ballooning of the sinusoids and the presence of inflammatory cells within the sinusoidal spaces (right high magnification) Low magnification x100, high magnification x400.

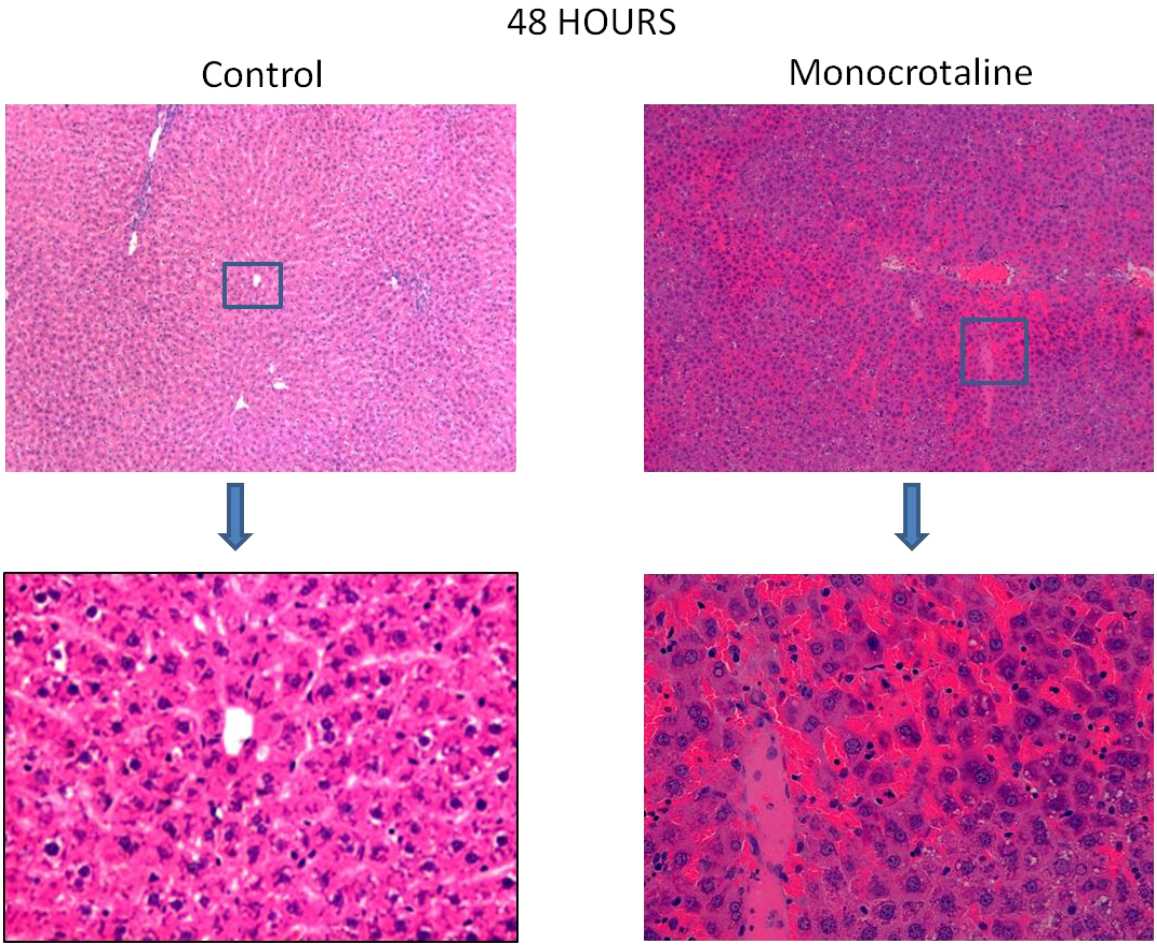

Figure 17 Histological examination of the liver in both studied groups at 48 hours. No liver damage could be detected at 48 hours in the control group (left); however in the MCT group there was severe congestion that was extensive over large areas of the liver (right low magnification). This was associated with areas of peliosis and beginning of necrosis in some areas of the liver (right high magnification). Low magnification x100, high magnification x400.

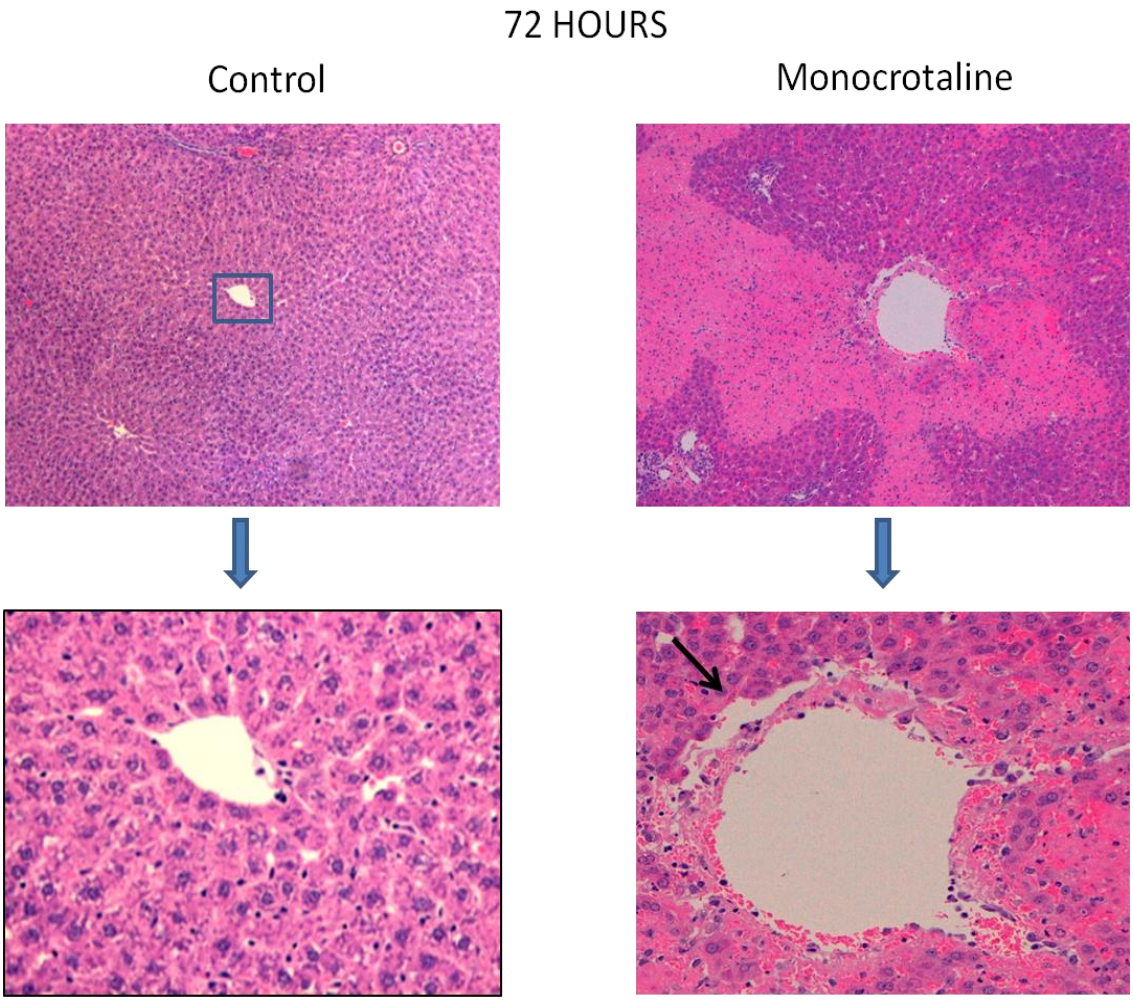

Figure 18 Histological examination of the liver in both studied groups at 72 hours. No damage could be detected in the control group at 72 hours (left). The liver in the MCT group shows extensive areas of coagulative necrosis in the centrilobular regions of the liver (right) with damage of the endothelial lining of the central vein and its separation from the basement membrane. (Right high magnification, solid arrow). Low magnification x100, high magnification x400.

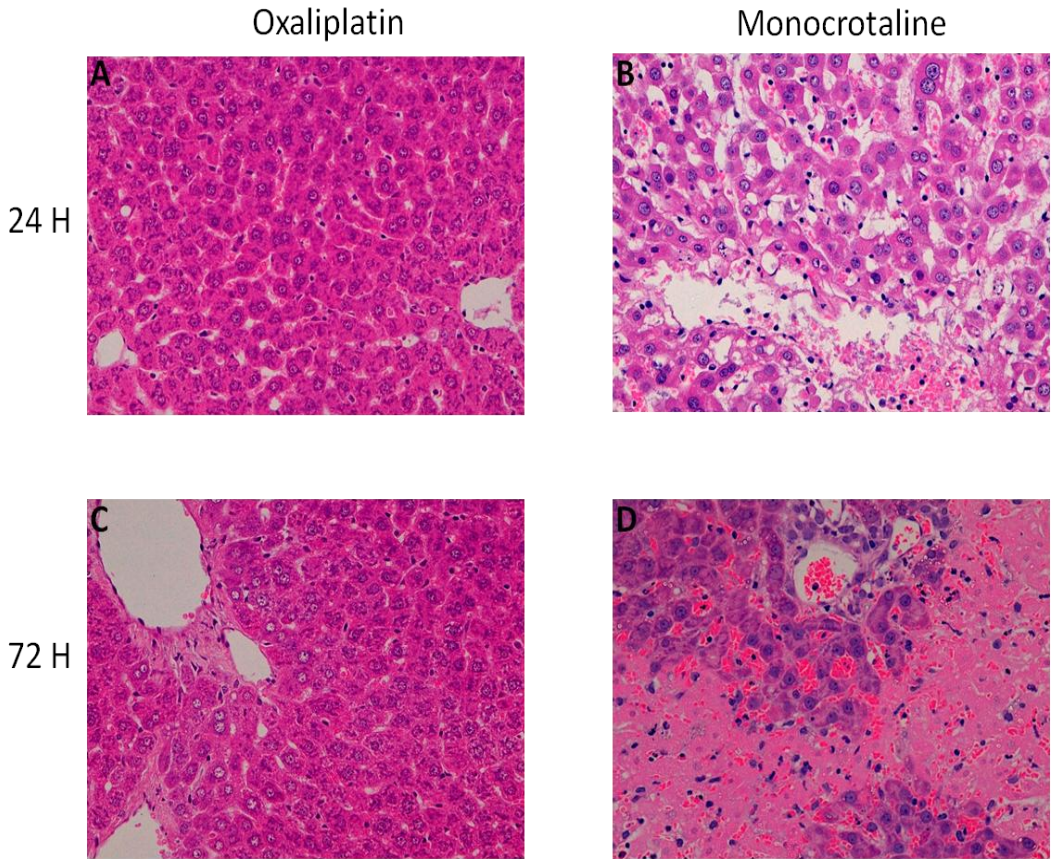

Figure 19 Histological changes in the liver following oxaliplatin and MCT treatment. A very mild degree of SOS could be seen in the livers of oxaliplatin treated rats at 24 hours when compared to MCT treated rats at 24 hours (A,B). There was no progression of liver injury with time in the oxaliplatin group. At 72 hours oxaliplatin treated rats lacked hepatocellular necrosis and inflammatory cells unlike in the MCT group which progressed from sinusoidal dilatation at 24 hours to frank necrosis at 72 hours (C,D).

4.2.4 Electron microscopic examination of Monocrotaline induced liver damage

EM was used to assess details that could not be detected using light microscopy. The EM study was conducted on liver samples preserved from both the control and the MCT treated rats at the 72 hour time point. This time point was chosen as it corresponded to the highest PP and enzymatic levels when compared to the other time points. On SEM it was possible to detect disruption of the sinusoidal endothelial lining and congestion of the sinusoids with erythrocytes in the MCT treated rats but not in the control group (Fig. 20A,B). Also an increase in the size of the fenestrae with gap formation was noted in the MCT treated group (Fig.20C,D).

On TEM gaping of the SECs was evident in the MCT group with dilatation of the fenestrae. The sinusoidal endothelial lining was intact in the control group with normal fenestrae size when compared to the MCT group (Fig.21). Detachment of the SEC lining from the basement membrane and disruption of the space of Disse was evident in the MCT treated group and not in the control group (Fig.22B). The detachment of the SECs obstructed the lumen of the sinusoid and allowed direct contact between the erythrocytes and hepatocytes inducing hepatocyte damage (Fig.22C). Also, hepatocytes from MCT treated group showed more glycogen depletion when compared to the control group (Fig.21,22).

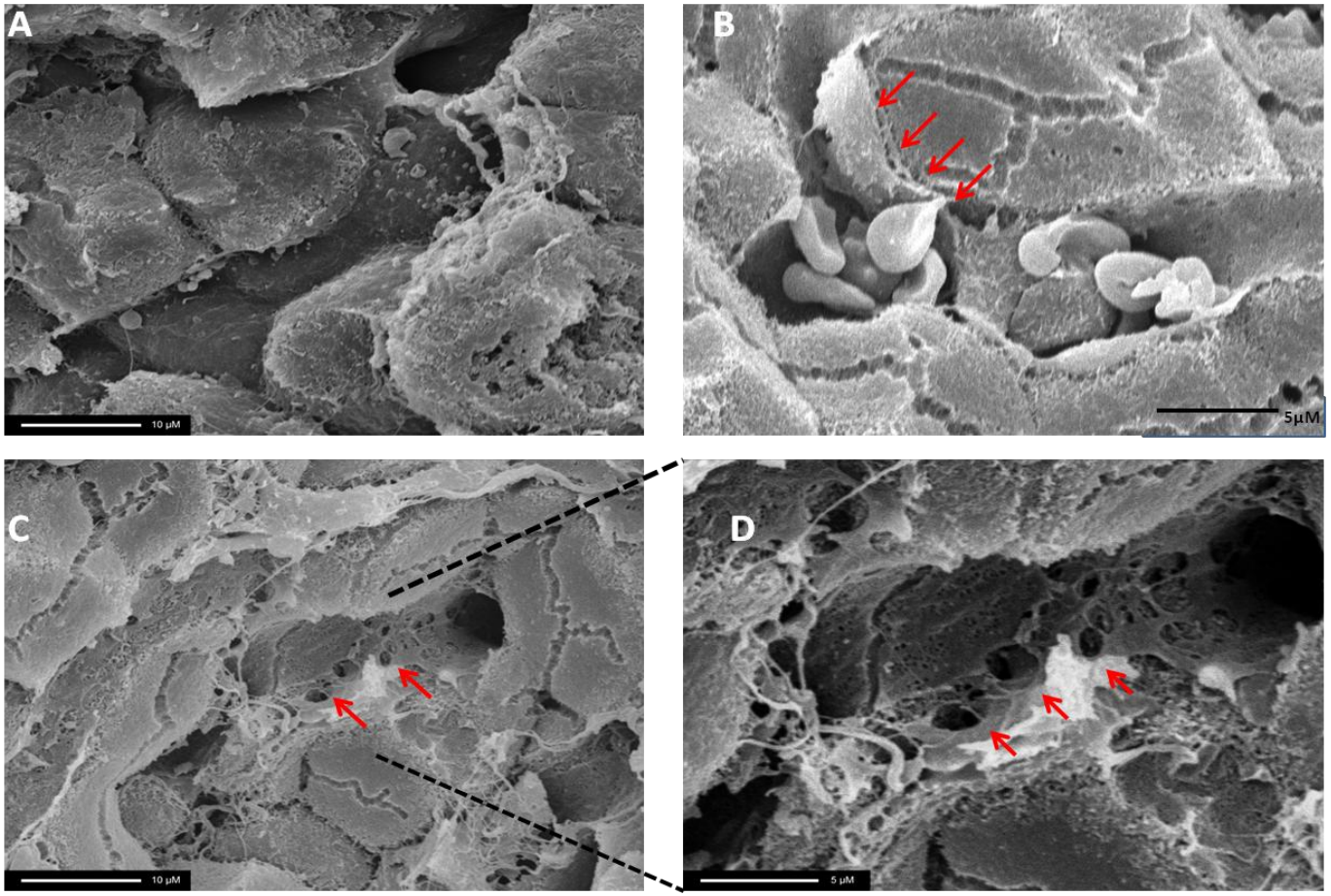

Figure 20 Scanning Electron Microscopy images of both control and MCT treated rats at 72 hours following gavage. The sinusoidal endothelial lining is intact in the control group receiving DMSO only with no detachment of the sinusoidal lining or gap formation (A x2500). In the MCT treated rats, there is detachment of the sinusoidal endothelial lining occluding the blood flow in the sinusoid and congestion with erythrocytes (B x5000). Dilatation of the fenestrae with formation of large gaps that develop in the sinusoidal lining of MCT treated rats (C x2500, D x5000 arrows pointing to gaps in sinusoids).

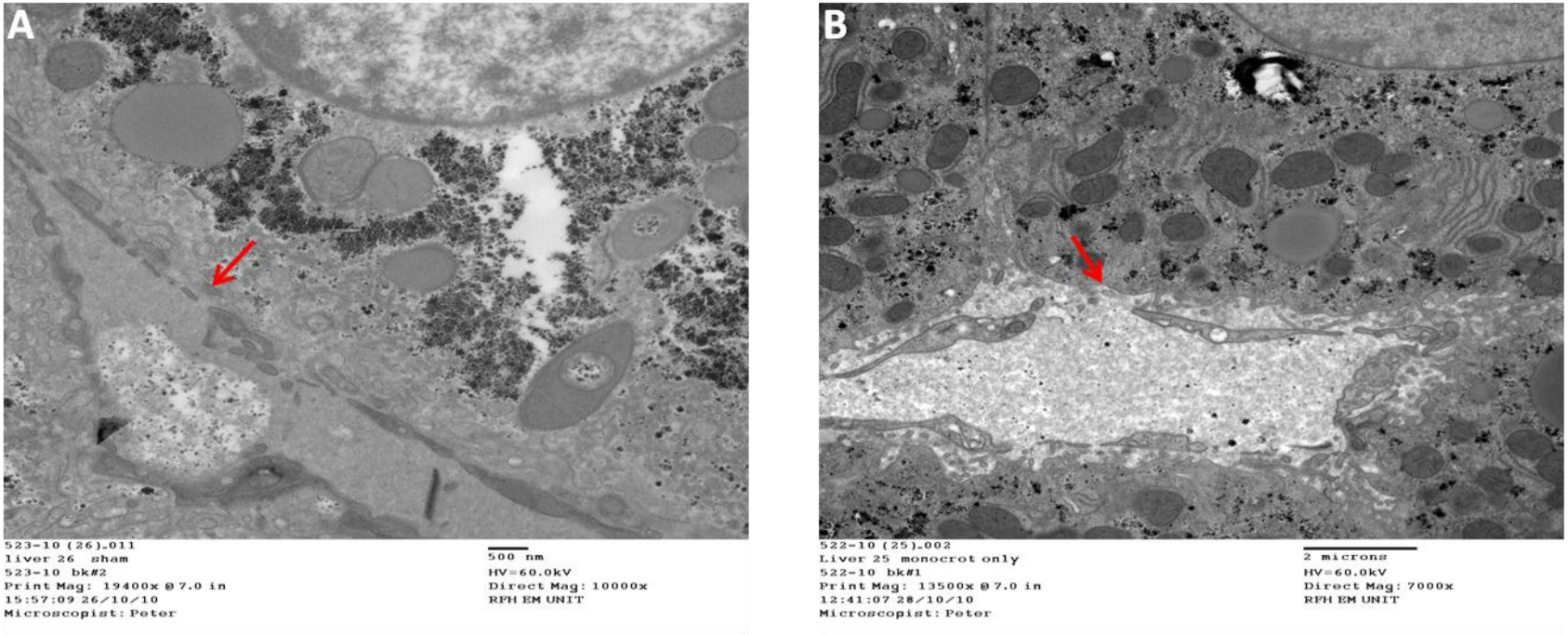

Figure 21 Transmission Electron Microscopy images of the sinusoidal lining in both the control and MCT treated groups. The SEC lining is intact and basement membrane with normal sized fenestrae (Arrow) and abundant glycogen in the control group (A). There is ballooning and detachment of the SEC lining from the basement membrane with an increase in the size of the fenestrae due to gaping of the SECs (Arrow). This is also associated with glycogen depletion (B).

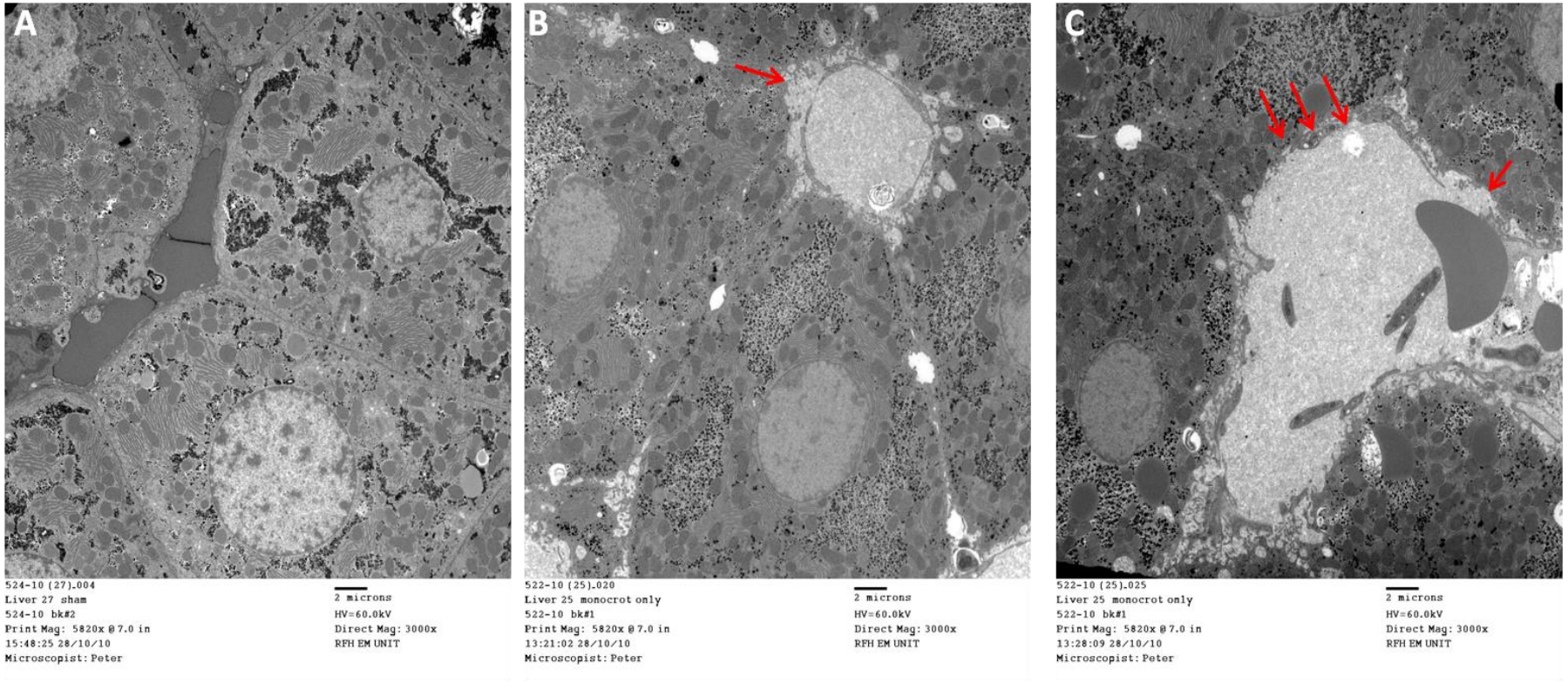

Figure 22 Transmission Electron Microscopy images of the sinusoids in both the control and MCT treated groups. Dilatation of the sinusoid with detachment of the SEC lining from the basement membrane with disruption of the space of Disse could be clearly seen in the MCT group (B). Separation of the SECs which are floating in the sinusoid and obstruct the lumen leading to dilatation and direct contact of erythrocytes with hepatocytes that have lost their SEC lining with loss of hepatocyte microvilli (arrow) (C). The sinusoids appear normal in the control group following DMSO gavage with abundant glycogen compared with the MCT group and intact SEC lining (A).

4.2.5 Role of Matrix Metalloproteinases in development MCT induced SOS

The role of MMP 2 and 9 was studied to determine their possible role in the pathogenesis of SOS. IHC was performed on liver samples with anti-MMP-2 and anti-MMP-9 antibodies. The basal expression of MMP-9 was slightly higher than that of MMP-2 in the control group (Fig.23A,B); however following MCT gavage MMP-9 expression was markedly higher than MMP-2 expression which did not seem to increase in response to MCT toxicity (Fig.23C,D).

The extent of MMP-9 expression was similar at different time points following MCT ingestion. MMP-9 was mainly localized in SEC lining and the inflammatory cells at 24 hours (Fig.24B,C). At 72 hours, in addition to expression in the SEC lining, MMP-9 was also expressed in hepatocytes in the vicinity of necrotic areas (Fig.24E,F).

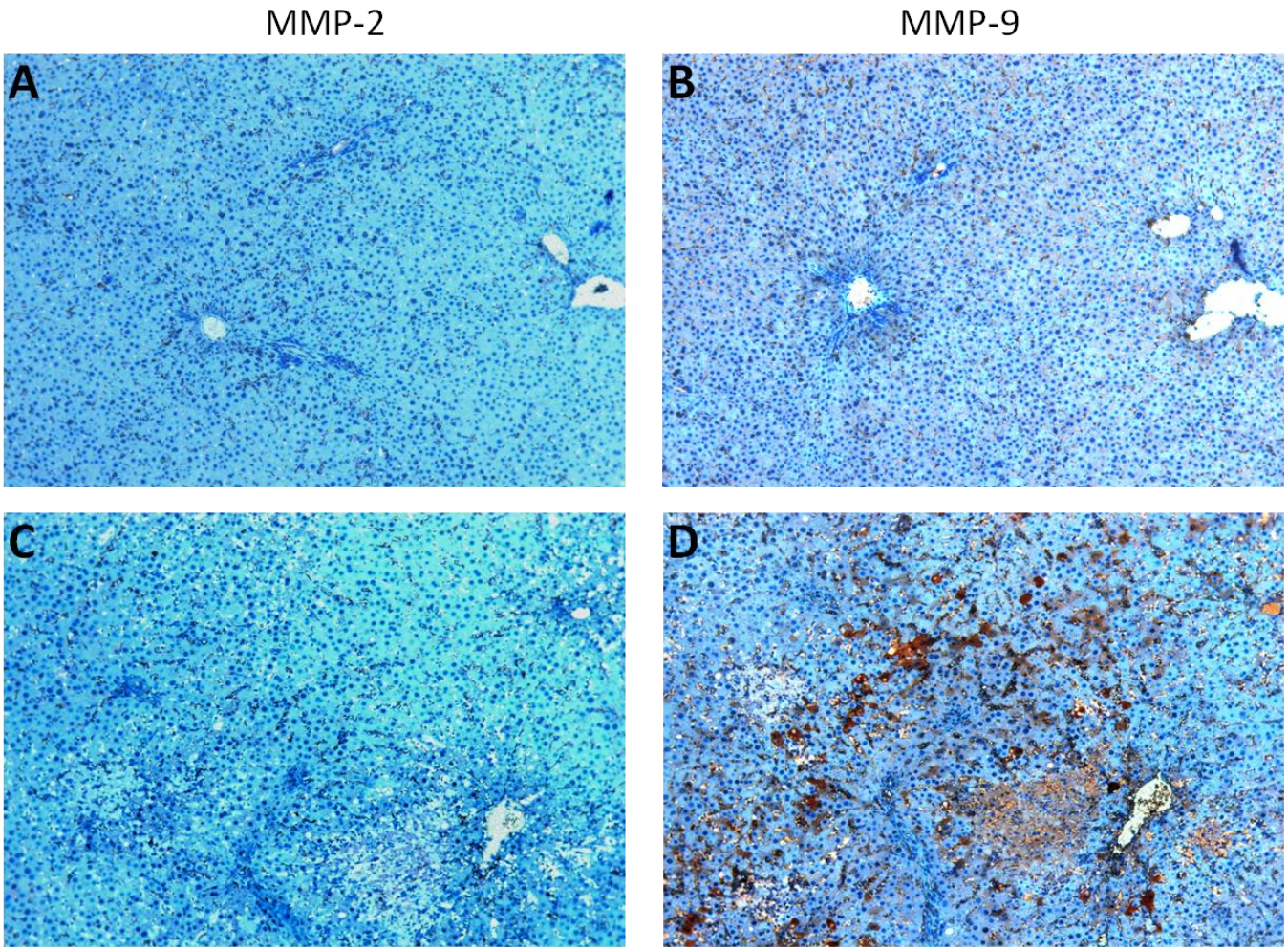

Figure 23 Difference in expression of MMP-2 and MMP-9 in control and MCT groups at 72 hours. There was no marked difference in MMP-2 and MMP-9 expression in the control group at 72 hours (A, B). In the MCT group however, MMP-9 was markedly expressed when compared to MMP-2 which was similar to the expression in the control group (C, D).

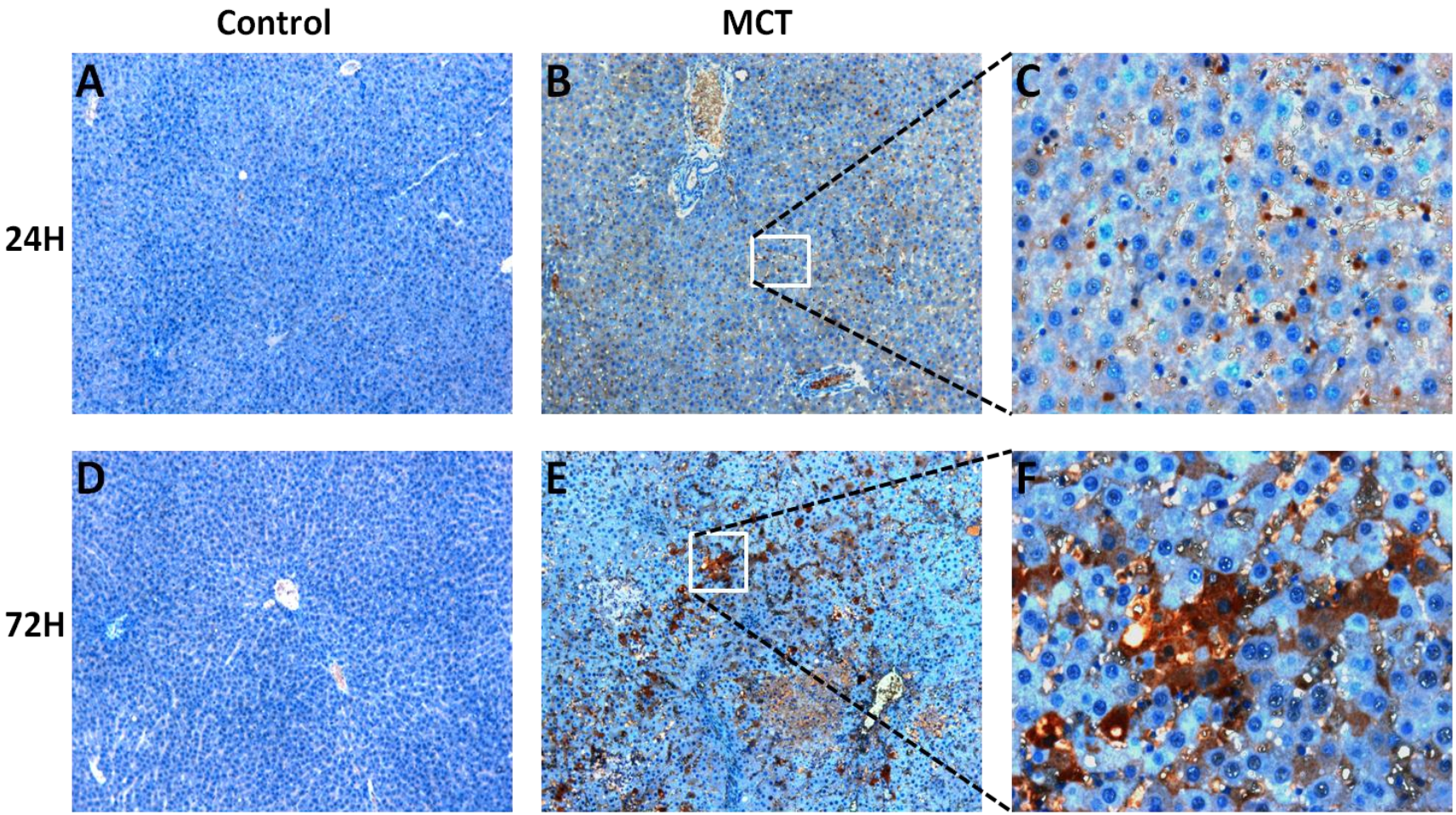

Figure 24 MMP-9 expression at different time points in the livers of the MCT group. A higher expression of MMP-9 could be detected in the MCT group when compared to the control group as early as 24 hours (A,B). Areas of MMP-9 expression included inflammatory cells and walls of the sinusoids (higher magnification C). An increase in the intensity of MMP-9 expression could be seen at 72 hours (E) with strong expression in damaged hepatocytes that show vacuolation (higher magnification F).

4.3 Discussion

Oxaliplatin-based chemotherapy has been strongly associated with development of SOS when given as part of the neoadjuvant protocol to downstage hepatic CLMs prior to liver resections. The most serious complication of this condition is development of portal hypertension leading to splenomegaly resulting in thrombocytopenia due to platelet sequestration, ascites and variceal bleeding when the PP exceeds 12 mmHg (64), (195). In this study we used MCT to induce SOS in rats; a model that is both reliable and reproducible and closely resembles both the histological and clinical features of SOS resulting from oxaliplatin based chemotherapy (182), (189).

It was not possible to establish the SOS rat model following treatment with oxaliplatin as we could not detect the pathological lesions that correlate with clinical SOS including sinusoidal dilatation, inflammatory cell infiltration and hepatocellular necrosis. Similarly, Schiffer et al (90) and Narita et al (196) used MCT and not oxaliplatin to develop an experimental SOS model in rats relating the model to oxaliplatin induced SOS in patients. This is in addition to the description of the first rat SOS model by DeLeve et al who used using MCT to simulate the clinical SOS that develops following myeloablative chemotherapy for HSC transplantation (182). The reason oxaliplatin was not successful in inducing SOS in rats might be related to the difference in metabolic pathways between humans and rats especially concerning the cytochrome P450 system since platinum based drugs have been shown to suppress the expression of some cytochrome P450 isoenzymes in the rat but not in the human liver (197).

The primary end point of this experiment was to establish the role of MCT in developing portal hypertension related to hepatocellular damage in rats. An animal model with established portal hypertension and pathological changes that correlate with clinical SOS would be of great value in order to investigate the potential therapeutic effects of a target drug. We showed that the PP measurements were significantly higher in the MCT treated rats when compared to the control group at all time points. This was also associated with liver congestion, the presence of bloody ascitic fluid and congested bowels which were most evident at 72 hours in the MCT group. It has been previously reported that hepatic venous pressure gradient greater than 10 mm Hg is specific for SOS (198). Hepatic venous pressure gradient is being used more frequently as an index for PPs as it is less invasive and correlates well with the direct PP measurements (199). In this study we measured the PPs directly through portal vein puncture with average values greater than 10 mm Hg at both 48 and 72 hour time points hence specific for SOS.

The pathogenesis of MCT induced portal hypertension differs however according to different time points. DeLeve et al divided the changes occurring in the SECs following MCT toxicity into early or preclinical SOS during the first 12-48 hours and late or clinical SOS starting from day three for a period of three days where separation of the sinusoidal lining occurs (200). Accordingly PP elevation in the first two days has been hypothesized to be due to swelling and rounding up of the SECs leading to impedance of the blood flow with development of gaps within the sinusoidal wall lining. The erythrocytes then penetrate the space of Disse from beneath the sinusoids and through the gaps in the wall dissecting and completely separating the SEC lining blocking the sinusoidal lumen and inducing clinical SOS by day three (200). We performed an EM study at the 72 hour time point which

corresponds to clinical SOS to correlate the changes in PP with the ultrastructural damage changes. The SEM images on day three showed complete detachment of the SEC lining obstructing the blood flow. In addition, the TEM images showed dilatation of the sinusoidal cell fenestrae with loss of the SEC lining leading to direct contact between the erythrocytes and hepatocytes. Also, TEM images showed evidence of glycogen depletion in the perisinusoidal hepatocytes reflecting hepatocyte damage. This is similar to the early phase of APAP toxicity where glutathione depletion has been noticed (201), (202).

Serum bilirubin levels were also significantly higher in the MCT group at 48 and 72 hours. Schiffer et al reported decreased bile flow and bile excretion in livers of MCT treated rats and attributed this to the toxic effect of MCT on hepatocytes (90). Although serum bilirubin levels are sensitive in detecting SOS in the clinic; they are not specific due to the presence of several other causes of jaundice in these patients including extensive metastatic liver disease and enlarged lymph nodes in the porta hepatis (189), (203). Serum bilirubin levels however are very specific in predicting the development of PLF when their values are greater than 50% and a peak bilirubin of 7.0 mg/dl has been considered a specific cut-off value for PLF related deaths (16).

Centrilobular sinusoidal dilatation with perisinusoidal erythrocyte extravasation could be detected on histological examination of the liver sections from the MCT group during the first 24 hours with progressive congestion, wide-spread haemorrhagic areas representing peliosis and extensive hepatocellular necrosis by day three. These findings were in-keeping with the pathological lesions seen in the non-neoplastic liver following oxaliplatin preoperative chemotherapy in patients (186). Drawbacks of the MCT-SOS model however included the extensive presence of coagulative hepatocellular necrosis which occurs less frequently in the liver

sections of patients following oxaliplatin treatment. Also, nodular regenerative hyperplasia (NRH) which is a common finding in a high percentage of patients could not be detected. In this study, the follow up period was only three days as we were interested in the acute phase of the disease and this time frame would not allow studying the NRH related to SOS. Moreover, even if we had longer follow up times it might still have not been possible to detect NRH due to the reversible nature of the model with complete resolution of SOS starting from day 10 in the animal model (182), (186).

A substantial inflammatory cell response was observed in the regions of sinusoidal damage following MCT gavage at all time points. This histological evidence of inflammation was associated with biochemical evidence in the form of significantly higher serum ALT measurements at 48 hours when compared to the control group. The highest serum ALT levels however were detected at 72 hours and this correlated with the development of hepatocellular necrosis. Deleve et al (182) also reported the highest inflammatory response to occur on day three with mixed mononuclear and polymorphonuclear (PMN) cell populations. PMNs have been shown to play a role in hepatocellular necrosis in the MCT-SOS model through detection of increased myeloperoxidase activity in areas of coagulative necrosis. Myeloperoxidase is released following activation and degranulation of PMNs which yields hypochlorous acid which is a major oxidant formed through a reaction between hydrogen peroxide and chloride ions. (194), (196).

Although inflammatory changes were not obvious in liver sections from patients with SOS, liver transaminases were significantly higher in high grade SOS lesions when compared to low grade SOS lesions (186), (204). Also, a recent study showed that acute phase pathway genes were upregulated in liver tissue following oxaliplatin

therapy including both the IL-6 pathway and STAT-1 gene which contribute directly to liver inflammation in clinical SOS (205), (206).

We also showed an increased expression of MMP-9 but not MMP-2 in liver tissue of rats treated with MCT. MMPs are known to be produced by SECs when subjected to injury through actin disassembly (207). They may play a key role in SOS pathogenesis due to the discontinuous and scanty nature of the sinusoidal basement membrane in the liver comprised principally of collagen IV which is easily degraded with MMPs (208). Deleve et al (209) used gelatin zymography to study MMP expression in rat liver following MCT gavage and showed that MMP-9 expression was much higher than MMP-2 expression and that SECs were the major source of MMP production in the liver. We also showed that in addition to SEC expression; MMP-9 was expressed in the inflammatory cells as early as 24 hours. Borregaard et al (210) showed that PMNs are a source of MMP-9 in response to injury however the role of PMN-released MMP-9 might be less significant than SECs in development of SOS (194).

The role of MMP-9 in pathogenesis of clinical SOS has been suggested when it was noticed that patients receiving bevacizumab in addition to oxaliplatin in the neoadjuvant chemotherapy protocol showed less severe SOS when compared to oxaliplatin alone (211). Bevacizumab is a monoclonal antibody directed against VEGF-A which has shown a higher expression in SOS following HSC transplantation (212). VEGF plays a role in maintenance of the fenestrae of the SECs and its expression is increased following SEC lining disruption and cellular hypoxia (213). VEGF is known to induce expression of MMP-9 by SECs, thus bevacizumab may lead to downregulation of MMP-9 resulting in less severe SOS. Surprisingly Rubbia-Brandt et al (205) showed that the VEGF-C mRNA levels were increased in

clinical SOS with no difference in VEGF-A levels when compared with the control. This would suggest that Bevacizumab has an anti-VEGF-C action as well. VEGF-C is responsible for lymphangiogensis and it has been reported that VEGF-C is released from macrophages activated via VEGF-A. In addition bevacizumab inhibited both angiogenesis and lymphangiogensis when added to the cornea suggesting a role of bevacizumab in VEGF-C suppression (214), (215).

To conclude, we established an SOS animal model with special emphasis on the clinical implications of the model in terms of oxaliplatin induced SOS. We showed that the functional and structural damage changes in the MCT-SOS model resemble closely the clinical SOS with similar pathways and hence preventing SOS in this model could be prospectively used in a clinical trial to prevent and treat SOS in patients.

5-Semi-synthetic flavonoid monoHER prevents development of sinusoidal obstruction syndrome in rats

5.1 Background

The main cause for development of SOS with its consequences of portal hypertension and increased incidence of PLF is the primary insult of the SECs with secondary hepatocellular damage. Prevention of SOS related PLF should focus primarily on identifying patients who are at high risk of developing SOS and who should be properly assessed before surgery. High risk patients include those who have received more than six cycles of neoadjuvant chemotherapy, patients with node positive tumours who received adjuvant chemotherapy following resection of the CRC, and those with a high APRI score which is considered a sensitive predictor of SOS (30), (216), (41).

It has also been recently reported that patients with high grade SOS have a worse prognosis, not only in relation to postoperative morbidity but also in terms of early intra-hepatic recurrence and decreased survival (216).

Prevention of the condition is of utmost importance and should focus on SEC protection. This should include both stabilization of sinusoidal endothelium and prevention of its detachment from the basement membrane in addition to inhibiting the upregulated inflammatory pathways associated with SOS. Prevention of SOS development has focused up until now on either inhibition of the coagulation cascade, deactivation of MMP activity which is upregulated in SOS, restoration of intracellular glutathione or preservation of sinusoidal perfusion (217), (40), (218).

The flavonoid monoHER could have a potential protective agent against SOS because of its favourable effect on the microvascular endothelium and its antioxidant and anti-inflammatory capacities (219). MonoHER is a component of the registered drug Venoruton, which is used to treat chronic venous insufficiency. MonoHER has

been shown to provide a protective effect against doxorubicin-induced cardiotoxicity in mice without interfering with its antitumour activity (220), (221). More recently, it has been used in healthy volunteers in a phase I clinical trial without any serious side effects. This has encouraged investigators to study its cardioprotective effects in patients with metastatic cancer being treated with doxorubicin (222), (223).

The aim of this study was to assess the protective effect of the semi-synthetic flavonoid monoHer on the development of MCT induced sinusoidal injury in rats. Furthermore, the effect of monoHER on cell growth of human CRC cells exposed to increasing concentrations of oxaliplatin was determined *in-vitro*.

5.2 Results

5.2.1 MonoHER reduces the portal pressure in SOS

In order to detect whether pretreatment with monoHER had an effect on reducing the PP, we compared PP measurements with the MCT group at all time points (Fig.25). The PP was significantly lower in rats pretreated with monoHER when compared to rats receiving MCT alone as early as 24 hours (7.43±0.93 vs. 9.37±0.99 mmHg respectively (p=0.005)). The PP measurements in the MCT+ monoHER group also remained significantly lower than in the MCT group at 48 hours (p=0.019) and 72 hours (p=0.016) (48h: 7.91±1.26 vs. 10.19±1.30 and 72h: 7.31±2.65 vs. 11.36±2.97 mmHg MCT+ monoHer vs. MCT respectively).

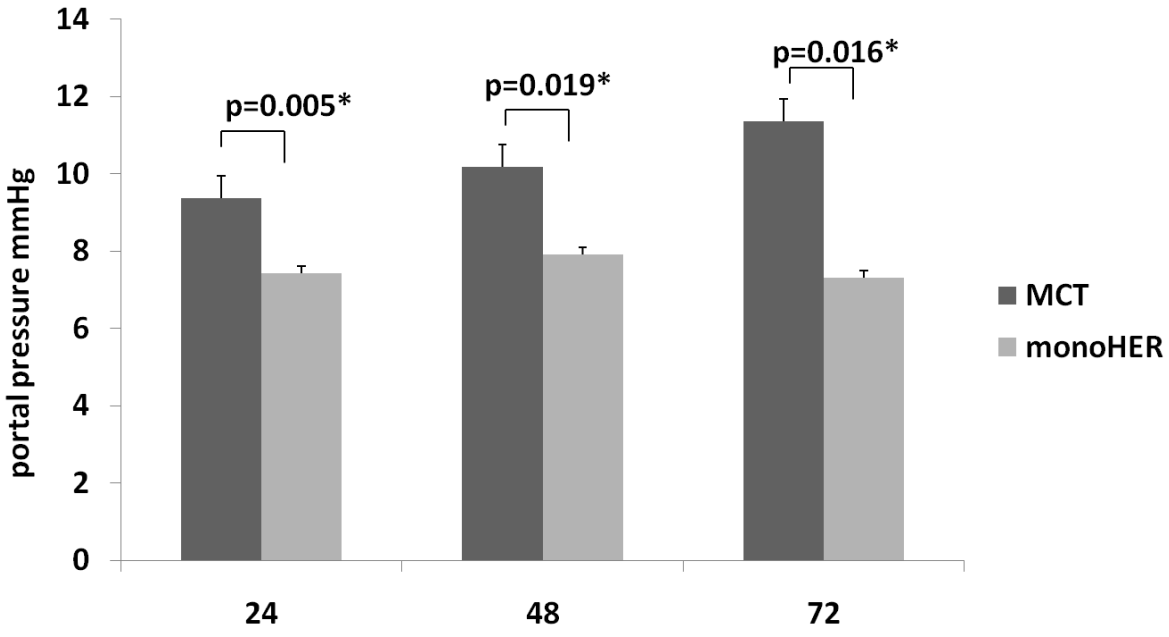

Figure 25 Portal pressure measurements in monoHER pretreated rats compared to MCT rats. Pretreatment with monoHER significantly reduced the portal pressure at all time points when compared to the MCT group.

5.2.2 Liver damage is attenuated by monoHER

Similar to the previous experiment no mortality occurred in either group. The livers of the MCT treated rats were more congested when compared to MCT+ monoHER group with multiple punctuate haemorrhagic spots at 48 hours and patches of necrosis at 72 hours in MCT only group (Fig.26).

No difference could be detected in serum bilirubin measurements at any time points between both groups. Serum ALT was significantly lower in MCT+ monoHER rats when compared to MCT rats at 72 hours (129.47±114.50 vs. 311.91±163.64) IU/L respectively, p=0.028). There was no significant difference in serum ALT levels between both groups at 24 hours (p=0.092) or 48 hours (p=1.00) (Fig.27).

Histological examination of liver sections revealed extensive sinusoidal dilatation following MCT administration with inflammatory cell infiltration at 24 hours (Fig.28A). Sinusoidal dilatation was also present in the MCT+ monoHER rats, however to a much lesser extent with fewer inflammatory cells when compared to the MCT group (Fig.28B). At 48 hours, marked congestion was observed in both groups with a more extensive inflammatory response in the MCT group when compared to the MCT+ monoHER group (Fig.29B,D). Frank hepatic necrosis extending over most of the liver was observed in the MCT group at 72 hours with dense inflammatory cell infiltration (Fig.30A). Also, detachment of the SEC lining from the space of Disse could be seen in the central vein with evidence of subendothelial haemorrhage (Fig.30B). In the monoHER group, congestion was still present however there was no necrosis and the SEC lining remained intact (Fig.30C,D).

The overall liver damage severity score was significantly lower in MCT+ monoHER rats when compared to MCT treated rats only at 72 hours (10.33±0.51 vs. 4.8±3.56) MCT+ monoHER vs. MCT respectively (p=0.002) (Fig.31A). Inflammatory cell infiltration/HPF was also significantly lower in the MCT+ monoHER group when compared to the MCT group at 72 hours but not at other time points (20.6±8.32 vs. 64.5±9.02) cells/HPF MCT+ monoHER vs. MCT respectively (P<0.0001) (Fig.31B).

5.2.3 MonoHER reduces MMP-9 expression in the liver

A scoring system based on both the intensity (0, 1, 2, 3) and extent of MMP-9 expression (1=<33%, 2=33-67%, 3=>67%) was used as a semi-quantitative measurement of MMP-9 expression in both groups (224). Livers of MCT treated rats had a significantly higher expression of MMP-9 when compared to the MCT+ monoHER rats at both 24 hours (p=0.016) and 72 hours (p=0.0001) (Fig.32). Areas of highest expression included SEC lining and inflammatory cells to a lesser extent; in addition, MMP-9 was also expressed in areas of hepatocellular necrosis at 72 hours (Fig.33). We could not detect significant differences in MMP-2 expression in MCT treated rats when compared to the sham group. Therefore MMP-2 expression was not used as a parameter to compare the liver damage between MCT and MCT+ monoHER groups.

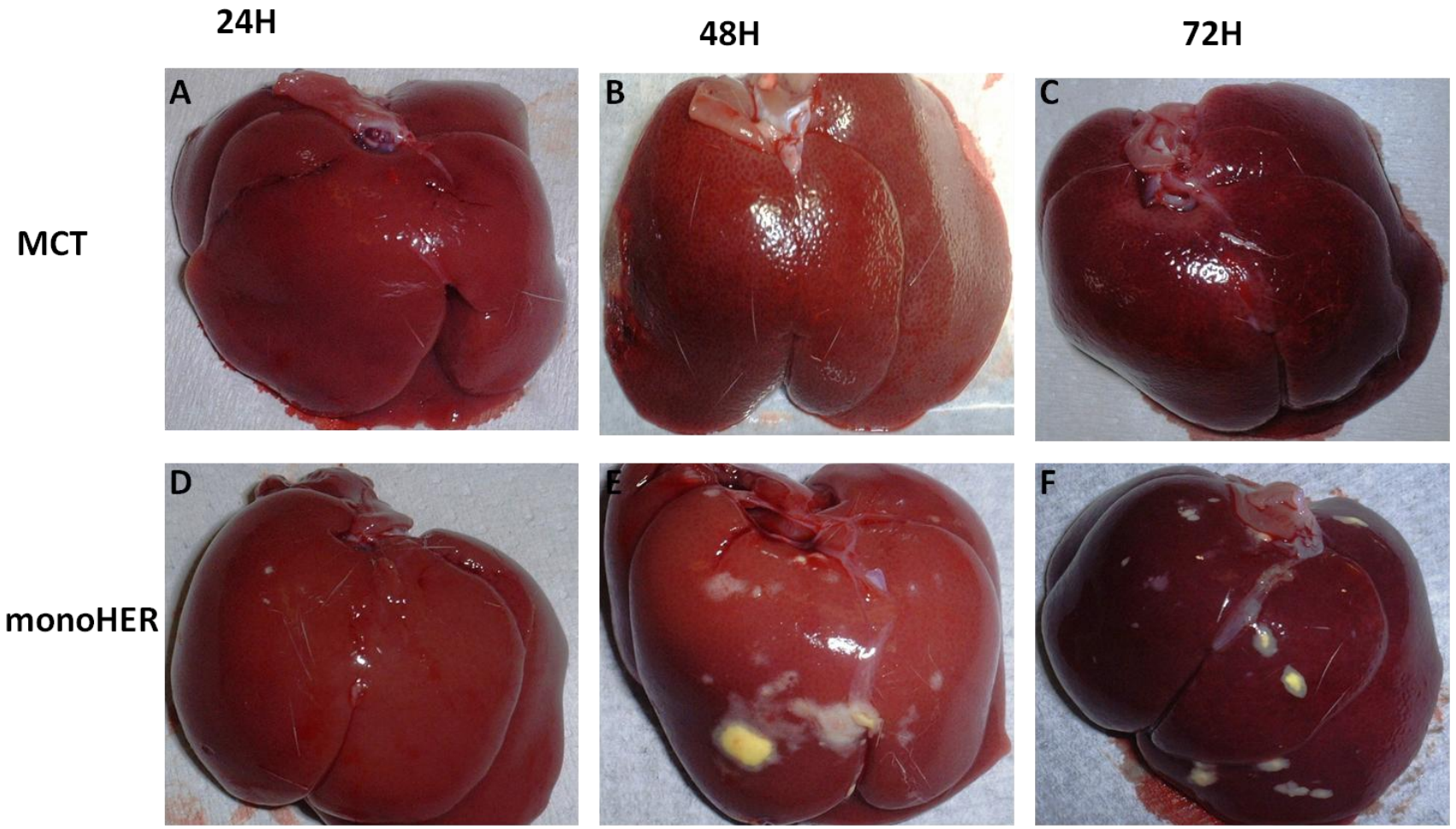

Figure 26 Representative samples showing morphological appearance of the liver at different time points. The congestion is evident at 24 hours in the MCT group (A), with appearance of punctuate hemorrhagic spots at 48 hours (B) and areas of frank necrosis in a deeply congested liver at 72 hours resembling the blue liver seen in the clinical scenario (C). Congestion also occurred in the MCT+ monoHER group however was much less severe than in the MCT group and without the development of punctuate hemorrhages or frank necrosis.

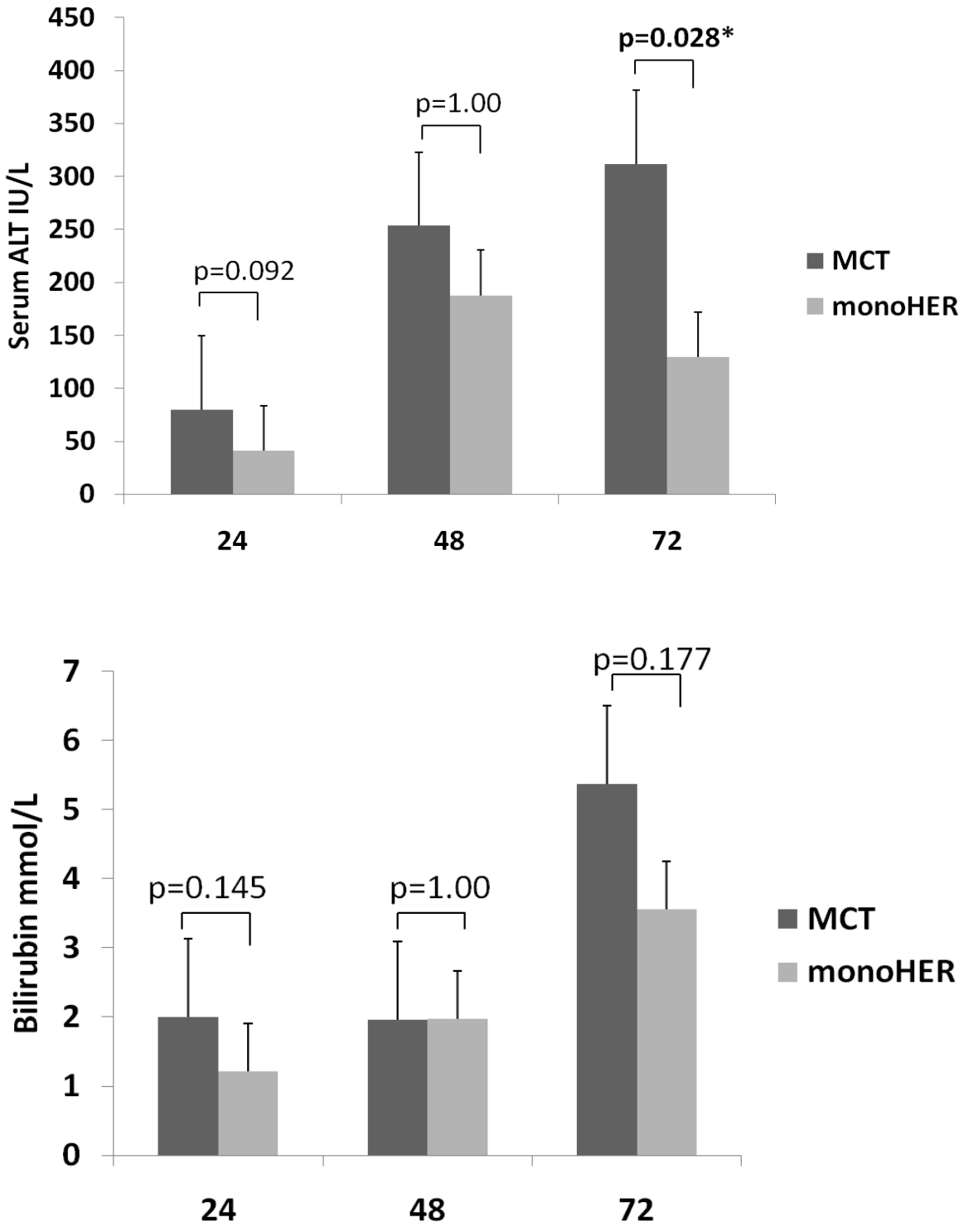

Figure 27 Serum ALT and bilirubin measurements in the two studied groups. Rats pretreated with monoHER had significantly reduced serum ALT at 72 hours when compared to MCT treated rats. There was no difference between both groups at 24 or 48 hours. There was no significant difference in bilirubin levels in both groups.

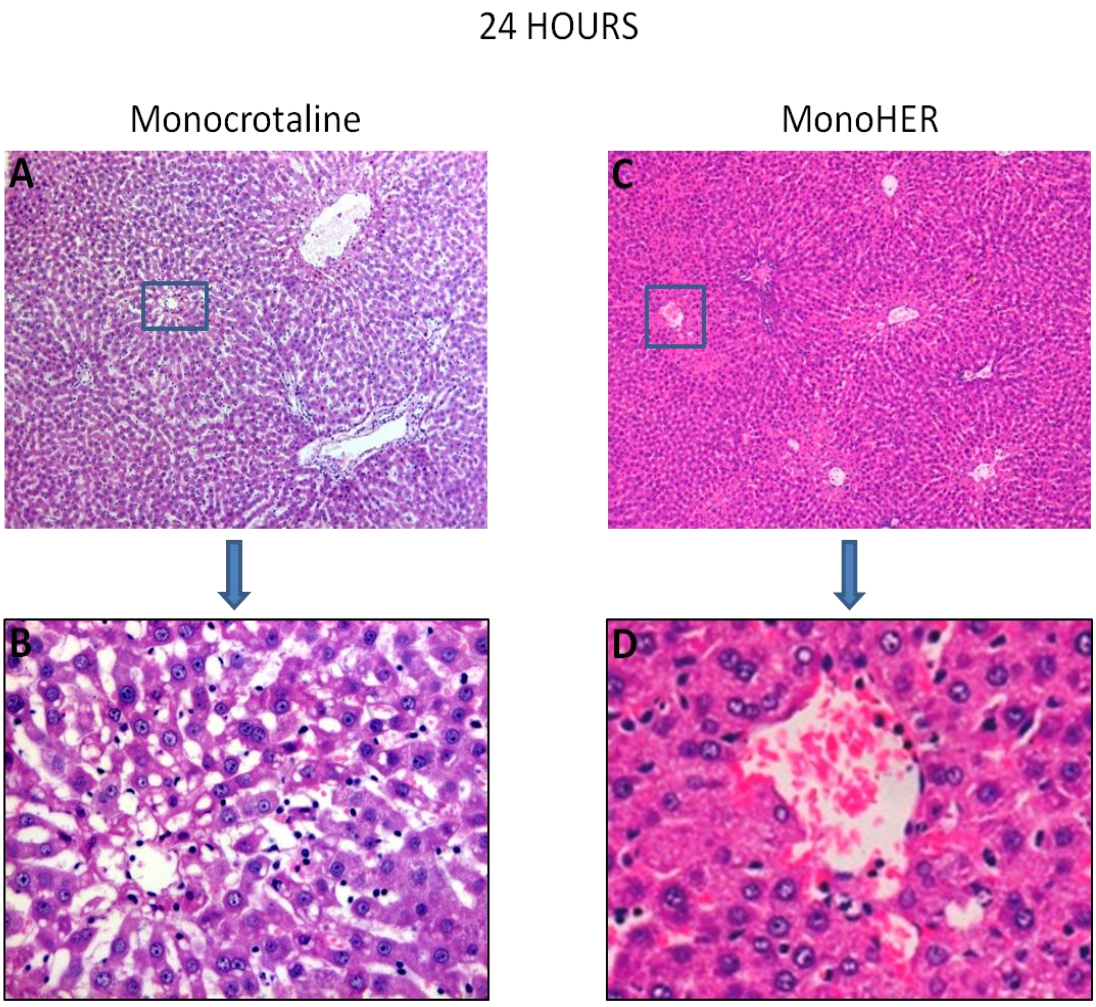

Figure 28 Histological examination of the liver in both studied groups at 24 hours. Generalized sinusoidal dilatation could be detected in the MCT group with inflammatory cell infiltration (A,B). The sinusoidal dilatation is less pronounced in the monoHER group with less inflammation (C,D). Low magnification x100, high magnification x400.

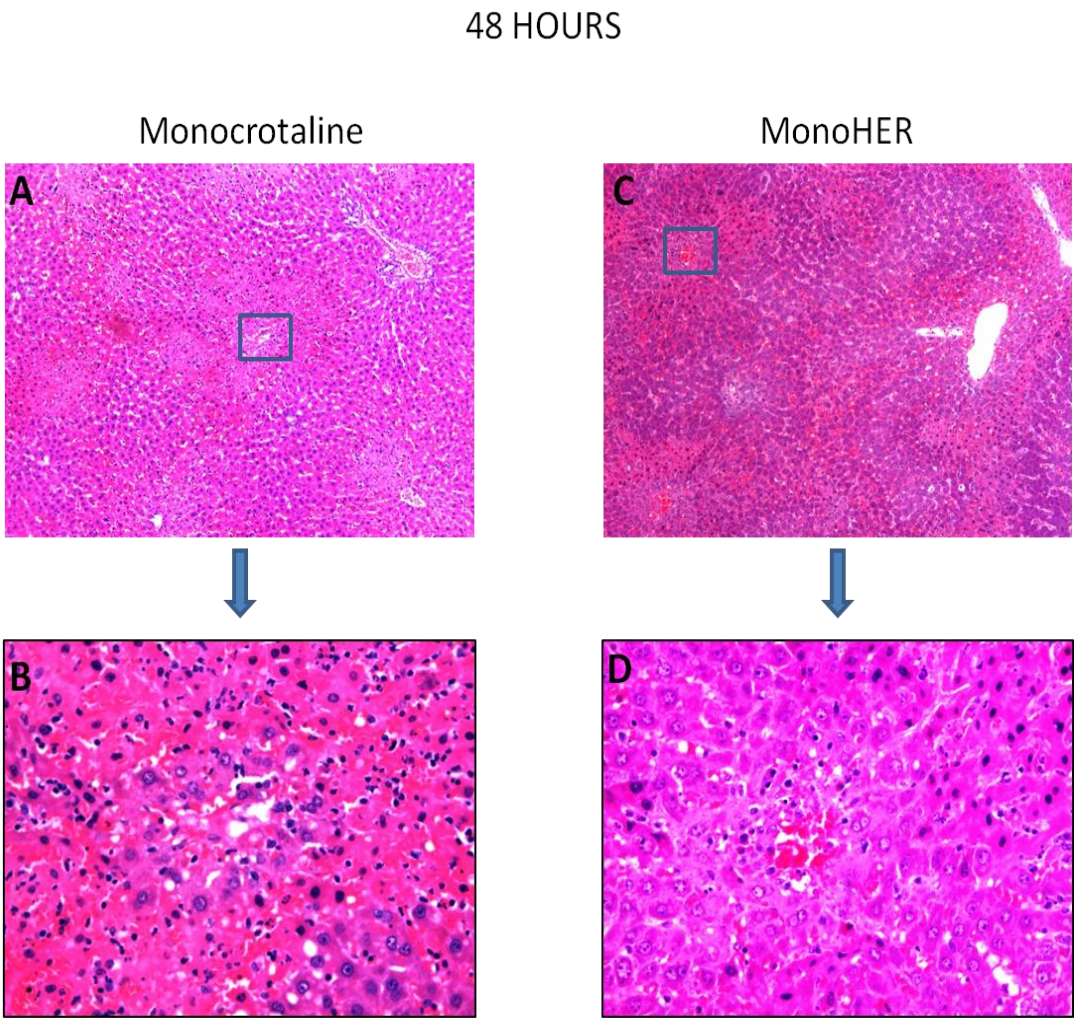

Figure 29 Histological examination of the liver in both studied groups at 48 hours. Extensive areas of congestion could be seen in both groups (A,C). Inflammation is less severe in the monoHER group (C,D).

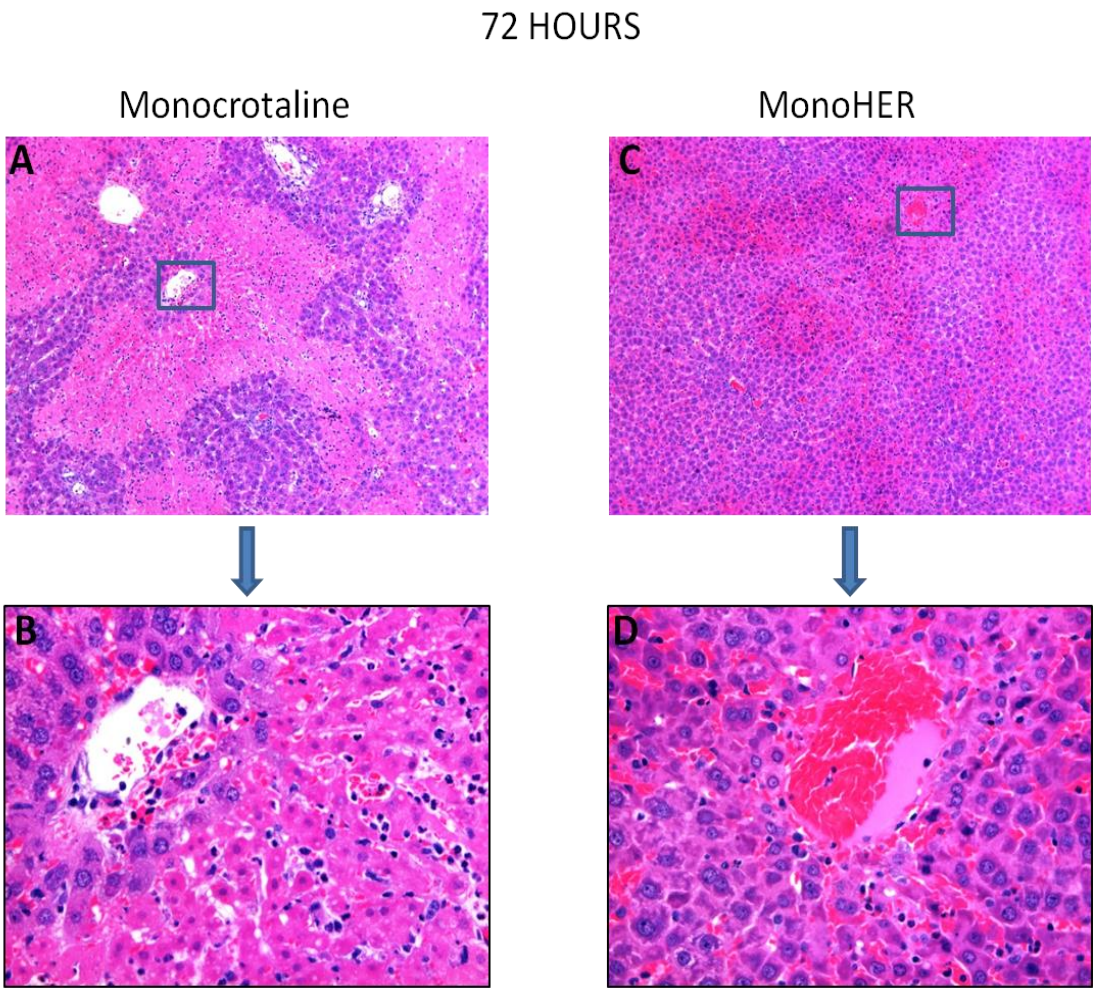

Figure 30 Histological examination of the liver in both studied groups at 72 hours. Massive areas of necrosis could be detected in the MCT treated liver (A), with detachment of the endothelial lining of the central vein and presence of subendothelial erythrocytes (B). No necrosis was detected in the monoHER liver at the same time point (C). Congestion was still present however the endothelial lining of the central vein was intact (D).

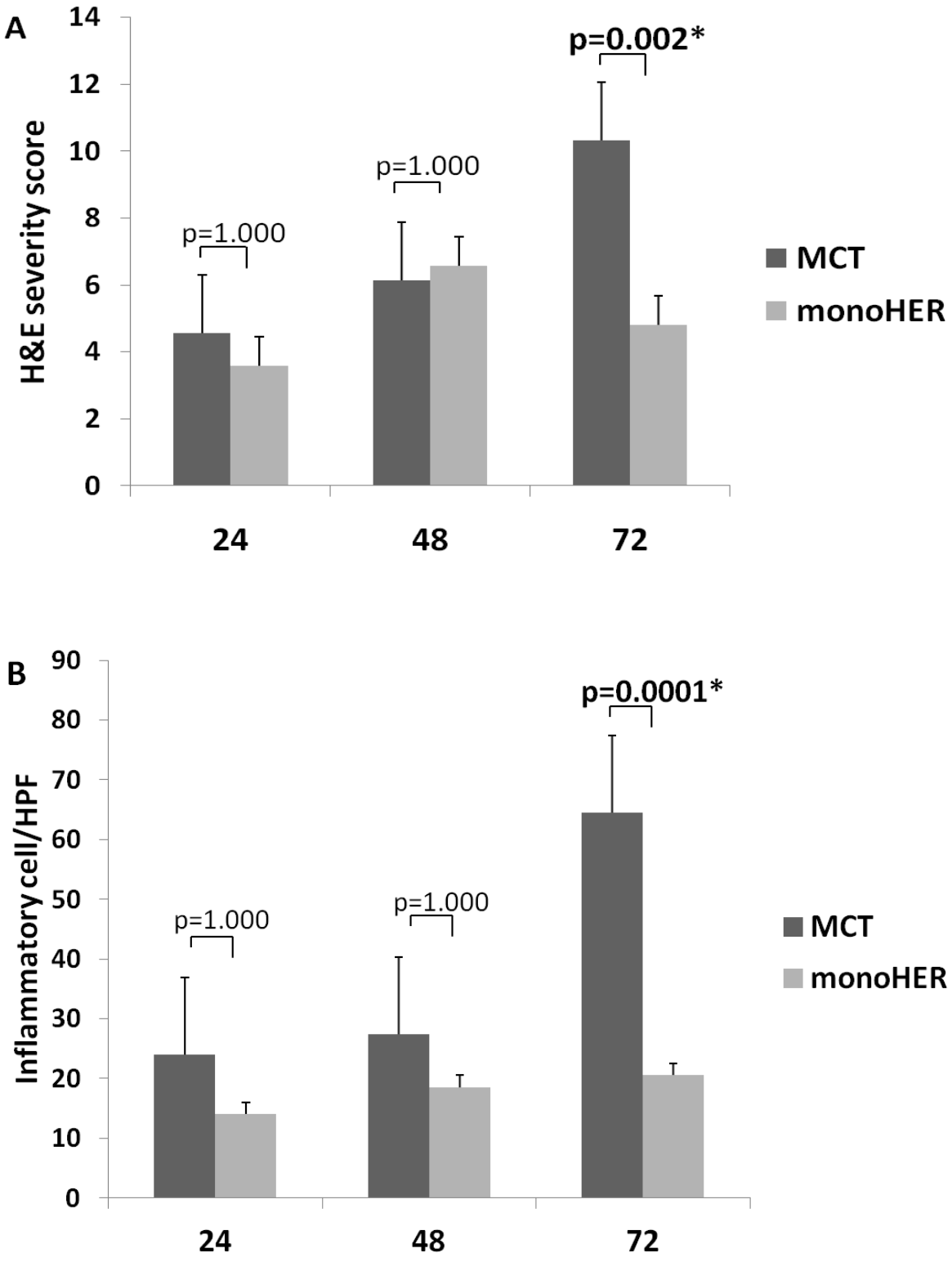

Figure 31 Semi-quantification of liver damage in studied groups. The overall H&E liver damage severity score (A) and inflammatory cell count /HPF were significantly lower in the MCT+monoHER group only at 72 hours (B).

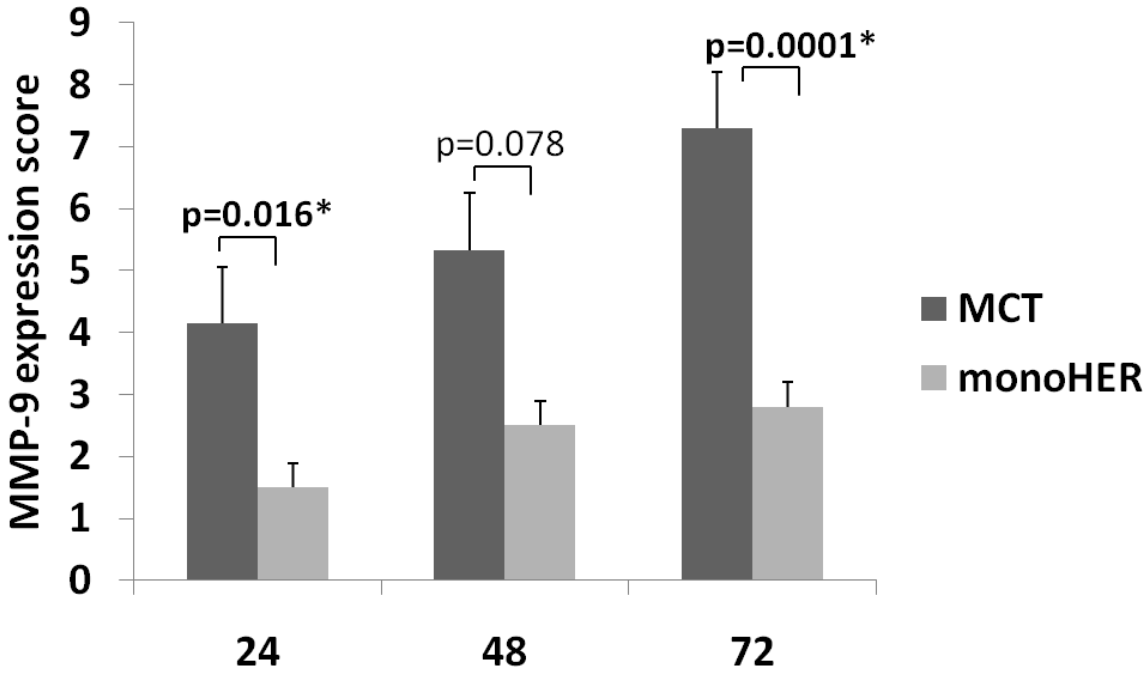

Figure 32 Semi-quantification of MMP-9 expression in the liver samples of both groups. The MMP-9 expression was significantly higher in the MCT group at 24 and 48 hours.

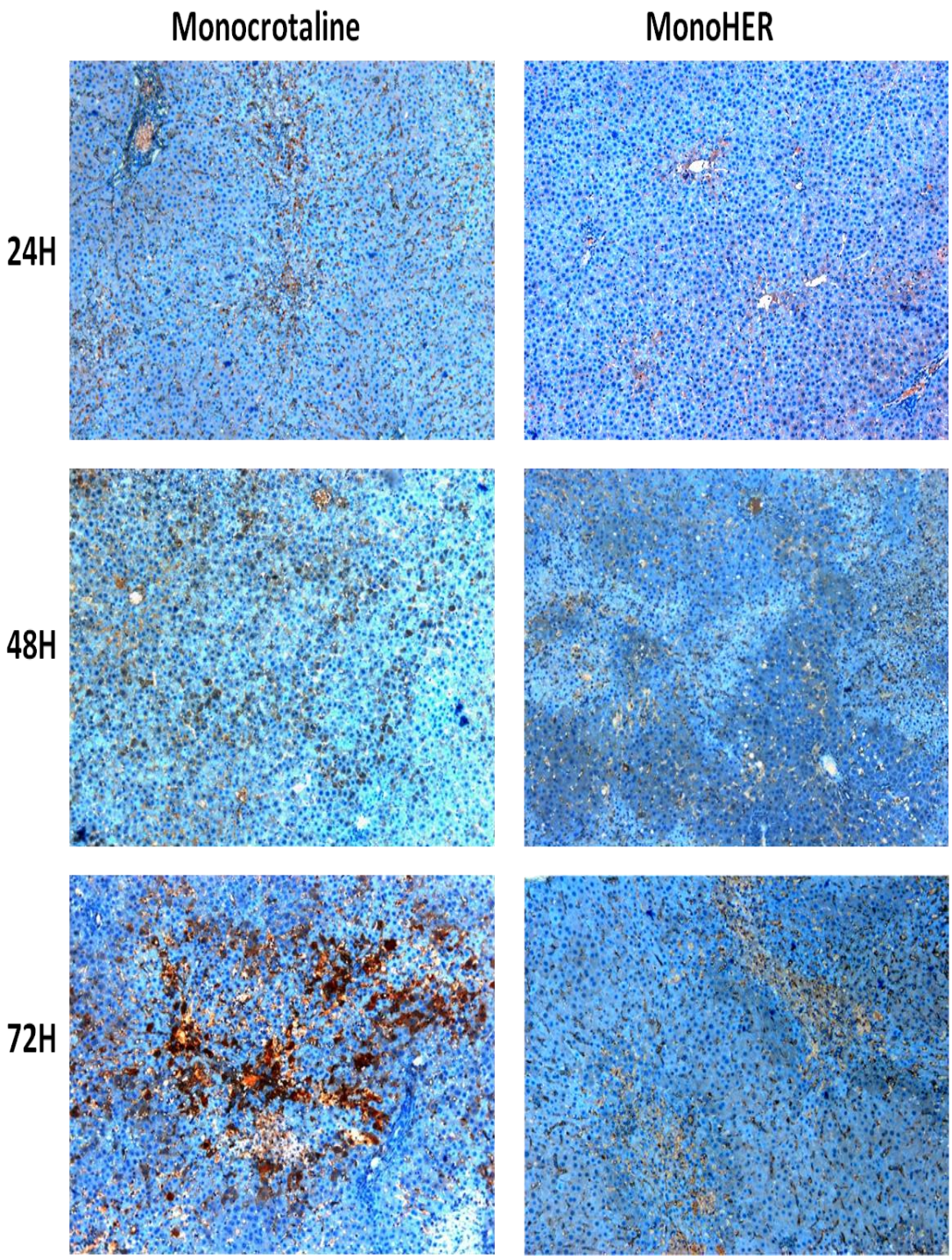

Figure 33 MMP-9 expression in both groups at different time points. The MMP-9 expression in the monoHER group was weaker than in the MCT group at all time points. The most striking difference could be seen at 72 hours where MMP-9 was greater in both extent and intensity in the MCT group.

5.2.4 Protective effect of monoHER on HUVEC cell line

To determine the effective drug concentrations, HUVEC cells were treated with various concentrations of oxaliplatin ranging from (0.5 µg/ml-8 µg/ml). No difference could be detected between oxaliplatin concentrations of 0.5µg/ml and 2µg/ml. With increasing the concentration to 8µg/ml, a sharp fall in cell number could be detected with less viable cells (Fig.34).

When similar numbers of HUVEC cells were pre-treated with monoHER, a very slight variation could be detected even with higher doses of oxaliplatin indicating a possible protective effect of monoHER on the HUVEC cell line (Fig.35).

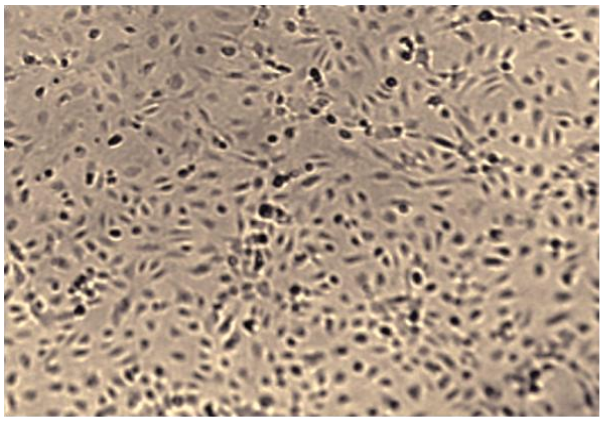

Oxaliplatin 0.5 µg/ml

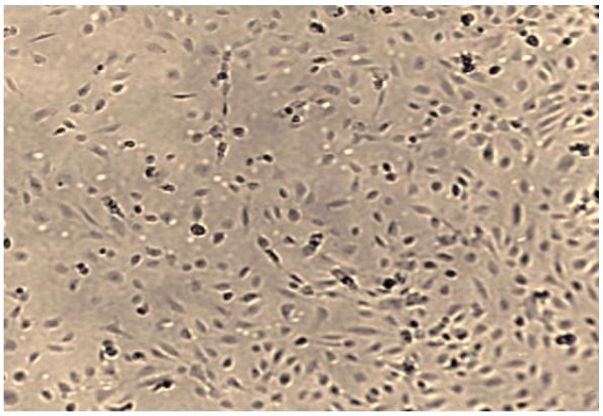

Oxaliplatin 2 µg/ml

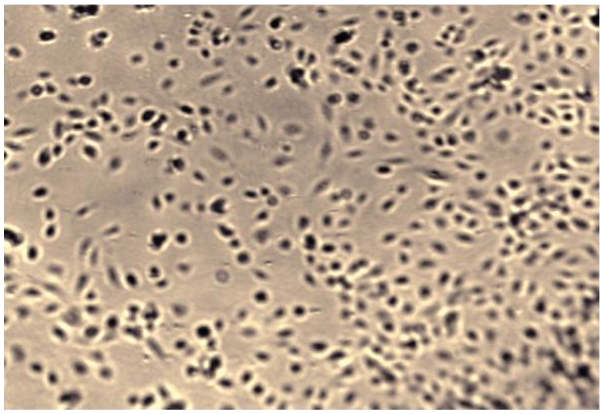

Oxaliplatin 4 µg/ml

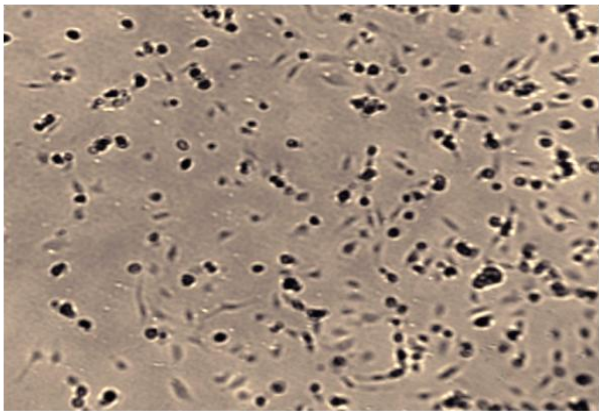

Oxaliplatin 8 µg/ml

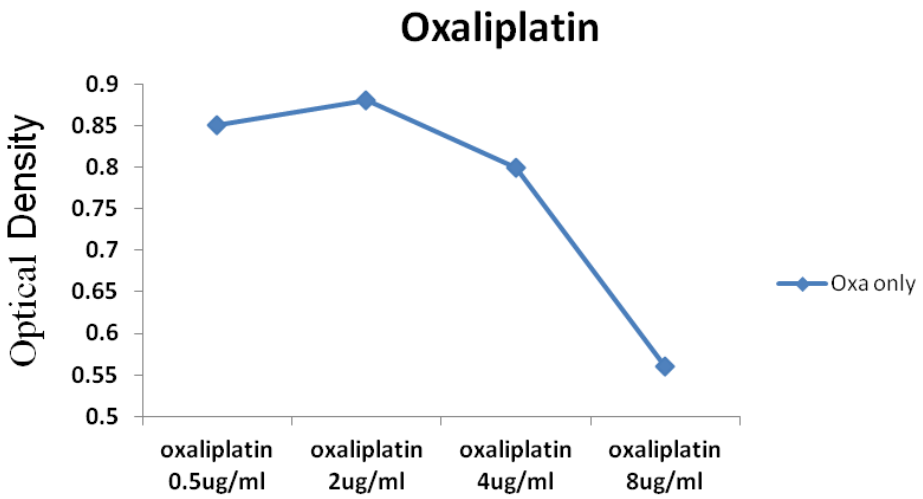

Figure 34 Oxaliplatin effect on HUVEC cell line. Oxaliplatin reduced the viability of HUVEC cells which was dose dependant.

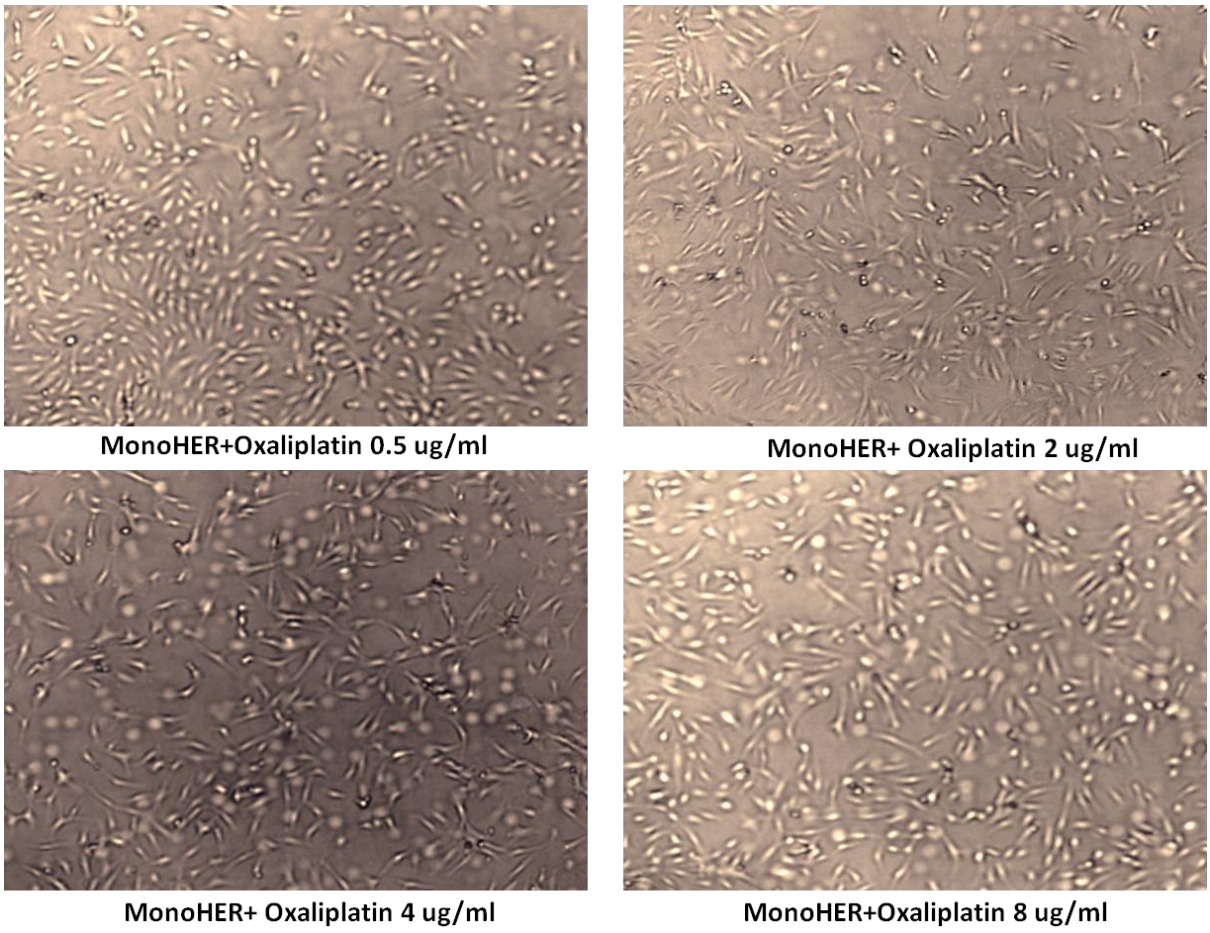

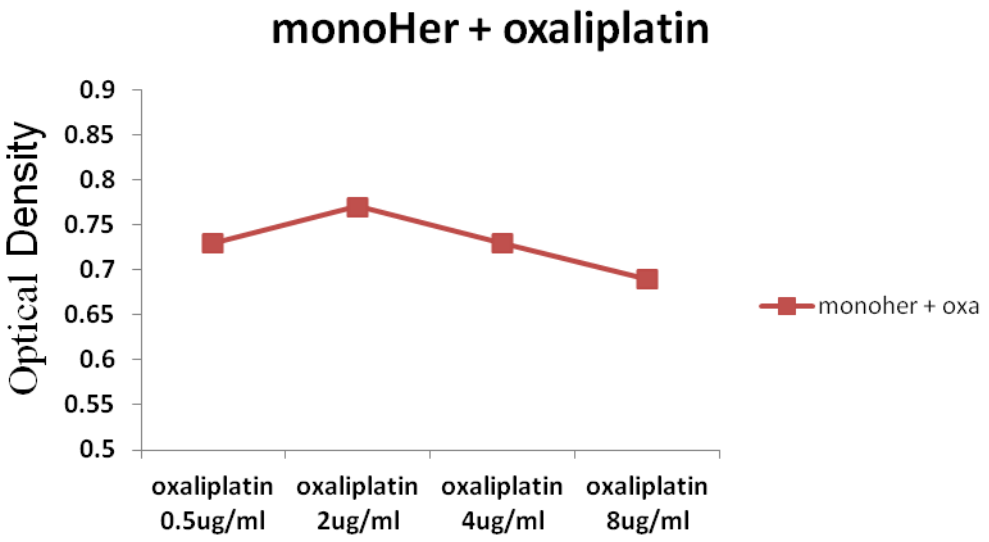

Figure 35 MonoHER attenuates the effect of oxaliplatin on HUVEC cells.

5.2.5 MonoHER does not interfere with oxaliplatin cytotoxicity

Both CRC cell lines incubated with oxaliplatin showed dose-dependent cytotoxicity. MCT and/or monoHER at different concentrations did not have an effect on cell numbers in both cell lines. Addition of monoHER to oxaliplatin even in high doses (100µM) did not interfere with the dose dependant cytotoxic effect established by oxaliplatin indicating that monoHER did not interfere with the anti-neoplastic properties of oxaliplatin (Fig 36).

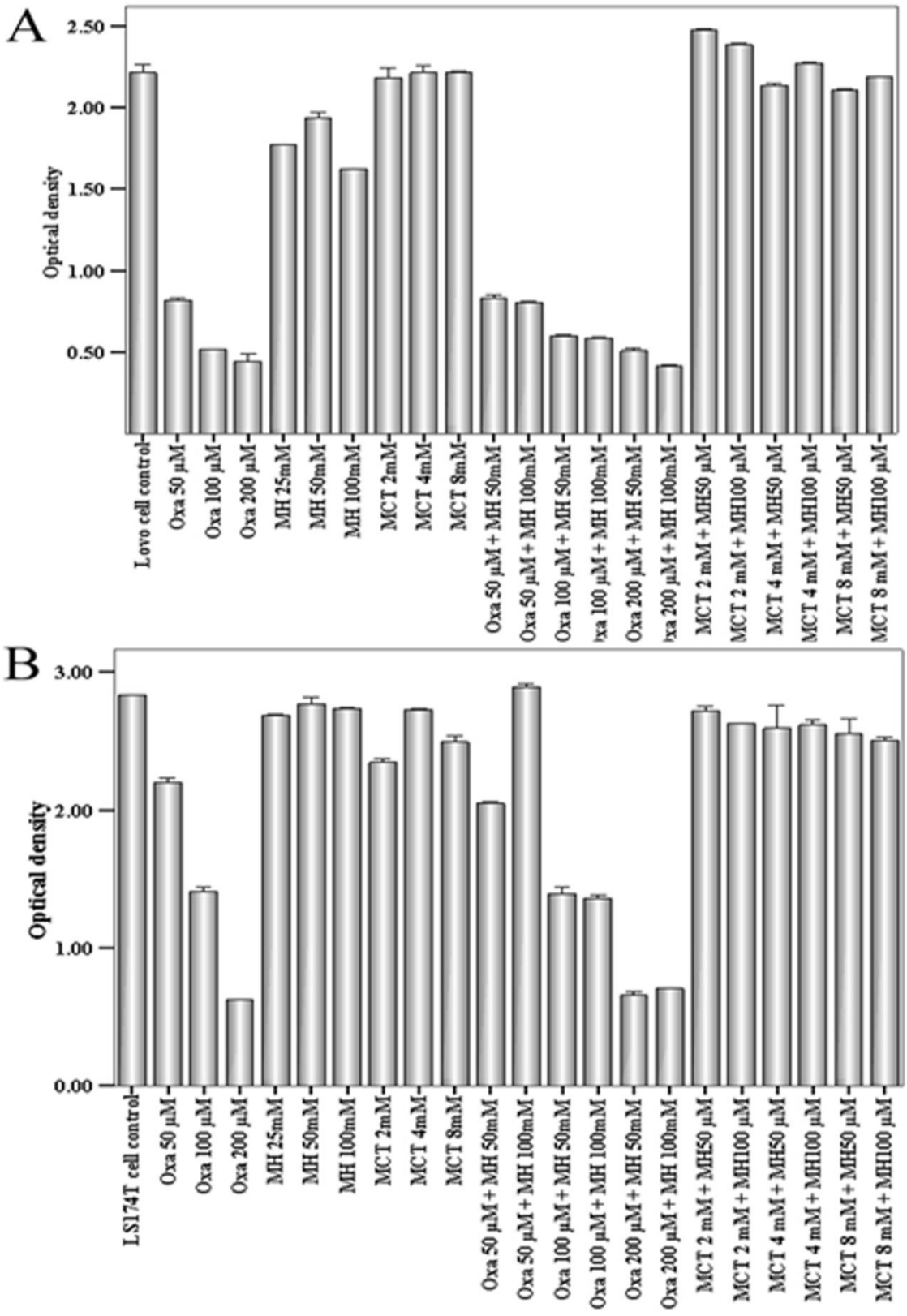

Figure 36 *In-vitro* analyses of proliferation of colorectal cancer cell lines using the MTS indirect colorimetric method and a spectrophotometer at 490nm. MonoHER did not interfere with the dose-dependent cytotoxic effects of oxaliplatin. MonoHER alone had no effect on viable cell count as measured by optical density in either cell line (OXA= Oxaliplatin, MH= MonoHER)

5.3 Discussion

The primary goal of this study was to investigate the role of monoHER in preventing the development of portal hypertension following MCT administration. The PP measurements in the MCT+ monoHER group were significantly lower than in the MCT group at all time points. The protective effect of monoHER was also reflected in the macroscopic appearance of the livers in the MCT+ monoHER group which demonstrated much less congestion and less haemorrhagic ascitic fluid in the abdominal cavity when compared to the MCT group specifically at 72 hours. Moreover, we showed that monoHER has a protective effect on HUVEC cells when added to oxaliplatin *in-vitro*.

This might be explained by understanding the role monoHER plays in endothelial cell stabilization since SEC detachment and occlusion of the sinusoidal lumen is the key factor in development of SOS and portal hypertension (200). MonoHER is the most potent constituent of Venoruton which has been shown to reduce the microvascular permeability and erythrocyte aggregation. Venoruton has also been shown to protect vascular endothelium and reduce the number of CECs which was considered as a marker of the severity of the disease in chronic venous insufficiency (225), (226). More recently, monoHER demonstrated a significant protective effect against doxorubicin-induced damage to human endothelial cells *in-vitro* (227).

It is known that a common pathway between MCT and oxaliplatin in the development of SOS is formation of reactive oxygen species and subsequent glutathione depletion (228). MonoHER has been shown to possess potent antioxidant free radical scavenging properties (220) which might play a role in prevention of SOS through sweeping free oxygen radicals and preventing SOS both in the MCT

animal model and in patients. Recently, serious concerns have been raised however towards the oxidation product formed following oxidation of monoHER. Similar to quercetin which is another well-established flavonoid that forms oxidation products in the process of free radical scavenging with resultant cell damage, a phenomenon known as the quercetin paradox (229) monoHER forms oxidation products which have been obtained *in-vitro* through oxidation of monoHER via horseradish peroxidase. These oxidation products have been shown to react with the thiol group in glutathione producing a monoHER-glutathione conjugate ultimately leading to glutathione depletion. This would lead to paradoxical catastrophic consequences in patients with SOS since the primary insult is depletion of glutathione which is the primary defence in the SECs. Fortunately, this has not been shown to occur in patients owing to a structural difference between monoHER and quercetin. A major difference exists in the interplay of these two compounds with the refined antioxidant network *in-vivo* owing to an intrinsic difference in their chemical structure leading to two energetically different products. Unlike quercetin which is a soft electrophile which directly reacts towards the thiol group in the soft nucleophile glutathione leading to its depletion, oxidized monoHER is a hard electrophile and is reduced through its preferential faster reaction with hard nucleophile plasma ascorbate preventing its reaction with thiols of glutathione hence avoiding its depletion (230), (231).

The structural damage changes seen by light microscopy in the H&E sections were significantly improved in the MCT+ monoHER group again only at 72 hours. This together with the significantly lower levels of both serum ALT and inflammatory cells at 72 hours is evidence that monoHER plays a role in reducing the inflammatory response elicited in the liver which has been shown to occur most

evidently between days three and five following MCT administration in rats (182). It is known that the inflammation induced oxygen free radicals play a role in endothelial cell damage and an increase in their vascular permeability (232). The anti-inflammatory properties of monoHER against doxorubicin-induced inflammation have been previously demonstrated through inhibition of neutrophil adhesion to endothelial cells and inhibition of overexpression of doxorubicin-induced VCAM and E-selectin (227). Narita et al has also demonstrated that inhibiting neutrophil adhesion to the sinusoids and hepatocytes is a key factor in prevention of SOS in rats. Moreover, the authors showed that the hepatic necrosis occurring following MCT intake was mainly due to both neutrophil infiltration and activation and that the resulting oncotic necrosis could be prevented by inhibiting the neutrophil-induced oxidative stress which leads to hepatocyte mitochondrial dysfunction (196), (233).

We also showed the possible role of monoHER in inhibiting another important pathway in SOS development which is through inhibiting the expression of MMP-9. When MCT is converted into its active metabolite MCT-P through the cytochrome P-450 system, it interacts with F-actin in SECs leading to its depolymerisation. This leads to upregulation of MMP-9 which degrades the collagen in the basement membrane leading to SEC detachment and occlusion of the sinusoids. MMP-9 upregulation may also be related to decreasing the NO concentration in the hepatic veins following MCT intake (40), (228).

The main sources of MMP-9 expression are PMNs and SECs (234), (235). We showed that localization of MMP-9 was mainly within the SEC lining in the first 24-48 hours, however at 72 hours, expression of MMP-9 could also be detected in areas of hepatocellular damage with significantly less expression in the MCT+ monoHER

group. Although we demonstrated that monoHER reduces the influx of inflammatory cells with a significantly lower inflammatory response, previous studies have undermined the role of PMNs in the pathogenesis of SOS following MCT (194). Hanumegowda et al showed that although infiltration and degranulation of PMNs occurs early in the MCT model, this seems to occur away from the centrilobular areas which represent the most heavily affected areas of sinusoidal damage. In addition, PMNs depletion did not prevent the occurrence of sinusoidal damage. Although PMNs might not apparently play a significant role in sinusoidal damage, they definitely play an integral role in hepatocellular damage when activated by thrombin which is released when the coagulation cascade is activated during the disease process (194). DeLeve et al also showed that MMP-9 and to a lesser extent MMP-2 were produced within the basement membrane of SECs and this allows for separation and dissection of the SEC lining by means of erythrocytes (218). This is also in-keeping with our findings as expression of MMP-2 was much weaker than MMP-9 and could not be quantified. Therefore monoHER plays a role in stabilizing the basement membrane of SECs early in the course of the disease and hence less expression of MMP-9 from SECs, and it also prevents hepatocytes damage which occurs as a later secondary event through inhibiting inflammatory cell infiltration and activation by means of its potent anti-oxidant and anti-inflammatory properties.

The importance of MMP-9 inhibition has been highlighted when bevacizumab added to oxaliplatin lead to a significant decrease in the severity of SOS through its role in inhibiting MMP-9 upregulation though blocking VEGF-A (186).

The cause of mortality in patients with severe SOS is usually multiorgan failure which is often triggered by a liver resection in a compromised patient. Treatment then requires a multidisciplinary team management and is mainly supportive,

maintaining the functions of vital organs with proper fluid and electrolyte balance. Specific drugs used in this setting include tissue plasminogen activators and heparin, however these patients are at risk of severe bleeding due to underlying thrombocytopenia (236), (237). Defibrotide is another drug that has been use for treatment of severe SOS with multiorgan failure with promising results in several uncontrolled trials (238), (239). It is a polydeoxoribonucleotide which increases PGE2, PGE1, thrombomodulin and tissue plasminogen activator with a decrease in plasminogen activator inhibitors that are released from the endothelial cells. Although beneficial, no randomized controlled trials exist up to the current date and therefore it cannot be recommended for use in established SOS (236). A recent phosphodiesterase inhibitor has been recently used to prevent SOS and preserve remnant liver function following hepatectomy in a MCT rat model *in-vitro* (240). This study however did not address the effect of this inhibitor on the PP; in addition its role in cancer cell progression is yet uncertain.

The ideal therapeutic agent therefore should be a preventive one, with low toxicity, and with no interference with the cytotoxic activity of the neoadjuvant chemotherapeutic agents. In the current study we used monoHER which is a potent semi-synthetic flavonoid and has been proven to be effective in reducing doxorubicin-induced cardiotoxicity both *in-vivo* and *in-vitro* (220), (221).

MonoHER has the advantage over other experimental therapeutic agents in that it has shown no interference with the cytotoxicity of oxaliplatin in two CRC cell lines when added at different concentrations. This is in agreement with previous studies on doxorubicin-induced cardiotoxicity where monoHER achieved adequate intracellular concentration without interfering with the pharmacokinetics of doxorubicin or its conversion to its active compound doxorubicinol (241),(221).

MCT had no effect on cell proliferation in either CRC cell line *in-vitro*, probably due to the need for its conversion to its active metabolite MCT-P which occurs via the cytochrome P450 system *in-vivo* (192). In addition, monoHER has proved to be safe in a phase I clinical trial and is currently in a phase two clinical trial (222) (223) which might expedite its use for prevention of SOS following oxaliplatin treatment in patients.

Conclusion

We have shown that monoHER is a potential therapeutic agent to be used in prevention of oxaliplatin induced SOS owing to its potent antioxidant and anti-inflammatory, without interfering with the cytotoxicity of the oxaliplatin.

6-Cell therapy and dynamic tracking in an experimental acute liver failure model

6.1 Background

SOS is not only involved in the development of portal hypertension and its sequelae but it has also been shown to have a significant negative impact on liver regeneration with an increased risk of early postoperative complications following partial hepatectomy (29). In a recent report it has been shown that SECs are of BM origin expressing the CD 133 marker. Moreover, BM CD133+ cells were capable of replacing damaged SECs following infusion in an SOS model in rats with a therapeutic benefit (168). Cell therapy therefore might play a role in improving the outcome of oxaliplatin-induced SOS through replacement of damaged SECs. It may also prevent the occurrence of PLF through enhancing hepatocyte regeneration and increasing the remnant liver volume following partial hepatectomy. It would be of great importance however to understand the dynamics of cell uptake in an animal model and to track their distribution and integration into the hepatic parenchyma. Cell tracking in the animal model could be achieved through cell labeling with fluorescent dyes.

We used mouse ESCs which are of unlimited potential and are capable of differentiating into several cell types. An obstacle which we faced was the inability to establish the SOS model in mice using MCT. We therefore used APAP which similar to MCT has an early primary insult to SECs with secondary effect on the hepatocytes (202). For the purpose of cell tracking in mice we established a novel dual labeling fluorescence system to enable *in-vivo* tracking of the transplanted cells without repetitive killing of the animals.

6.2 Results

6.2.1 Dual labeling of mouse embryonic stem cells using the near infra red dye DiR

For the purpose of a meaningful transplantation allowing the possibility to track the cells *in-vivo* using IVIS, we used ESCs which have an unlimited potential to divide and differentiate into different cell types. We used GFP +ve ESCs in order to allow IHC analysis of the tissue using the anti-GFP antibody. Immediate tracking of GFP +ve cells was not possible due to the low wave length of GFP which was associated with high background fluorescence. Therefore we used a NIR dye DiR which proved effective allowing accurate identification of the cells with low background noise using the ICG filter (Fig.37).

6.2.2 MCT-SOS model could not be established in mice

It was not possible to establish SOS in mice using MCT. There was no change in the naked eye appearance of the liver in the MCT mice when compared to the control group. Also, no sinusoidal dilatation or histological evidence of hepatocellular damage could be elicited at any of the time points (Fig.38A). We used APAP which is known to have an early toxic effect on the SECs followed by hepatocellular necrosis (202). At a dose of 300mg/Kg given i.p, it was possible to achieve histological evidence of hepatocyte damage and necrosis comparable to that of MCT in rats at 72 hours (Fig.38B). The mortality from APAP administration was 47.5% (19/40) at 24 hours in both groups and there was no mortality following the first 24 hours.

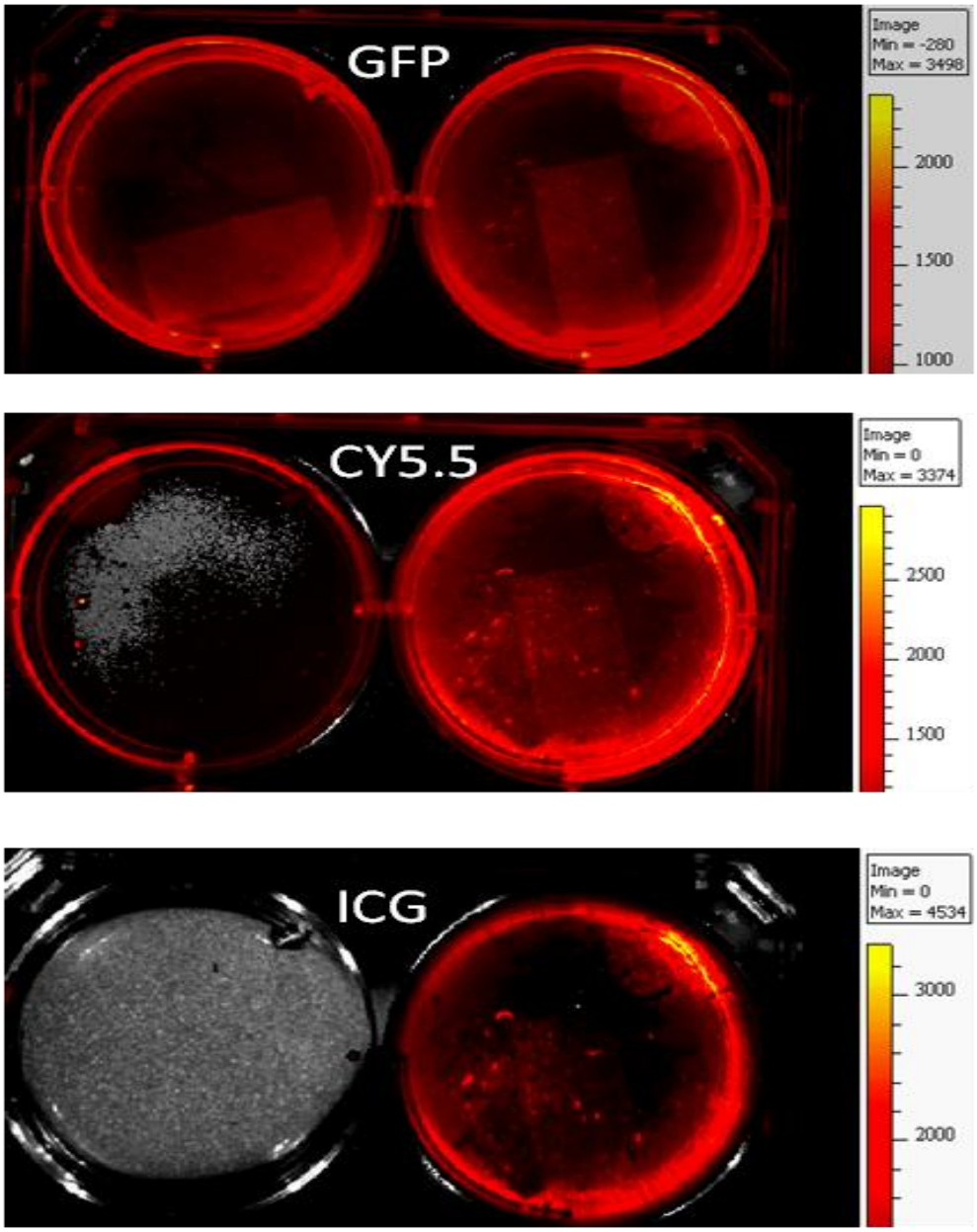

Figure 37 IVIS images of two sets of cell culture plates with GFP +ve ESCs without DiR staining (LT) and with DiR staining (RT) showing background fluorescence using the GFP and CY5.5 filters, but not with the ICG filter.

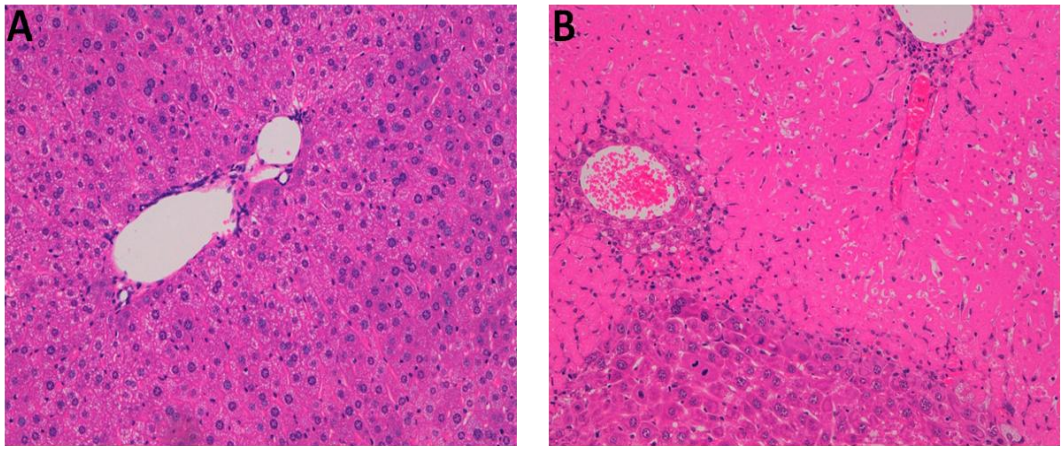

Figure 38 Histological appearance of the liver following MCT administration in mice. No sinusoidal dilatation or hepatocellular damage could be detected in mice treated with MCT at 72 hours (A). When the mice were treated with APAP 300 mg/kg, marked hepatic necrosis was evident at 72 hours (B).

6.2.3 Transplantation and *in-vivo* imaging

$5x10^6$ GFP +ve labeled ESCs with DiR were used per transplantation in 20 mice. IVIS proved to be effective in precisely identifying the cells labeled with DiR in the liver and spleen at different time points. This was possible only using the ICG filter due to its high background passband of 665-695 nm with minimal background fluorescence. At 30 minutes post transplantation, the cells were confined inside the spleen and then gradually moved into the splenic vein and part of the liver at the three hour time point. By 24 hours, the cells spread out over almost all areas of the liver and residual signal was received over the spleen as well. The signal of DiR emitted from the liver faded out at 72 hours. No signal could be detected in any of the other organs (Fig.39).

6.2.4 Ex-vivo imaging

A very clear fluorescent signal was detectable from both the liver and spleen when the organs were taken out and imaged directly with the IVIS. Eliminating the barrier effect of the anterior abdominal wall allowed signal detection at time points when the signal could not be detected by *in-vivo* imaging. Similar to *in-vivo* imaging the ICG filter was the most accurate filter to localize the cells with no autoflourescence from the organs. A weak signal was also detectable in the lungs and kidneys in contrast to the *in-vivo* imaging (Fig.40A). DiR uptake in the liver was significantly higher than the sum of uptake in all other organs at 72 hours ($p<0.0001$). At two weeks, the total number of photons emitted from the liver decreased significantly from $3.67\times10^{10} \pm 1.7\times10^{10}$ photons/sec at 72 hours to $5.18\times10^{9}\pm1.58\times10^{9}$ ($p=0.002$). However, in the liver, the emission was still significantly higher than the spleen ($p=0.002$), lungs ($p<0.0001$) and kidneys ($p<0.0001$) (Fig.40B).

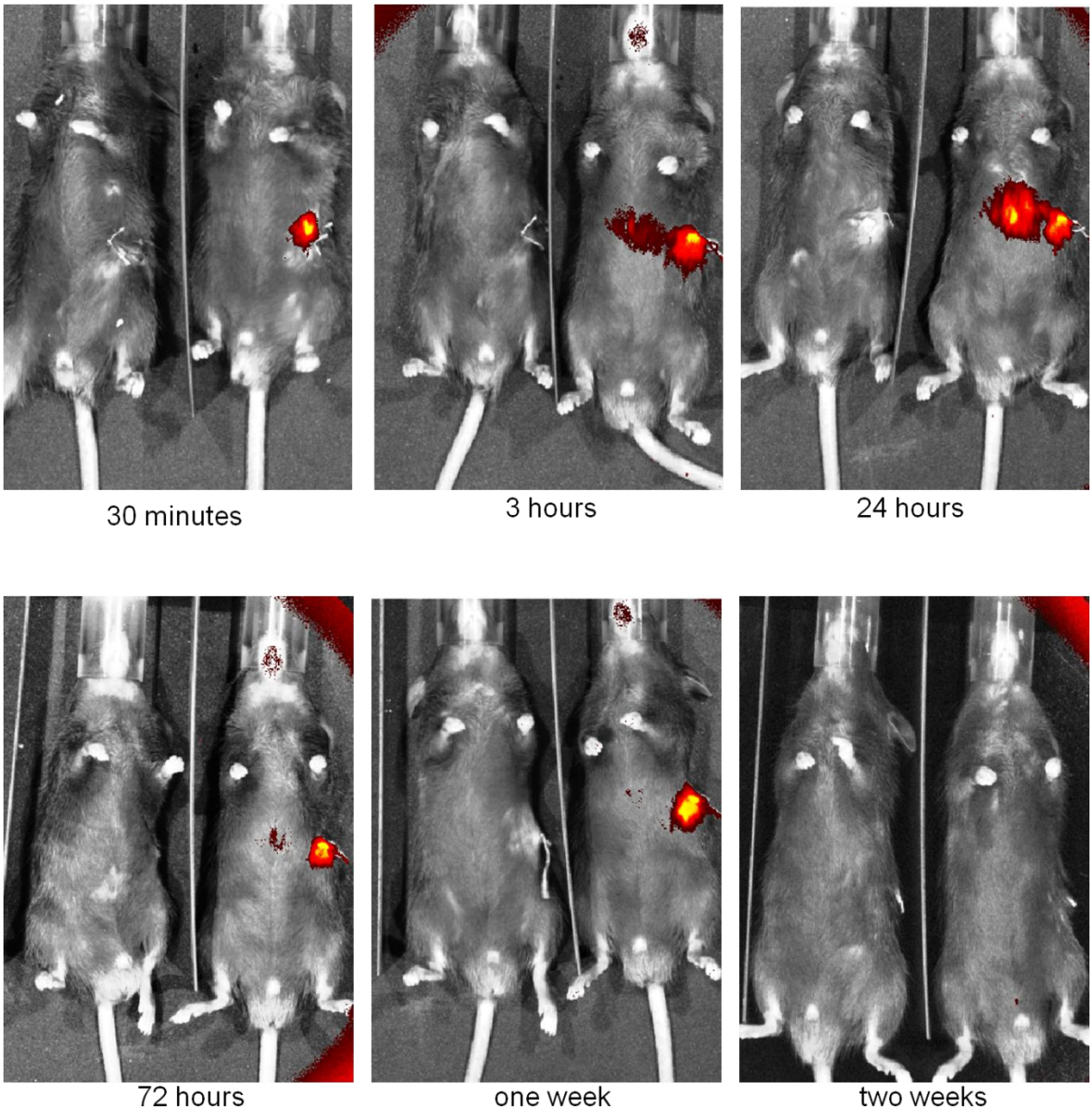

Figure 39 Labeling and tracking of the fluorescent ESCs following APAP administration. Images of a pair of mice (cell therapy group-RT) compared with the (control group-LT) using IVIS. At 30 minutes following transplantation, a strong signal could only be detected from the spleen where the cells were injected. Between 3 and 24 hours following the cell transplantation, signal started to intensify between the spleen and the liver which is most probably the splenic vein owing to its tortuous course. A strong signal was detected over the liver 24 hours post-transplantation which faded out by 72 hour time period. At one week, the signal could not be detected over the liver but still strong was detectable over the spleen which completely disappeared by two weeks.

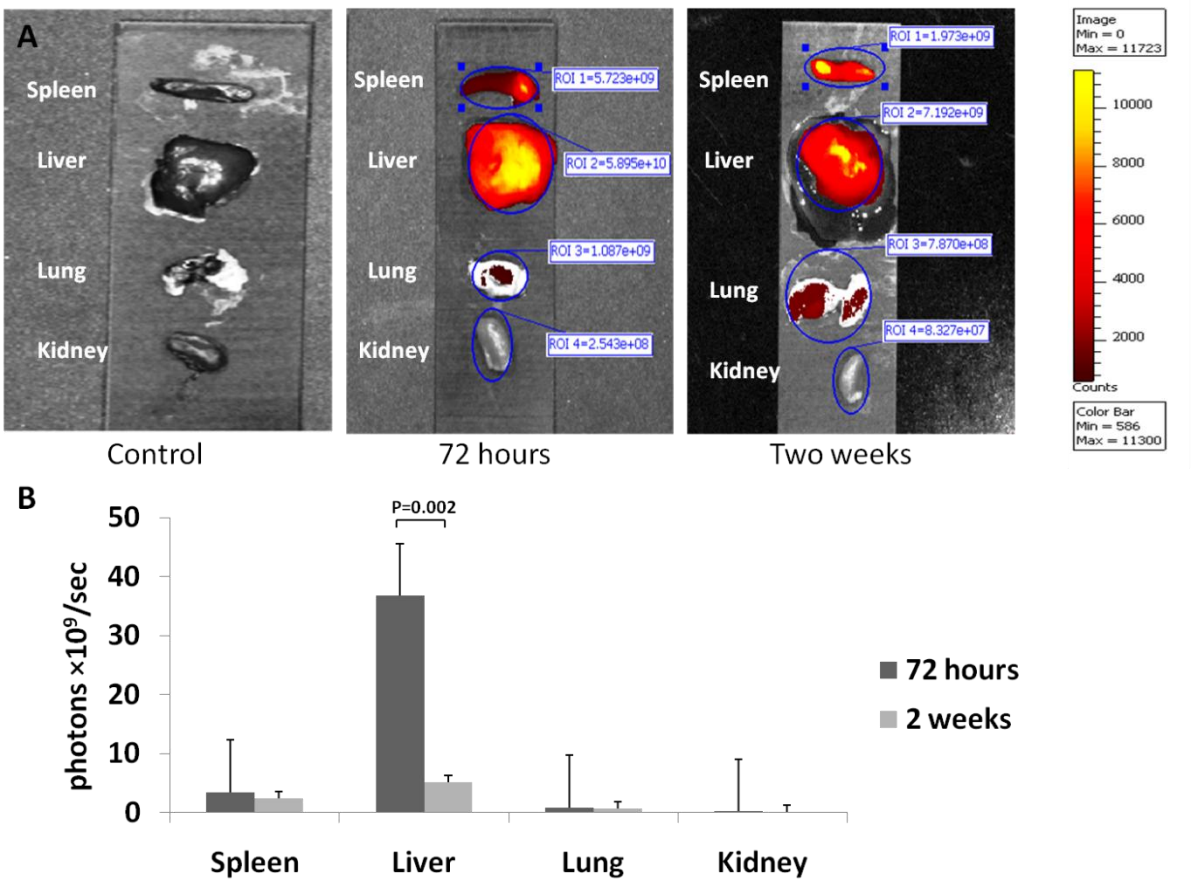

Figure 40 *Ex-vivo* images showing the distribution of fluorescent cells in different organs as detected by the ICG filter of the IVIS. A signal was detected at the site of injection in the spleen however; the highest signal was noticed in the centre of the liver at 72 hours, which faded out after two weeks. A weak fluorescent signal was also detected in the lungs at 72 hours and two weeks but not seen in kidneys at any of the designated time points (A). A graph showing the highest uptake of cells in the liver at all time points with a significant drop at two weeks (B).

6.2.5 Engraftment of the transplanted cells in the liver

Frozen liver sections were examined under the fluorescent microscope to detect GFP +ve transplanted cells in the liver parenchyma. This was to confirm that the signal detected using the IVIS was definitely emitted from the engrafted cells and not from the fluorescent DiR dye released following cell death. GFP fluorescence from the transplanted cells was easily detectable by direct fluorescence microscopy at 72 hours, however, the signal was much weaker at two weeks and therefore, we relied on IHC using an anti-GFP antibody for detection. At 72 hours, discrete GFP +ve colonies were located under the liver capsule and around the central veins (Fig. 41A). At two weeks, GFP +ve cells resembling hepatocytes were seen dispersed throughout the hepatic parenchyma with the presence of a larger number of GFP +ve cells incorporated within the sinusoidal endothelial lining (Fig. 41E). GFP +ve cells could still be detected after two weeks in the spleen, mainly around the central arteriole and the trabeculae (Fig. 41F).

6.2.6 Liver functions

All mortality occurred during the first 24 hours following APAP administration with 10/40 (25%) mice in the control group and 9/40 (22.5%) in the cell therapy group. All animals surviving the initial 24 hours lived till the time of sacrifice. Liver damage was detected at 72 hours, most prominent in the centrilobular regions with hepatocyte necrosis and secondary infiltration of inflammatory cells in both the cell therapy and the control group (Fig.41C,D). Improvement in liver histology was noticed both in the cell therapy and the control groups at two weeks with less inflammatory cell infiltration in the treatment group (Fig.41G,H).

In order to identify the nature of the transplanted cells, we stained the sections with anti-albumin antibody which revealed very faint albumin expression in the GFP+ cells at 72 hours (Fig.42A,B). However, at two weeks cells positive for GFP were also strongly positive for albumin (Fig.42C,D). There was a significant improvement in serum levels of ALT, albumin and bilirubin in both groups at two weeks when compared to the 72 hour time point (Fig.43). Cell therapy itself had no effect on any of these parameters at the 72 hour time point when compared with the control group. However, at two weeks, serum ALT was significantly lower in the cell therapy group when compared to the control group ($p=0.016$) (Fig. 43A). Also, serum albumin level was significantly higher in the cell therapy group ($p=0.009$) (Fig.43B). No significant changes occurred in serum bilirubin or urea levels between both groups at two weeks. (Fig.43C, D)

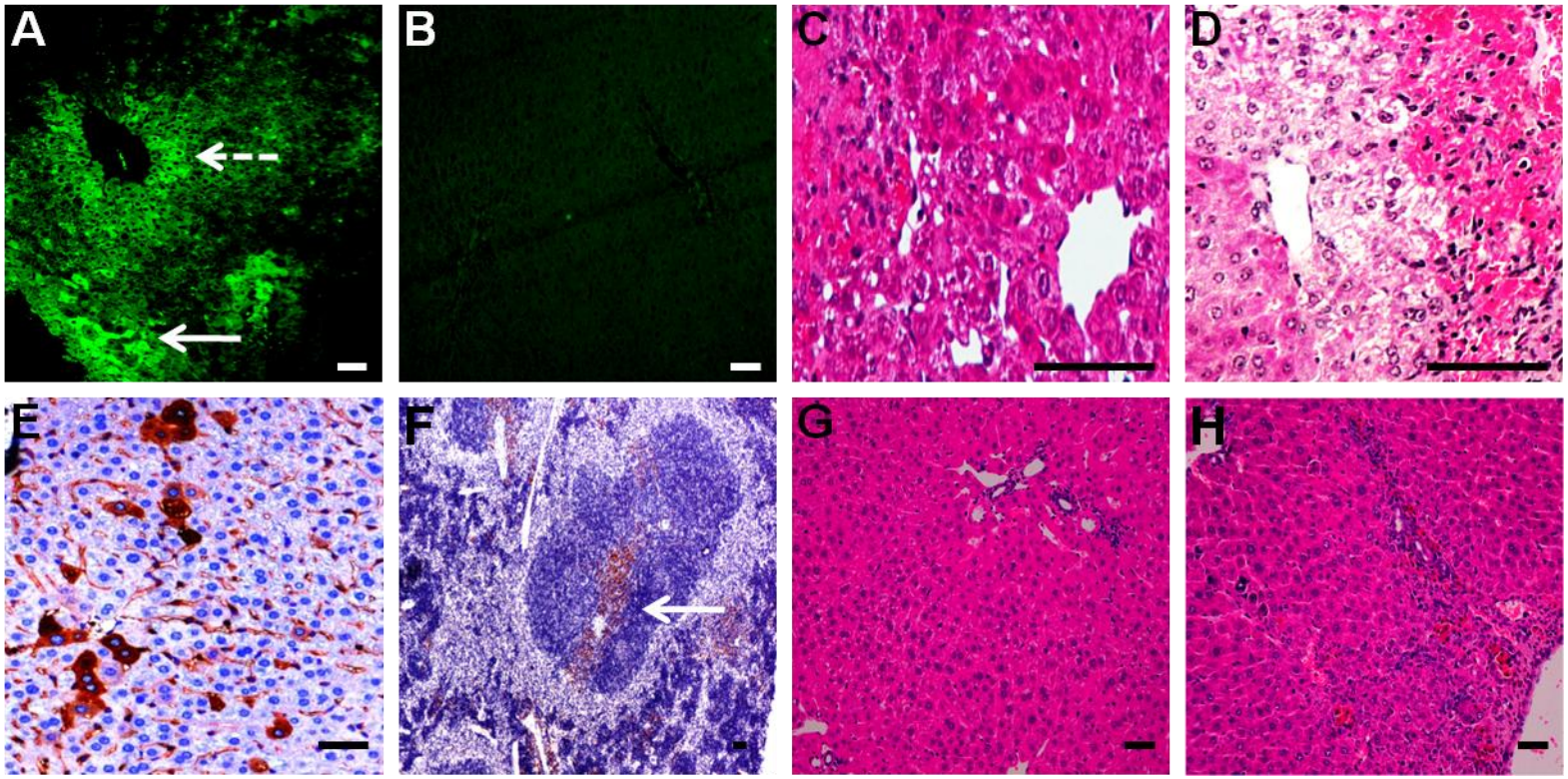

Figure 41 ESC liver engraftment following APAP induced damage. GFP +ve cells were present under the liver capsule (A-solid arrow) and around the central veins of the liver at 72 hours as seen under direct fluorescence (A-dashed arrow) with no fluorescence detected in the control group (B). Characteristic pattern of APAP induced liver damage after 72 hours affecting mainly the centrilobular portions of the liver with marked damage of the pericentral hepatocytes in both the cell therapy and control groups although pericentral vacuolation was more evident in the control group (C,D). At 2wks, the GFP +ve cells could be detected using IHC in the hepatic parenchyma and within the sinusoidal lining (E). Localized colonies of GFP +ve cells were also detected in the spleen at 2 weeks (F). After 2 weeks the liver recovered in both groups with the liver sections from the cell therapy group (G) showing less inflammatory cells and congestion than in the control group (H)(Scale bar=200µ)**.**

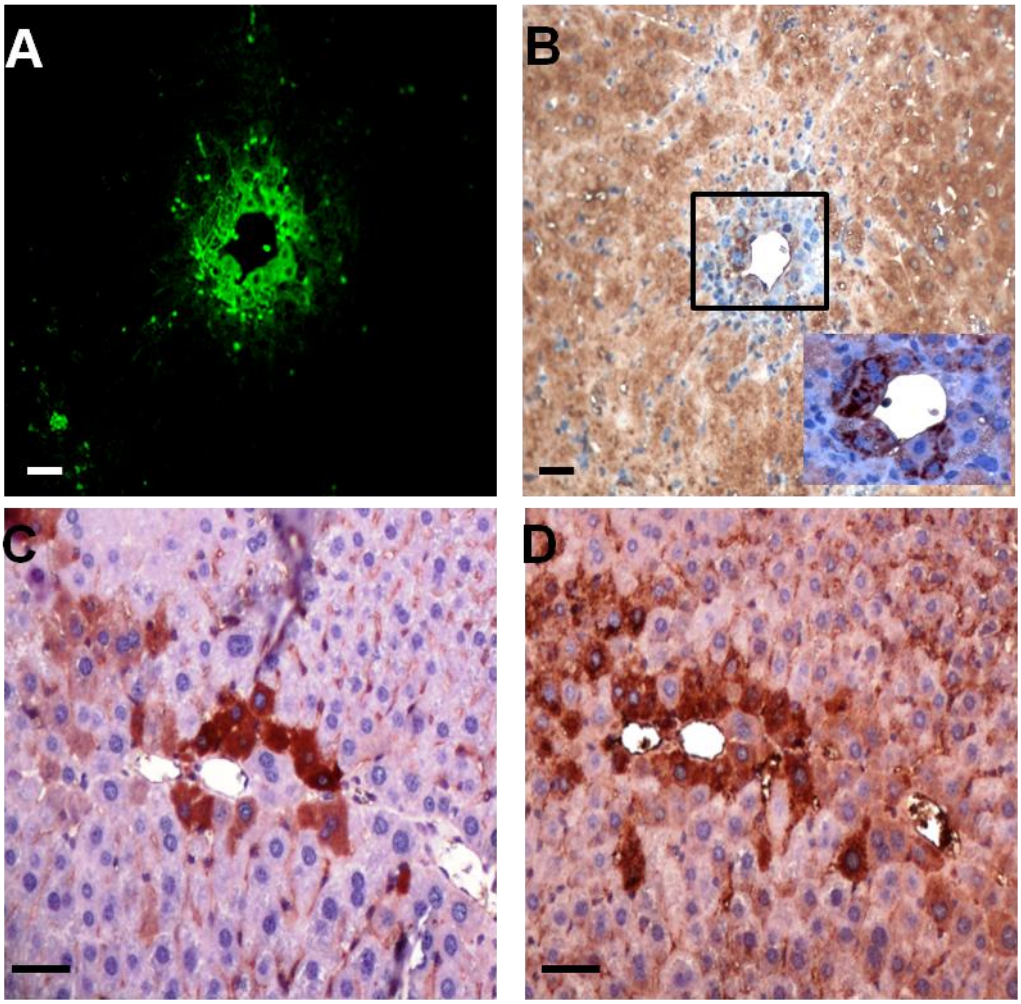

Figure 42 Serial sections examined for GFP and Albumin expressions. GFP +ve transplanted cells (A) showed very faint albumin expression at the cell periphery of dividing cells at 72 (B), whereas areas stained with anti-GFP antibody (C) were positive for albumin (D) at 2 weeks following cell therapy (Scale bar=100µ).

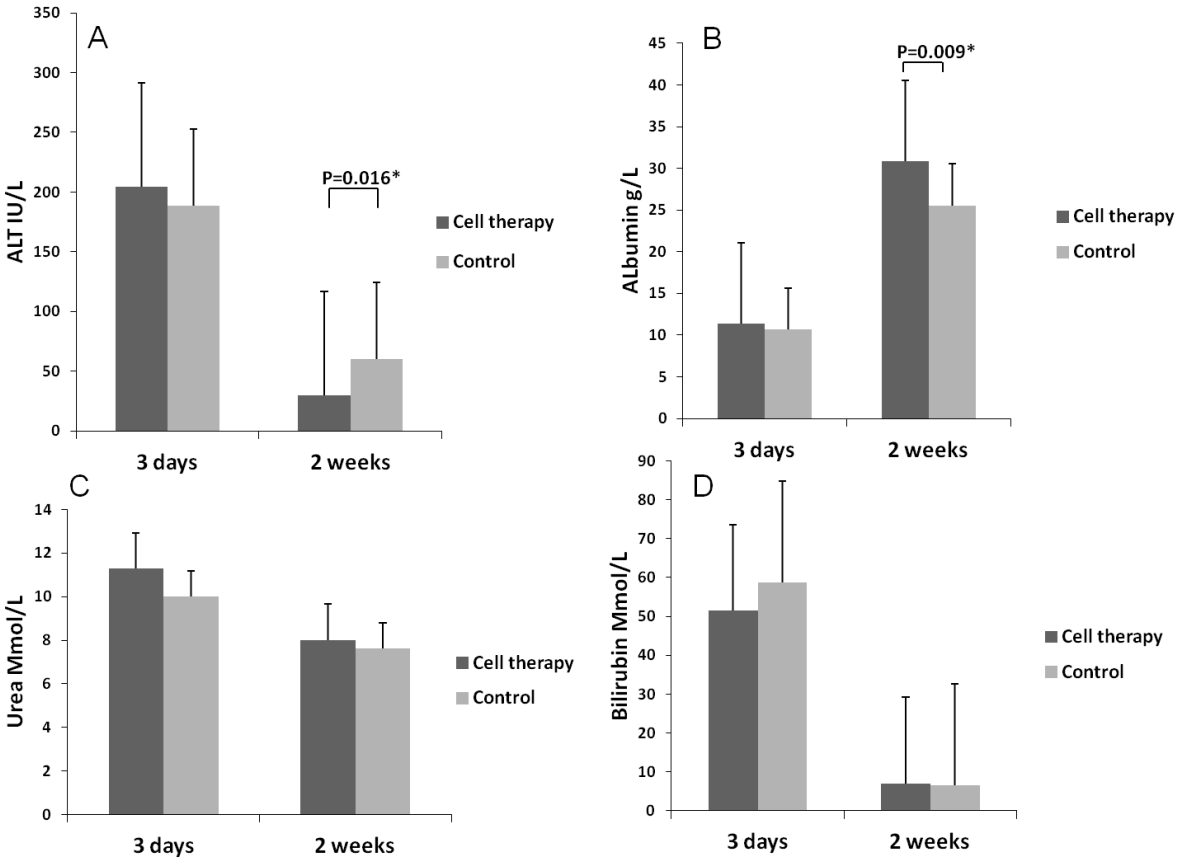

Figure 43 Serum levels of ALT, Albumin, Bilirubin and Urea are shown. ALT level significantly dropped in both groups at two weeks when compared with the 72 hour time point. When compared with the 72 hours, there was a significant reduction in serum ALT level at two weeks in the ESC treatment group only but not in the control group (A). Albumin level also improved in both groups with level being significantly higher in the cell therapy group when compared with the control group at two weeks (B). The drop in urea levels was not significant in both groups. (C) Bilirubin levels dropped significantly from 72 hours to two weeks with no significant differences between groups at similar time points (D).

6.3 Discussion

In this study we used mouse ESCs which have an unlimited supply and an enormous potential to differentiate into different cell types including hepatocytes. We also developed a novel model in which we were able to monitor both the immediate and late kinetics of transplanted ESC cells. In this way, we were able to track the cells real-time over days after the injection and had a better understanding of the dynamics of the cells in an experimental model of ALF without the need to sacrifice animals at different time points.

Although it was possible to induce SOS in rats by using MCT, similar results could not be established in mice. It is known that MCT is converted into MCT-P which is the active metabolite produced by cytochrome P-450 3A (242). There are no studies that support the role of MCT in SOS development in mice, furthermore, when MCT was used to induce the pulmonary hypertension in mice the effects were much more attenuated when compared to rats and this again has been attributed to differences in metabolic pathways involved in MCT activation between rats and mice (243). We therefore used APAP to induce sinusoidal damage and ALF in mice. The sinusoidal damage in APAP similar to MCT precedes hepatocellular necrosis disrupting the space of Disse with gap formation in SEC lining eventually leading to SEC separation from the hepatocytes (244) (245). Also similar to MCT-induced SOS, MMP-9 is upregulated with APAP toxicity and its inhibition attenuated both the sinusoidal and hepatic parenchymal injury in C57BL/6 mice (246).

So far, most of the existing animal models looked into the role of cell therapy in liver regeneration following partial hepatectomy or hepatocellular damage induced by CCL4, (247), (248),(249), (250). In these models the roles of cell therapy were not

studied in a pathophysiological milieu reciprocating the clinical scenario of ALF (251). For example, following liver resection the liver bed reduces drastically and resection itself mobilizes the CD 133+ subset of cells from BM into the circulation, which might have played an independent role in liver regeneration (252). Moreover, CCL4-induced liver damage builds up over a period of time and does not produce the similar profound effects of ALF (251). In this study, we used an ALF model induced by APAP at a relatively moderate dose of 300 mg/kg and transplanted the undifferentiated ESCs four hours following induction of injury so that most of the APAP would have been metabolized and would not interfere with ESCs survival (183). In order to track the cells *in-vivo*, we used a reproducible imaging system for continuous real-time monitoring of the injected cells following transplantation. The IVIS is a relatively new optical imaging system that is being widely used in the fields of oncology and immunology allowing non-invasive cell detection and migration (253). NIR dyes have been previously used for monitoring cells *in-vivo* with improved quality of signal detection through increasing the contrast between the signal and the background which is comprised mainly of water, oxyhaemoglobin and deoxyhaemoglobin (254). This has made it possible to track labeled cells located in deep seated organs with minimal background fluorescence. To achieve that goal, we labeled the ESCs with a NIR lipophilic tracer dye DiR which has the advantage of very low cell toxicity and laterally diffuses within the cell membrane, hence staining the whole cell. Very recently, Chois *et al* (255) used luciferase transfected fetal hepatocyte cells for repopulating liver in a MCT injected mice model and nicely showed the uptake of the cells by a CCD camera generated images. The advantages of the imaging we used in this study lies with the simplicity of the method. This technique is relatively cheap and easy to use without any necessity of genetic

manipulation of the cells. Also there is no necessity to inject any extra dye for visualisation of the cells which might interfere with body chemistry and prolong the anaesthetic duration for the animals. The cells could be clearly seen migrating from the spleen to the liver. The signal intensity in the liver was highest between the second and third days post-transplantation, possibly because cell proliferation is highest at that time (78). A rapid drop in the signal intensity was noticed after the third day and continued to fade till it completely disappeared at two weeks post transplantation. Similar to the DiR dye we used, the signal from firefly luciferase also dropped on day 10 following HT (255). However, visualisation and quantification of the transplanted cells was still possible at two weeks by DiR imaging when the organs were extracted and imaged directly under the IVIS.

Because the ESCs were transfected with GFP; it was possible to observe the distribution of the transplanted cells in tissue sections directly under the fluorescent microscope or by IHC using the anti-GFP antibody. Engraftment of the ESCs was confirmed in liver tissue sections in the post-transplantation period by direct visualization of GFP+ cells, which appeared in the close vicinity of the central veins where the main brunt of the damage has occurred. The homed pericentral cells subsequently proliferated and spread throughout the liver parenchyma. The mechanism through which the ESCs integrate into the liver plate depends primarily on the disruption of the SECs (256). Although APAP overdose characteristically affects the centrilobular regions of the liver causing extensive necrosis; there is also a direct toxic effect on the SECs through glutathione depletion (202) and thus might have played a role in uptake of cells into the liver parenchyma particularly since GFP +ve cells were also detected in the sinusoidal endothelial lining at two weeks.

ESC transplantation did not improve either survival or liver functions at 72 hours. At two weeks, some transplanted cells expressed albumin and morphologically resembled hepatocytes. In accordance, there was a significant reduction in serum ALT and an increase in serum albumin production at two weeks in the cell therapy group when compared to the control group. It is unlikely that the differentiation of transplanted cells into hepatocytes could explain the improved liver functions at two weeks in the cell therapy group since the cells were few and we did not perform additional studies to confirm differentiation as this was not the purpose of the study. The paracrine effect of the transplanted cells rather than direct differentiation seems to be a more possible reason for improved liver functions. MSC conditioned media has been shown to improve liver functions following induction of ALF in rats. (257), also proteins released from human undifferentiated ESCs was shown to improve cardiac functions (258).

ESC therapy has been riddled with several problems including allogenic rejection, ethical concerns and most importantly, possibilities of malignant transformation. Although Moriya et al did not detect any teratoma formation following transplantation of undifferentiated ESCs in a liver cirrhosis model in mice (259), the transformation of undifferentiated ESCs into teratomas is very likely after a period of time. We used undifferentiated ESCs in this study to develop a suitable model to study the kinetics of transplanted cells in ALF; however, to study the therapeutic effect of ESCs in ALF, ideally we should have used differentiated ESCs, pluripotent stem cells or primary hepatocytes. Differentiation of ESCs *in-vitro* into hepatocytes has been extensively studied by several groups and could be achieved by formation of EBs (146), or directly by adding growth factors to the ESCs in monolayer cultures (147). However, full maturation of hepatocytes is not complete without the influence

of the intrinsic environment (260). Several studies have been conducted to simulate the inductive microenvironment *in-vitro*, either through co-cultures with hepatocytes (261) or using conditioned media in *in-vitro* cultures (262).

We concluded that serial longitudinal tracking of transplanted cells in a mouse model of ALF induced by APAP is possible using IVIS and that dual labeling would allow both immediate and longterm tracking of the transplanted cells which would allow us to better understand their differentiation and fate.

7-Discussion and future directions

SOS is a serious clinical condition that has been known to result from myeloablative chemo-radiotherapy in preparation for HSC transplantation. SOS has also been shown to occur following oxaliplatin based neoadjuvant chemotherapy in order to downstage CLMs prior to liver resections. This condition leads to increased blood loss during liver resections with increased hospital stay and a higher occurrence of PLF in the immediate postoperative period with high morbidity and mortality. The only effective treatment of PLF is LT however may not always be possible due to shortage of liver donors and the high mortality associated with PLF and the problem of cancer and immunosuppression. Recent studies have also reported the important role of SECs in liver regeneration through the release of certain growth factors which stimulate hepatocyte regeneration. Moreover, in an experimental rat model of SOS, delayed liver regeneration following liver resection has been proven (189), (263), (64), (191), (90), (95).

The ideal management of PLF should therefore be a preventive one with a strategy to eliminate the predisposing factors; one of which is oxaliplatin-induced SOS prior to liver resection for CLMs. There is also difficulty in estimating the functional liver reserve following liver resections as the non-tumorous liver may not have an adequate regenerative capacity owing to the SEC damage and delayed hepatocyte proliferation (90).

From here comes the importance of planning a strategy to prevent the occurrence of SOS in addition to increasing the functional residual liver reserve to prevent the development of PLF.

We used MCT to induce SOS in rats simulating clinical SOS, in addition to showing the structural and ultra-structural events that occur following MCT administration

through H&E and EM studies. We also studied the MMP pathways through IHC and showed that SOS is mainly related to upregulation of MMP-9.

In order to prevent SOS, we used a semi-synthetic flavonoid monoHER which has been previously used in prevention of doxorubicin-induced cardiotoxicity. We showed that monoHER was effective in reducing SOS induced portal hypertension in rats with significantly lower ALT measurements especially at the 72 hour time point corresponding with the peak of MCT induced liver damage. We also showed that monoHER improved the liver damage score through a decrease in sinusoidal dilatation, hepatic necrosis and inflammatory cell infiltration. MonoHER proved to be effective in significantly downregulating the MMP-9 activity at 72 hours post-MCT administration. The advantage of monoHER over other drugs is its safety to be used in patients and that it does not interfere with the cytotoxic effect of oxaliplatin which would make it an ideal preventive drug owing to its potent vascular protective and anti-inflammatory properties (225), (227).

Predicting the subgroup of patients who are more likely to develop high grade SOS and hence PLF has been investigated by several groups, however with no convincing evidence. Importance of this would be to postpone surgery in patients who are at risk of high grade SOS in order to prevent SOS (51), (41). There is a growing interest in using Micro RNA (MIR) which is a short non-encoding RNA sequence for diagnostic purposes. We performed a preliminary experiment to investigate whether MIR-126 which is expressed in and specific to endothelial cells would be upregulated in SOS. We confirmed this by detecting a 26-fold increase in expression of MIR-126 in HUVEC cell lines when compared to normal control liver tissue. We showed that miRNA-126 expression in liver tissue increased with the severity of MCT injury but remained stable in the control group (Fig.44). Harris et al, showed

that MIR-126 was specific to endothelial cells as they were not expressed in vascular smooth muscle cells or in lymphocytic cells. They also showed that MIR-126 regulates the expression of VCAM-1 which increases with damage to endothelial cells and is responsible for leukocyte adhesion to endothelial cells at the site of injury (264). Therefore MIR-126 expression might be related to the inflammatory response which was significantly higher at 72 hours in this study. When the rats were pretreated with monoHER, MIR-126 expression was lower in the MCT+ monoHER group when compared to the MCT group. This might be explained by the fact that monoHER reduces MIR-126-VCAM overexpression (227) (Fig.44). (Appendix 1).

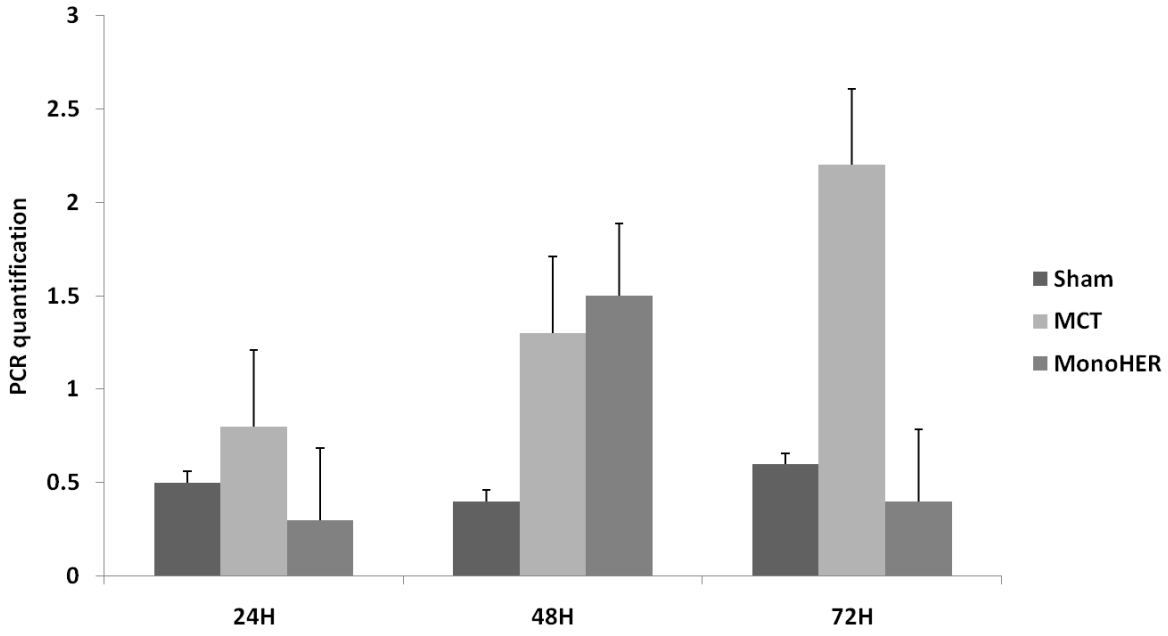

Figure 44 Mir126 expression in the three studied groups at different time points. A steady increase with time in the MCT group; however expression was five-fold lower in the MCT+ monoHER group when compared to the MCT group at 72 hours.

MIR-126 could serve as a potential marker to predict SOS development and patient stratification into low and high risk groups according to the expression. More experiments need to be conducted including isolating MIR-126 from the serum of

patients which if proved successful would be a simple non-invasive predictive marker.

In addition to preventing the development of SOS, it would be important to increase the functional liver reserve following partial hepatectomy. This would be possible through either stimulating the endogenous hepatocyte population or through an exogenous cell transplantation. Since the regenerative drive of hepatocytes is suppressed in the chemotherapy liver (90); therefore future therapies should focus on either hepatocyte or ESC transplantation with the potential to differentiate into hepatocytes either. It is important however to understand the dynamics of the transplanted cells and the time points at which they engraft in the liver and start to function which would dictate the time points when a cell transplantation would be effective.

We developed a dual labeling tracking system in order to track the cellular events in an APAP model of ALF in mice. It was not possible to induce SOS using MCT in mice, however APAP-induced ALF has several advantages as it simulates the events occurring in SOS with early SEC damage followed by hepatocyte necrosis (265), (245). In addition, it represents a more acute liver damage model providing an adequate drive for cell engraftment. APAP-induced ALF therefore resembles PLF with chemical injury in the non-tumorous liver and serves as a good model for the purpose of cell tracking.

We showed that cell tracking in the acute liver failure setting is possible with the real time events easily monitored using the IVIS without the need to sacrifice the animals at several time points. The dual labeling methodology allowed IHC studies on tissue sections once the animals were sacrificed. In this study we used ESCs in order to

achieve a meaningful population for transplantation. ESCs can be grown indefinitely *in-vitro* and provide sufficient numbers of cells for transplantation. We used DiR for labeling the ESCs which has an excitation peak at 750nm and an emission peak at 782 nm which are well within the NIR range and higher than background tissue autoflourescence. Advantages of this dye include minimum lateral cell to cell transfer and very low toxicity. Although DiR has not been approved for use in patients; it shares very similar excitation/emission spectra with FDA-approved ICG which has been used for labeling human ESC derived cardiomyocytes (181). Although several studies have investigated the role of ICG in cell labeling *in-vitro*, there have been no studies to report its use *in-vivo* (266), (267). In the present study, we could track the migration of transplanted cells as early as three hours from the spleen to the liver with a signal appearing in the liver at 24 hours. There was decay in the transmitted signal starting from day three with complete loss of the signal at two weeks. This was not due to death of transplanted cells as a signal could be detected when the organs were displayed and imaged *ex-vivo*. Similar to our study, Boddington et al reported a rapid decay of the signal at 48 hours when the cells were imaged *in-vitro* using ICG labeling (181). Therefore labeling with NIR dyes is considered an efficient method for acute phase cell tracking providing useful information on cell migration and engraftment optimizing stem cell delivery schedules and techniques. This imaging technique carries great potential for clinical application in various fields of research including islet and stem cell transplantation.

In terms of therapy, undifferentiated ESCs would not be optimal for rescuing patients with ALF as the amount of time required for differentiation would extend beyond the acute events of PLF. The improvement in liver functions following undifferentiated ESCs transplantation could not be explained by the small number of

albumin positive cells which have differentiated from the transplanted ESCs. This improvement might be related to certain factors released from the ESCs might have reduced the inflammatory response and stimulated the regenerative drive of the resident hepatocytes through HGF and VEGF production (258), (268). There is a significant risk of teratoma formation if ESCs were to be transplanted in the undifferentiated state (269). Alternative options might include the use of bile duct cells which share the common embryological origin with the liver and have been previously shown to transdifferentiate into hepatocytes (88). It would be ideal to isolate biliary epithelial cells from the gall bladders that would be removed at the time of partial hepatectomy and discarded. The isolated cell population would be expanded *in-vitro* and then transplanted back to the patient in the postoperative period preventing and/or stabilizing the developing PLF without the need for immunosuppression. We attempted a preliminary experiment to isolate rat bile duct cells and culture them *in-vitro*, however most cells were transformed into fibroblasts after 10 days of culture (Appendix-2). There are two main obstacles to using biliary epithelial cells in patients with acute liver failure; first of which is the need for a stressful stimulus to expand the oval cell population in the gall bladder which is achieved experimentally via bile duct ligation (BDL). Irie et al could not culture or identify cells with hepatocyte phenotypes when biliary epithelial cells were isolated from normal mouse and they showed that BDL was essential for the appearance of the C-Kit^{+} epithelial cells which are considered hepatocyte progenitor cells (270). Lee et al used gallbladder cells from normal mice and transplanted into mice with induced liver failure to investigate whether these cells could acquire phenotypic characteristics of hepatocytes and whether these would repopulate the damaged liver. Of interest, is that partial hepatectomy was a weak stimulus for engraftment when

compared to chemical injury, in addition freshly transplanted cells had a much better engraftment rate than when cultured *in-vitro* and then transplanted. The overall percentage of engraftment however was very low and colonies were localized in discrete areas of the liver. A few of these cells acquired a hepatocyte phenotype however this occurred several months following transplantation (88).

Another alternative would be *in-vitro* differentiation of ESCs into functional mature hepatocytes to achieve therapeutic benefit. Several methods of differentiation have been described (147), (262), (271), (272). We attempted *in-vitro* differentiation of ESCs into hepatocytes via formation of EBs (Fig.45) (Protocol for EB formation. Appendix 3).

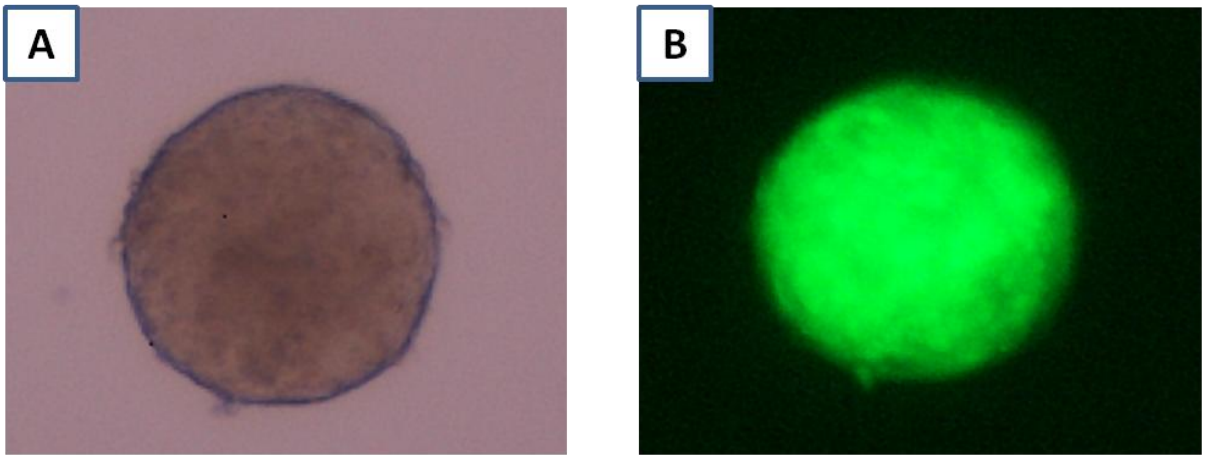

Figure 45 well-formed EBs in culture using GFP+ C57BL6 mouse embryonic stem cells using the static suspension method (A) Under fluorescence microscopy (B).

The next step would be a directed differentiation into definitive endoderm followed by hepatocyte differentiation and maturation. Directed definitive endoderm differentiation is essential step as visceral endoderm which may give rise to cells with hepatocyte markers would be fated to form tumours *in-vivo* (273). It is therefore essential also to achieve a large population of uniform cells which would be suitable for transplantation. These problems still need to be addressed as large numbers of

cells are lost during the differentiation process leading to a small cell yield that would not be sufficient for function replacement in the setting of PLF.

Conclusions

Surgeons are often confronted with a big challenge to perform partial hepatectomy for intended curative resections in patients with advanced tumours or with advanced cirrhosis. While neoadjuvant chemotherapy is effective in shrinking CLMs, it has deleterious effects on the non-tumorous liver predisposing to PLF. None of the current therapies have proven to be effective in treating PLF and LT which might be curative remains a debatable option due to the high mortality associated with the condition. Prevention of the condition from occurrence should therefore be the best approach and this may be through prevention of development of SOS through monoHER administration and by expanding the remnant liver volume following liver resection using cell therapy. Currently, HT is being effectively used to treat in born errors of metabolism especially in children, however in order to replace LT; greater numbers of differentiated cells from other sources with hepatocyte functions need to be used. The timing and degree of optimum differentiation of these cells and the capacity of the *in-vivo* inductive microenvironment to complete the differentiation process without tumour formation needs to be further investigated.

Presentations arising from the studies contained in this thesis

1- Tarek Ezzat, Dipok Dhar, Steven OldeDamink, Massimo Malago. Dual labeling of embryonic stem cells for dynamic tracking in an acetaminophen induced model of injury in mice. *World congress of stem cells and regenerative medicine*, San Francisco, USA. Jan 20-21/ 2010

Winner of UCL poster award for faculty of biomedical sciences, 2010

2- Tarek Ezzat, Dipok Dhar, Massimo Malago, Steven OldeDamink. Embryonic stem cells improve liver functions and express albumin following transplantation in a model of acute liver failure in mice. *Stem cells, development and regulation, Amsterdam***,** NL. October 12-14, 2010

3- **Tarek Ezzat**, Dhar D, Malago M, Steven OldeDamink. Novel semi-synthetic flavonoid prevents MCT Induced Sinusoidal Obstruction Syndrome in Rats. The Royal Free and University College London Medical School, Pearce Gould Visiting Professor, October 2010

4- **Tarek Ezzat**, Dhar D, Malago M, Steven OldeDamink. The role of a novel semi-synthetic flavonoid (MonoHer) in preventing monocrotaline induced sinusoidal obstruction syndrome in rats. SARS annual meeting, Dublin, January 4-5, 2011

BRITISH JOURNAL OF SURGERY Volume: 98 Pages: 20-20 Supplement: Suppl. 2 Published: APR 2011

Publications arising from the studies contained in this thesis

1- **Ezzat TM**, Dhar DK, Newsome PN, Malagó M, Olde Damink SW. Use of hepatocyte and stem cells for treatment of post-resectional liver failure: are we there yet? *Liver Int* 2011;31:773-84.

2- **Ezzat TM**, Dhar DK, Malagó M, Olde Damink SW. A simple and effective way for *in-vivo* dynamic tracking of embryonic stem cells in an acute liver failure model in mice. *World Journal of Gastroenterology* 2011;18:498-506

3- **Ezzat TM**, van den Broek M, Davies A, Dejong C, Bast A, Malagó M, Dhar D, Olde Damink SW. The flavonoid monoHER prevents monocrotaline-induced hepatic sinusoidal injury in rats. *Journal of Surgical Oncology* 2012 Jan 27. doi: 10.1002/jso.23046. [Epub ahead of print]

References

1. Squires RH Jr, Shneider BL, Bucuvalas J, Alonso E, Sokol RJ, Narkewicz MR, et al. Acute liver failure in children: the first 348 patients in the pediatric acute liver failure study group. J Pediatr 2006;148:652-8.

2. R, Williams. Classification, etiology, and considerations of outcome in acute liver failure. Semin Liver Dis 1996;16:343-8.

3. Sokal EM, Goldstein D, Ciocca M, Lewindon P, Ni YH, Silveira T, et al. End-stage liver disease and liver transplant: current situation and key issues. J Pediatr Gastroenterol Nutr 2008;47:239-46.

4. Lucey MR, Schaubel DE, Guidinger MK, Tome S, Merion RM. Effect of alcoholic liver disease and hepatitis C infection on waiting list and posttransplant mortality and transplant survival benefit. Hepatology 2009;50:400-6.

5. van den Broek MA, van Dam RM, Malagó M, Dejong CH, van Breukelen GJ, Olde Damink SW. Feasibility of randomized controlled trials in liver surgery using surgery-related mortality or morbidity as endpoint. Br J Surg 2009;96:1005-14.

6. Otsuka Y, Duffy JP, Saab S, Farmer DG, Ghobrial RM, Hiatt JR, Busuttil RW. Postresection hepatic failure: successful treatment with liver transplantation. Liver Transpl 2007;13:672-9.

7. Mayo SC, Pawlik TM. Current management of colorectal hepatic metastasis. Expert Rev Gastroenterol Hepatol 2009;3:131-4.

8. Khan SA, Toledano MB, Taylor-Robinson SD. Epidemiology, risk factors, and pathogenesis of cholangiocarcinoma. HPB (Oxford) 2008;10:77-82.

9. Geoghegan JG, Scheele J. Treatment of colorectal liver metastases. Br J Surg 1999;86:158-69.

10. Abdalla EK, Adam R, Bilchik AJ, Jaeck D, Vauthey JN, Mahvi D. Improving resectability of hepatic colorectal metastases: expert consensus statement. Ann Surg Oncol 2006;13:1271-80.

11. Pawlik TM, Schulick RD, Choti MA. Expanding criteria for resectability of colorectal liver metastases. Oncologist 2008;13:51-64.

12. Lytratzopoulos G, Tyrrell C, Smith P, Yelloly J. Recent trends in liver resection surgery activity and population utilization rates in English regions. HPB (Oxford) 2007;9:277-80.

13. Cescon M, Vetrone G, Grazi GL, Ramacciato G, Ercolani G, Ravaioli M, et al. Trends in perioperative outcome after hepatic resection: analysis of 1500 consecutive unselected cases over 20 years. Ann Surg 2009;249:995-1002.

14. Kiuchi T, Kasahara M, Uryuhara K, Inomata Y, Uemoto S, Asonuma K, et al. Impact of graft size mismatching on graft prognosis in liver transplantation from living donors. Transplantation 1999;67: 321-7.

15. Mullen JT, Ribero D, Reddy SK, Donadon M, Zorzi D, Gautam S, et al. Hepatic insufficiency and mortality in 1,059 noncirrhotic patients undergoing major hepatectomy. J Am Coll Surg 2007;204:854-62.

16. van den Broek MA, Olde Damink SW, Dejong CH, Lang H, Malagó M, Jalan R, et al. Liver failure after partial hepatic resection: definition, pathophysiology, risk factors and treatment. Liver Int 2008;28:767-80.

17. Schindl MJ, Redhead DN, Fearon KC, Garden OJ, Wigmore SJ and (eLISTER), Edinburgh Liver Surgery and Transplantation Experimental Research Group. The value of residual liver volume as a predictor of hepatic dysfunction and infection after major liver resection. Gut 2005;54:289-96.

18. Giacchetti S, Itzhaki M, Gruia G, Adam R, Zidani R, Kunstlinger F, et al. Long-term survival of patients with unresectable colorectal cancer liver metastases following infusional chemotherapy with 5-fluorouracil, leucovorin, oxaliplatin and surgery. Ann Oncol 1999;10:663-9.

19. Mathijssen RH, van Alphen RJ, Verweij J, Loos WJ, Nooter K, Stoter G, et al. Clinical pharmacokinetics and metabolism of irinotecan (CPT-11). Clin Cancer Res 2001;7:2182-94.

20. Mentha G, Majno PE, Andres A, Rubbia-Brandt L, Morel P, Roth AD. Neoadjuvant chemotherapy and resection of advanced synchronous liver metastases before treatment of the colorectal primary. Br J Surg 2006;93:872-8.

21. Karoui M, Penna C, Amin-Hashem M, Mitry E, Benoist S, Franc B, et al. Influence of preoperative chemotherapy on the risk of major hepatectomy for colorectal liver metastases. Ann Surg 2006;243:1-7.

22. Saltz LB, Cox JV, Blanke C, Rosen LS, Fehrenbacher L, Moore MJ, et al. Irinotecan plus fluorouracil and leucovorin for metastatic colorectal cancer. Irinotecan Study Group. N Engl J Med 2000;343:905-14.

23. Vauthey JN, Pawlik TM, Ribero D, Wu TT, Zorzi D, Hoff PM, et al. Chemotherapy regimen predicts steatohepatitis and an increase in 90-day mortality after surgery for hepatic colorectal metastases. J Clin Oncol 2006;24:2065-72.

24. Rixe O, Ortuzar W, Alvarez M, Parker R, Reed E, Paull K, et al. Oxaliplatin, tetraplatin, cisplatin, and carboplatin: spectrum of activity in drug-resistant cell lines and in the cell lines of the National Cancer Institute's Anticancer Drug Screen panel. Biochem Pharmacol 1996;52:1855-65.

25. Raymond E, Lawrence R, Izbicka E, Faivre S, Von Hoff DD. Activity of oxaliplatin against human tumor colony-forming units. Clin Cancer Res 1998;4:1021-9.

26. Raymond E, Faivre S, Chaney S, Woynarowski J, Cvitkovic E. Cellular and molecular pharmacology of oxaliplatin. Mol Cancer Ther 2002;1:227-35.

27. André T, Boni C, Navarro M, Tabernero J, Hickish T, Topham C, et al. Improved overall survival with oxaliplatin, fluorouracil, and leucovorin as adjuvant treatment in stage II or III colon cancer in the MOSAIC trial. J Clin Oncol 2009;27:3109-16.

28. Rubbia-Brandt L, Audard V, Sartoretti P, Roth AD, Brezault C, Le Charpentier M, et al. Severe hepatic sinusoidal obstruction associated with oxaliplatin-based chemotherapy in patients with metastatic colorectal cancer. Ann Oncol 2004;15:460-6.

29. Pessaux P, Chenard MP, Bachellier P, Jaeck D. Consequences of chemotherapy on resection of colorectal liver metastases. J Visc Surg 2010;147:e193-201

30. Nakano H, Oussoultzoglou E, Rosso E, Casnedi S, Chenard-Neu MP, Dufour P, et al. Sinusoidal injury increases morbidity after major hepatectomy in patients with colorectal liver metastases receiving preoperative chemotherapy. Ann Surg 2008;247:118-24.

31. Collardeau-Frachon S, Scoazec JY. Vascular development and differentiation during human liver organogenesis. Anat Rec (Hoboken) 2008;29:614-27.

32. RS, McCuskey. The hepatic microvascular system in health and its response to toxicants. Anat Rec (Hoboken) 2008;291:661-71.

33. Wisse E, De Zanger RB, Charels K, Van Der Smissen P, McCuskey RS. The liver sieve: considerations concerning the structure and function of endothelial fenestrae, the sinusoidal wall and the space of Disse. Hepatology 1985;5:683-92.

34. Jacobs F, Wisse E, De Geest B. The role of liver sinusoidal cells in hepatocyte-directed gene transfer. Am J Pathol 2010;176:14-21.

35. DeLeve LD, Wang X, Hu L, McCuskey MK, McCuskey RS. Rat liver sinusoidal endothelial cell phenotype is maintained by paracrine and autocrine regulation. Am J Physiol Gastrointest Liver Physiol 2004;287:G757-63.

36. Wang X, Kanel GC, DeLeve LD. Support of sinusoidal endothelial cell glutathione prevents hepatic veno-occlusive disease in the rat. Hepatology 2000;31:428-34.

37. DeLeve LD, Wang X, Kuhlenkamp JF, Kaplowitz N. Toxicity of azathioprine and monocrotaline in murine sinusoidal endothelial cells and hepatocytes: the role of glutathione and relevance to hepatic venoocclusive disease. Hepatology 1996;23:589-99.

38. Rabik CA, Dolan ME. Molecular mechanisms of resistance and toxicity associated with platinating agents. Cancer Treat Rev 2007;33:9-23.

39. LD, DeLeve. Hepatic microvasculature in liver injury. Semin Liver Dis 2007;27:390-400.

40. DeLeve LD, Wang X, Kanel GC, Ito Y, Bethea NW, McCuskey MK, et al. Decreased hepatic nitric oxide production contributes to the development of rat sinusoidal obstruction syndrome. Hepatology 2003;38:900-8.

41. Soubrane O, Brouquet A, Zalinski S, Terris B, Brézault C, Mallet V, et al. Predicting high grade lesions of sinusoidal obstruction syndrome related to oxaliplatin-based chemotherapy for colorectal liver metastases: correlation with post-hepatectomy outcome. Ann Surg 2010;251:454-60.

42. Tamandl D, Klinger M, Eipeldauer S, Herberger B, Kaczirek K, Gruenberger B, et al. Sinusoidal obstruction syndrome impairs long-term outcome of colorectal liver metastases treated with resection after neoadjuvant chemotherapy. Ann Surg Oncol 2011;18:421-30.

43. Morris-Stiff G, Gomez D, Prasad R. Quantitative assessment of hepatic function and its relevance to the liver surgeon. J Gastrointest Surg 2009;13:374-85.

44. Poon RT, Fan ST, Lo CM, Liu CL, Lam CM, Yuen WK, et al. Improving perioperative outcome expands the role of hepatectomy in management of benign and malignant hepatobiliary diseases: analysis of 1222 consecutive patients from a prospective database. Ann Surg 2004;240:708-10.

45. Fraser JR, Laurent TC, Laurent UB. Hyaluronan: its nature, distribution, functions and turnover. J Intern Med 1997;1:27-33.

46. U, Lindqvist. Is serum hyaluronan a helpful tool in the management of patients with liver diseases? J Intern Med 1997;242:67-71.

47. Lindqvist U, Westerberg G, Bergström M, Torsteindottir I, Gustafson S, Sundin A, et al. [11C]Hyaluronan uptake with positron emission tomography in liver disease. Eur J Clin Invest 2000;30:600-7.

48. Fried MW, Duncan A, Soroka S, Connaghan DG, Farrand A, Peter J, et al. Serum hyaluronic acid in patients with veno-occlusive disease following bone marrow transplantation. Bone Marrow Transplant 2001;27:635-9.

49. Blann AD, Taberner DA. A reliable marker of endothelial cell dysfunction: does it exist? Br J Haematol 1995;90:244-8.

50. Nürnberger W, Michelmann I, Burdach S, Göbel U. Endothelial dysfunction after bone marrow transplantation: increase of soluble thrombomodulin and PAI-1 in patients with multiple transplant-related complications. Ann Hematol 1998;76:61-5.

51. Woywodt A, Haubitz M, Buchholz S, Hertenstein B. Counting the cost: markers of endothelial damage in hematopoietic stem cell transplantation. Bone Marrow Transplant 2004;34:1015-23.

52. Wai CT, Greenson JK, Fontana RJ, Kalbfleisch JD, Marrero JA, Conjeevaram HS, et al. A simple noninvasive index can predict both significant fibrosis and cirrhosis in patients with chronic hepatitis C. Hepatology 2003;38:518-26.

53. Vallet-Pichard A, Mallet V, Nalpas B, Verkarre V, Nalpas A, Dhalluin-Venier V, et al. FIB-4: an inexpensive and accurate marker of fibrosis in HCV infection. comparison with liver biopsy and fibrotest. Hepatology 2007;46:32-6.

54. Bedossa P, Dargère D, Paradis V. Sampling variability of liver fibrosis in chronic hepatitis C. Hepatology 2003;38:1449-57.

55. Richter B, Schmandra TC, Golling M, Bechstein WO. Nutritional support after open liver resection: a systematic review. Dig Surg 2006;23:139-45.

56. Sewnath ME, Karsten TM, Prins MH, Rauws EJ, Obertop H, Gouma DJ. A meta-analysis on the efficacy of preoperative biliary drainage for tumors causing obstructive jaundice. Ann Surg 2002;236:17-27.

57. van der Gaag NA, Rauws EA, van Eijck CH, Bruno MJ, van der Harst E, Kubben FJ, et al. Preoperative biliary drainage for pancreatic head tumours. N Engl J Med 2010;14:129-37.

58. Kishi Y, Zorzi D, Contreras CM, Maru DM, Kopetz S, Ribero D, et al. Extended preoperative chemotherapy does not improve pathologic response and increases postoperative liver insufficiency after hepatic resection for colorectal liver metastases. Ann Surg Oncol 2010;17:2870-6.

59. Broering DC, Hillert C, Krupski G, Fischer L, Mueller L, Achilles EG, et al. Portal vein embolization vs. portal vein ligation for induction of hypertrophy of the future liver remnant. J Gastrointest Surg 2002;6:905-13.

60. Farges O, Belghiti J, Kianmanesh R, Regimbeau JM, Santoro R, Vilgrain V, et al. Portal vein embolization before right hepatectomy: prospective clinical trial. Ann Surg 2003;237:208-17.

61. Liu H, Zhu S. Present status and future perspectives of preoperative portal vein embolization. Am J Surg 2009;197:686-90.

62. Mochida S, Ogata I, Hirata K, Ohta Y, Yamada S, Fujiwara K. Provocation of massive hepatic necrosis by endotoxin after partial hepatectomy in rats. Gastroenterology 1990;99:771-7.

63. Aloia T, Sebagh M, Plasse M, Karam V, Lévi F, Giacchetti S, et al. Liver histology and surgical outcomes after preoperative chemotherapy with fluorouracil plus oxaliplatin in colorectal cancer liver metastases. J Clin Oncol 2006;24:4983-90.

64. Slade JH, Alattar ML, Fogelman DR, Overman MJ, Agarwal A, Maru DM, et al. Portal hypertension associated with oxaliplatin administration: clinical manifestations of hepatic sinusoidal injury. Clin Colorectal Cancer 2009;8:225-30.

65. Vassiliou I, Arkadopoulos N, Stafyla V, Theodoraki K, Yiallourou A, Theodosopoulos T, et al. The introduction of a simple maneuver to reduce the risk of postoperative bleeding after major hepatectomies. J Hepatobiliary Pancreat Surg 2009;16:552-6.

66. Gurusamy KS, Kumar Y, Pamecha V, Sharma D, Davidson BR. Ischaemic pre-conditioning for elective liver resections performed under vascular occlusion. Cochrane Database Syst Rev 2009;21:CD007629.

67. Gomez D, Homer-Vanniasinkam S, Graham AM, Prasad KR. Role of ischaemic preconditioning in liver regeneration following major liver resection and transplantation. World J Gastroenterol 2007;13:657-70.

68. Onodera K, Sakata H, Yonekawa M, Kawamura A. Artificial liver support at present and in the future. J Artif Organs 2006;9:17-28.

69. Sen S, Williams R, Jalan R. Emerging indications for albumin dialysis. Am J Gastroenterol 2005;100:468-75.

70. Chamuleau RA, Poyck PP, van de Kerkhove MP. Bioartificial liver: its pros and cons. Ther Apher Dial 2006;10:168-74.

71. Selden C, Hodgson H. Cellular therapies for liver replacement. Transpl Immunol 2004;12:273-88.

72. Yu CB, Pan XP, Li LJ. Progress in bioreactors of bioartificial livers.Hepatobiliary Pancreat Dis Int 2009;8:134-40.

73. JD, Sipe. Tissue engineering and reparative medicine. Ann N Y Acad Sci 2002;961:1-9.

74. Ehnert S, Glanemann M, Schmitt A, Vogt S, Shanny N, Nussler NC, et al. The possible use of stem cells in regenerative medicine: dream or reality? Langenbecks Arch Surg 2009;394:985-97.

75. Fausto N, Laird AD, Webber EM. Liver regeneration. 2. Role of growth factors and cytokines in hepatic regeneration. FASEB J 1995;9:1527-36.

76. N, Fausto. Liver regeneration and repair: hepatocytes, progenitor cells, and stem cells. Hepatology 2004;39:1477-87.

77. Flohr TR, Bonatti H Jr, Brayman KL, Pruett TL. The use of stem cells in liver disease. Curr Opin Organ Transplant 2009;14:64-71.

78. Garcea G, Maddern GJ. Liver failure after major hepatic resection. J Hepatobiliary Pancreat Surg 2009;16:145-55.

79. Sowa JP, Best J, Benko T, Bockhorn M, Gu Y, Niehues EM, et al. Extent of liver resection modulates the activation of transcription factors and the production of cytokines involved in liver regeneration. World J Gastroenterol 2008;14:7093-100.

80. E, FARBER. Similarities in the sequence of early histological changes induced in the liver of the rat by ethionine, 2-acetylamino-fluorene, and 3'-methyl-4-dimethylaminoazobenzene. Cancer Res 1956;16:142-8.

81. Faris RA, Konkin T, Halpert G. Liver stem cells: a potential source of hepatocytes for the treatment of human liver disease.Artif Organs 2001;25:513-21.

82. Alison M, Golding M, Lalani EN, Nagy P, Thorgeirsson S, Sarraf C. Wholesale hepatocytic differentiation in the rat from ductular oval cells, the progeny of biliary stem cells.,J Hepatol 1997;26:343-52.

83. Fausto N, Campbell JS. The role of hepatocytes and oval cells in liver regeneration and repopulation. Mech Dev 2003;120:117-30.

84. Kuwahara R, Kofman AV, Landis CS, Swenson ES, Barendswaard E, Theise ND. The hepatic stem cell niche: identification by label-retaining cell assay. Hepatology 2008;47:1994-2002.

85. Gaudio E, Carpino G, Cardinale V, Franchitto A, Onori P, Alvaro D. New insights into liver stem cells. Dig Liver Dis 2009;41:455-62.

86. S, Sell. Heterogeneity and plasticity of hepatocyte lineage cells. Hepatology 2001;33:738-50.

87. Tremblay KD, Zaret KS. Distinct populations of endoderm cells converge to generate the embryonic liver bud and ventral foregut tissues. Dev Biol 2005;280:87-99.

88. Lee SP, Savard CE, Kuver R. Gallbladder epithelial cells that engraft in mouse liver can differentiate into hepatocyte-like cells. Am J Pathol 2009;174:842-53.

89. Hewes JC, Riddy D, Morris RW, Woodrooffe AJ, Davidson BR, Fuller B. A prospective study of isolated human hepatocyte function following liver resection for colorectal liver metastases: the effects of prior exposure to chemotherapy. J Hepatol 2006;45:263-70.

90. Schiffer E, Frossard JL, Rubbia-Brandt L, Mentha G, Pastor CM. Hepatic regeneration is decreased in a rat model of sinusoidal obstruction syndrome. J Surg Oncol 2009;99:439-46.

91. Narita M, Oussoultzoglou E, Chenard MP, Rosso E, Casnedi S, Pessaux P, et al. Sinusoidal obstruction syndrome compromises liver regeneration in patients undergoing two-stage hepatectomy with portal vein embolization. Surg Today 2011;41:7-17.

92. Lesurtel M, Graf R, Aleil B, Walther DJ, Tian Y, Jochum W, et al. Platelet-derived serotonin mediates liver regeneration. Science 2006;312:104-7.

93. Murata S, Ohkohchi N, Matsuo R, Ikeda O, Myronovych A, Hoshi R. Platelets promote liver regeneration in early period after hepatectomy in mice. World J Surg 2007;31:808-16.

94. LeCouter J, Moritz DR, Li B, Phillips GL, Liang XH, Gerber HP, et al. Angiogenesis-independent endothelial protection of liver: role of VEGFR-1. Science 2003;299:890-3.

95. Ding BS, Nolan DJ, Butler JM, James D, Babazadeh AO, Rosenwaks Z, et al. Inductive angiocrine signals from sinusoidal endothelium are required for liver regeneration. Nature 2010;468:310-5.

96. Mellick AS, Plummer PN, Nolan DJ, Gao D, Bambino K, Hahn M, et al. Using the transcription factor inhibitor of DNA binding 1 to selectively target endothelial progenitor

cells offers novel strategies to inhibit tumor angiogenesis and growth. Cancer Res 2010;70:7273-82.

97. Groth CG, Arborgh B, Björkén C, Sundberg B, Lundgren G. Correction of hyperbilirubinemia in the glucuronyltransferase-deficient rat by intraportal hepatocyte transplantation. Transplant Proc 1977;9:313-36.

98. Fisher RA, Strom SC. Human hepatocyte transplantation: worldwide results. Transplantation 2006;82:441-9.

99. Nussler A, Konig S, Ott M, Sokal E, Christ B, Thasler W, et al. Present status and perspectives of cell-based therapies for liver diseases. J Hepatol 2006;45:144-59.

100. Baccarani U, Sanna A, Cariani A, Sainz-Barriga M, Adani GL, Zambito AM, et al. Isolation of human hepatocytes from livers rejected for liver transplantation on a national basis: results of a 2-year experience. Liver Transpl 2003;9:506-12.

101. Allen KJ, Soriano HE. Liver cell transplantation: the road to clinical application. J Lab Clin Med 2001;138:298-312.

102. Pietrosi G, Vizzini GB, Gruttadauria S, Gridelli B. Clinical applications of hepatocyte transplantation. World J Gastroenterol 2009;15:2074-7.

103. Sigot V, Mediavilla MG, Furno G, Rodríguez JV, Guibert EE. A simple and effective method to improve intrasplenic rat hepatocyte transplantation. Cell Transplant 2004;13:775-81.

104. Gupta S, Rajvanshi P, Sokhi R, Slehria S, Yam A, Kerr A , et al. Entry and integration of transplanted hepatocytes in rat liver plates occur by disruption of hepatic sinusoidal endothelium. Hepatology 1999;29:509-19.

105. Mula N, Cubero FJ, Codesal J, de Andrés S, Escudero C, García-Barrutia S, et al. Survival of allogeneic hepatocytes transplanted into the thymus. Cells Tissues Organs 2008;188:270-9.

106. Mei J, Sgroi A, Mai G, Baertschiger R, Gonelle-Gispert C, Serre-Beinier V, et al. Improved survival of fulminant liver failure by transplantation of microencapsulated cryopreserved porcine hepatocytes in mice. Cell Transplant 2009;18:101-10.

107. Glanemann M, Gaebelein G, Nussler N, Hao L, Kronbach Z, Shi B, et al. Transplantation of monocyte-derived hepatocyte-like cells (NeoHeps) improves survival in a model of acute liver failure. Ann Surg 2009;249:149-54.

108. Rajvanshi P, Kerr A, Bhargava KK, Burk RD, Gupta S. Efficacy and safety of repeated hepatocyte transplantation for significant liver repopulation in rodents. Gastroenterology 1996;111:1092-102.

109. Smalley M, Leiper K, Tootle R, McCloskey P, O'Hare MJ, Hodgson H. Immortalization of human hepatocytes by temperature-sensitive SV40 large-T antigen. In Vitro Cell Dev Biol Anim 2001;37:166-8.

110. Khetani SR, Bhatia SN. Microscale culture of human liver cells for drug development. Nat Biotechnol 2008;26:120-6.

111. Ito M, Nagata H, Miyakawa S, Fox IJ. Review of hepatocyte transplantation. J Hepatobiliary Pancreat Surg 2009;16:97-100.

112. Becker AJ, Mcculloch EA, Till JE.Cytological demonstration of the clonal nature of spleen colonies derived from transplanted mouse marrow cells. Nature 1963;197:452-4.

113. Mitalipov S, Wolf D. Totipotency, pluripotency and nuclear reprogramming. Adv Biochem Eng Biotechnol 2009;114:185-99.

114. Toma JG, Akhavan M, Fernandes KJ, Barnabé-Heider F, Sadikot A, Kaplan DR, et al. Isolation of multipotent adult stem cells from the dermis of mammalian skin. Nat Cell Biol 2001;3:778-84.

115. Okita K, Ichisaka T, Yamanaka S. Generation of germline-competent induced pluripotent stem cells. Nature 2007;448:313-7.

116. Shamblott MJ, Axelman J, Wang S, Bugg EM, Littlefield JW, Donovan PJ, et al. Derivation of pluripotent stem cells from cultured human primordial germ cells. Proc Natl Acad Sci U S A 1998;95:13726-31.

117. Shamblott MJ, Axelman J, Littlefield JW, Blumenthal PD, Huggins GR, Cui Y, et al. Human embryonic germ cell derivatives express a broad range of developmentally distinct markers and proliferate extensively in vitro. Proc Natl Acad Sci U S A 2001;98:113-8.

118. Nagy A, Gócza E, Diaz EM, Prideaux VR, Iványi E, Markkula M, et al. Embryonic stem cells alone are able to support fetal development in the mouse. Development 1990;110:815-21.

119. Xu RH, Chen X, Li DS, Li R, Addicks GC, Glennon C, et al. BMP4 initiates human embryonic stem cell differentiation to trophoblast. Nat Biotechnol 2004;20:1261-4.

120. Polak JM, Bishop AE. Stem cells and tissue engineering: past, present, and future. Ann N Y Acad Sci 2006;1068:352-66.

121. Takahashi K, Yamanaka S. Induction of pluripotent stem cells from mouse embryonic and adult fibroblast cultures by defined factors. Cell 2006;126:663-76.

122. Aoi T, Yae K, Nakagawa M, Ichisaka T, Okita K, Takahashi K, et al. Generation of pluripotent stem cells from adult mouse liver and stomach cells. Science 2008;321:699-702.

123. Park IH, Zhao R, West JA, Yabuuchi A, Huo H, Ince TA, et al. Reprogramming of human somatic cells to pluripotency with defined factors. Nature 2008;451:141-6.

124. Zhou Q, Brown J, Kanarek A, Rajagopal J, Melton DA. In vivo reprogramming of adult pancreatic exocrine cells to beta-cells. Nature 2008;455:627-32.

125. Berninger B, Costa MR, Koch U, Schroeder T, Sutor B, Grothe B, et al. Functional properties of neurons derived from in vitro reprogrammed postnatal astroglia. J Neurosci 2007;27:8654-64.

126. Colman A, Dreesen O. Induced pluripotent stem cells and the stability of the differentiated state. EMBO Rep 2009;10:714-21.

127. Lyra AC, Soares MB, dos Santos RR, Lyra LG. Bone marrow stem cells and liver disease. Gut 2007;56:1640-1.

128. Pittenger MF, Mackay AM, Beck SC, Jaiswal RK, Douglas R, Mosca JD, et al. Multilineage potential of adult human mesenchymal stem cells. Science 1999;284:143-7.

129. Bobis S, Jarocha D, Majka M. Mesenchymal stem cells: characteristics and clinical applications. Folia Histochem Cytobiol 2006;44:215-30.

130. Liu ZJ, Zhuge Y, Velazquez OC. Trafficking and differentiation of mesenchymal stem cells. J Cell Biochem 2009;106:984-91.

131. Kassem M, Kristiansen M, Abdallah BM. Mesenchymal stem cells: cell biology and potential use in therapy. Basic Clin Pharmacol Toxicol 2004;95:209-14.

132. Vassilopoulos G, Wang PR, Russell DW. Transplanted bone marrow regenerates liver by cell fusion. Nature 2003;4226934:901-4.

133. Harris RG, Herzog EL, Bruscia EM, Grove JE, Van Arnam JS, Krause DS. Lack of a fusion requirement for development of bone marrow-derived epithelia. Science 2004;305:90-3.

134. Simonsen JL, Rosada C, Serakinci N, Justesen J, Stenderup K, Rattan SI, et al. Telomerase expression extends the proliferative life-span and maintains the osteogenic potential of human bone marrow stromal cells. Nat Biotechnol 2002;20:592-6.

135. Huang YC, Yang ZM, Chen XH, Tan MY, Wang J, Li XQ, et al. Isolation of mesenchymal stem cells from human placental decidua basalis and resistance to hypoxia and serum deprivation. Stem Cell Rev 2009;5:247-55.

136. D'Alessandro A, Liumbruno G, Grazzini G, Pupella S, Lombardini L, Zolla L. Umbilical cord blood stem cells: towards a proteomic approach. J Proteomics 2010;73:468-82.

137. H, Mizuno. Adipose-derived stem and stromal cells for cell-based therapy: current status of preclinical studies and clinical trials. Curr Opin Mol Ther 2010;12:442-9.

138. Burt RK, Loh Y, Pearce W, Beohar N, Barr WG, Craig R, et al. Clinical applications of blood-derived and marrow-derived stem cells for nonmalignant diseases. JAMA 2008;299:925-36.

139. Vaquero J, Zurita M. Bone marrow stromal cells for spinal cord repair: a challenge for contemporary neurobiology. Histol Histopathol 2009;24:107-16.

140. Schächinger V, Erbs S, Elsässer A, Haberbosch W, Hambrecht R, Hölschermann H, et al. Intracoronary bone marrow-derived progenitor cells in acute myocardial infarction. N Engl J Med 2006;355:1210-21.

141. Witkowski P, Zakai SB, Rana A, Sledzinski Z, Hardy MA. Pancreatic islet transplantation, what has been achieved since Edmonton break-through. Ann Transplant 2006;11:5-13.

142. Baeyens L, Bouwens L. Can beta-cells be derived from exocrine pancreas? Diabetes Obes Metab 2008;10:170-8.

143. GR, Martin. Isolation of a pluripotent cell line from early mouse embryos cultured in medium conditioned by teratocarcinoma stem cells. Proc Natl Acad Sci U S A 1981;78:7634-8.

144. Liedtke C, Streetz KL. Hepatocytes from embryonic stem cells: Prometheus revisited? Hepatology 2007;45:829-30.

145. Pan YL, Cai JY, Hu AB. Differentiation of hepatocytes from mouse embryonic stem cells and its significance. Hepatobiliary Pancreat Dis Int 2005;4:291-4.

146. Chinzei R, Tanaka Y, Shimizu-Saito K, Hara Y, Kakinuma S, Watanabe M, et al. Embryoid-body cells derived from a mouse embryonic stem cell line show differentiation into functional hepatocytes. Hepatology 2002;36:22-9.

147. Hamazaki T, Iiboshi Y, Oka M, Papst PJ, Meacham AM, Zon LI, et al. Hepatic maturation in differentiating embryonic stem cells in vitro.FEBS Lett 2001;497:15-9.

148. umashiro Y, Asahina K, Ozeki R, Shimizu-Saito K, Tanaka Y, Kida Y, et al. Enrichment of hepatocytes differentiated from mouse embryonic stem cells as a transplantable source. Transplantation 2005;79:550-7.

149. Moriya K, Yoshikawa M, Ouji Y, Saito K, Nishiofuku M, Matsuda R, et al. Embryonic stem cells reduce liver fibrosis in CCl4-treated mice. Int J Exp Pathol 2008;89:401-9.

150. Moore RN, Dasgupta A, Rajaei N, Yarmush ML, Toner M, Larue L, et al. Enhanced differentiation of embryonic stem cells using co-cultivation with hepatocytes. Biotechnol Bioeng 2008;101:1332-43.

151. Kubo A, Shinozaki K, Shannon JM, Kouskoff V, Kennedy M, Woo S, et al. Development of definitive endoderm from embryonic stem cells in culture. Development 2004;131:1651-62.

152. Zhou M, Li P, Tan L, Qu S, Ying QL, Song H. Differentiation of mouse embryonic stem cells into hepatocytes induced by a combination of cytokines and sodium butyrate.J Cell Biochem 2010;109: 606-14.

153. Chen L, Tredget EE, Liu C, Wu Y. Analysis of allogenicity of mesenchymal stem cells in engraftment and wound healing in mice. PLoS One 2009;4:e7119.

154. Krampera M, Glennie S, Dyson J, Scott D, Laylor R, Simpson E, et al. Bone marrow mesenchymal stem cells inhibit the response of naive and memory antigen-specific T cells to their cognate peptide. Blood 2003;101:37223729.

155. Di Nicola M, Carlo-Stella C, Magni M, Milanesi M, Longoni PD, Matteucci P, et al. Human bone marrow stromal cells suppress T-lymphocyte proliferation induced by cellular or nonspecific mitogenic stimuli. Blood 2002;99:3838-43.

156. Taniguchi H, Toyoshima T, Fukao K, Nakauchi H. Presence of hematopoietic stem cells in the adult liver. Nat Med 1996;2:198-203.

157. Tang YL, Zhao Q, Qin X, Shen L, Cheng L, Ge J, et al. Paracrine action enhances the effects of autologous mesenchymal stem cell transplantation on vascular regeneration in rat model of myocardial infarction. Ann Thorac Surg 2005;80:229-36.

158. Bruno S, Grange C, Deregibus MC, Calogero RA, Saviozzi S, Collino F, et al. Mesenchymal stem cell-derived microvesicles protect against acute tubular injury. J Am Soc Nephrol 2009;20:1053-67.

159. van Poll D, Parekkadan B, Cho CH, Berthiaume F, Nahmias Y, Tilles AW, et al. Mesenchymal stem cell-derived molecules directly modulate hepatocellular death and regeneration in vitro and in vivo. Hepatology 2008;47:1634-43.

160. Herrera MB, Fonsato V, Gatti S, Deregibus MC, Sordi A, Cantarella D, et al. Human liver stem cell-derived microvesicles accelerate hepatic regeneration in hepatectomized rats. J Cell Mol Med 2010;14:1605-18.

161. Yu Y, Yao AH, Chen N, Pu LY, Fan Y, Lv L, et al. Mesenchymal stem cells over-expressing hepatocyte growth factor improve small-for-size liver grafts regeneration. Mol Ther 2007;15:1382-89.

162. Son BR, Marquez-Curtis LA, Kucia M, Wysoczynski M, Turner AR, Ratajczak J, et al. Migration of bone marrow and cord blood mesenchymal stem cells in vitro is regulated by stromal-derived factor-1-CXCR4 and hepatocyte growth factor-c-met axes and involves matrix metalloproteinases. Stem Cells 2006;24:1254-64.

163. Hattori K, Heissig B, Tashiro K, Honjo T, Tateno M, Shieh JH, et al. Plasma elevation of stromal cell-derived factor-1 induces mobilization of mature and immature hematopoietic progenitor and stem cells. Blood 2001;97:3354-60.

164. Mao L, Qiu YD, Fang S, Wu YF, Liu H, Ding YT. Liver progenitor cells activated after 30% small-for-size liver transplantation in rats: a preliminary study. Transplant Proc 2008;40:1635-40.

165. Peichev M, Naiyer AJ, Pereira D, Zhu Z, Lane WJ, Williams M, et al. Expression of VEGFR-2 and AC133 by circulating human CD34(+) cells identifies a population of functional endothelial precursors. Blood 2000;95:952-8.

166. Lemoli RM, Catani L, Talarico S, Loggi E, Gramenzi A, Baccarani U, et al. Mobilization of bone marrow-derived hematopoietic and endothelial stem cells after orthotopic liver transplantation and liver resection. Stem Cells 2006;24:2817-25.

167. Stutchfield BM, Rashid S, Forbes SJ, Wigmore SJ. Practical barriers to delivering autologous bone marrow stem cell therapy as an adjunct to liver resection. Stem Cells Dev 2010;19:155-62.

168. Harb R, Xie G, Lutzko C, Guo Y, Wang X, Hill CK, et al. Bone marrow progenitor cells repair rat hepatic sinusoidal endothelial cells after liver injury. Gastroenterology 2009;137:704-12.

169. To LB, Haylock DN, Simmons PJ, Juttner CA. The biology and clinical uses of blood stem cells. Blood 1997;89:2233-58.

170. Pai M, Zacharoulis D, Milicevic MN, Helmy S, Jiao LR, Levicar N, et al. Autologous infusion of expanded mobilized adult bone marrow-derived CD34+ cells into patients with alcoholic liver cirrhosis. Am J Gastroenterol 2008;103:1952-8.

171. Gehling UM, Willems M, Dandri M, Petersen J, Berna M, Thill M, et al. Partial hepatectomy induces mobilization of a unique population of haematopoietic progenitor cells in human healthy liver donors. J Hepatol 2005;43:845-53.

172. am Esch JS 2nd, Knoefel WT, Klein M, Ghodsizad A, Fuerst G, Poll LW, et al. Portal application of autologous CD133+ bone marrow cells to the liver: a novel concept to support hepatic regeneration. Stem Cells 2005;23:463-70.

173. Fürst G, Schulte am Esch J, Poll LW, Hosch SB, Fritz LB, Klein M, et al. Portal vein embolization and autologous CD133+ bone marrow stem cells for liver regeneration: initial experience. Radiology 2007;243:171-9.

174. Bulte JW, Douglas T, Witwer B, Zhang SC, Strable E, Lewis BK, et al. Magnetodendrimers allow endosomal magnetic labeling and in vivo tracking of stem cells. Nat Biotechnol 2001;19:1141-7.

175. Toso C, Vallee JP, Morel P, Ris F, Demuylder-Mischler S, Lepetit-Coiffe M, et al. Clinical magnetic resonance imaging of pancreatic islet grafts after iron nanoparticle labeling. Am J Transplant 2008;8:701-6.

176. Budde MD, Frank JA. Magnetic tagging of therapeutic cells for MRI. J Nucl Med 2009;50:171-4.

177. Welling MM, Duijvestein M, Signore A, van der Weerd L. In vivo biodistribution of stem cells using molecular nuclear medicine imaging. J Cell Physiol 2011;226:1444-52.

178. Chalfie M, Tu Y, Euskirchen G, Ward WW, Prasher DC. Green fluorescent protein as a marker for gene expression. Science 1994;263:802-5.

179. K, König. Multiphoton microscopy in life sciences. J Microsc 2000;200(Pt 2):83-104.

180. Koenig S, Krause P, Hosseini AS, Dullin C, Rave-Fraenk M, Kimmina S, et al. Noninvasive imaging of liver repopulation following hepatocyte transplantation. Cell Transplant 2009;18:69-78.

181. Boddington SE, Henning TD, Jha P, Schlieve CR, Mandrussow L, DeNardo D, et al. Labeling human embryonic stem cell-derived cardiomyocytes with indocyanine green for noninvasive tracking with optical imaging: an FDA-compatible alternative to firefly luciferase. Cell Transplant 2010;19:55-65.

182. DeLeve LD, McCuskey RS, Wang X, Hu L, McCuskey MK, Epstein RB, et al. Characterization of a reproducible rat model of hepatic veno-occlusive disease. Hepatology 1999;29:1779-91.

183. Saito C, Zwingmann C, Jaeschke H. Novel mechanisms of protection against acetaminophen hepatotoxicity in mice by glutathione and N-acetylcysteine. Hepatology 2010;51:246-54.

184. Scorticati C, Prestifilippo JP, Eizayaga FX, Castro JL, Romay S, Fernández MA, et al. Hyperammonemia, brain edema and blood-brain barrier alterations in prehepatic portal hypertensive rats and paracetamol intoxication. World J Gastroenterol 2004;10:1321-4.

185. Ponder KP, Gupta S, Leland F, Darlington G, Finegold M, DeMayo J, et al. Mouse hepatocytes migrate to liver parenchyma and function indefinitely after intrasplenic transplantation. Proc Natl Acad Sci U S A 1991;88:1217-21.

186. Rubbia-Brandt L, Lauwers GY, Wang H, Majno PE, Tanabe K, Zhu AX, et al. Sinusoidal obstruction syndrome and nodular regenerative hyperplasia are frequent oxaliplatin-associated liver lesions and partially prevented by bevacizumab in patients with hepatic colorectal metastasis. Histopathology 2010;56:430-9.

187. Chun YS, Vauthey JN. Extending the frontiers of resectability in advanced colorectal cancer. Eur J Surg Oncol 2007;33:S52-8.

188. Rubbia-Brandt L, Audard V, Sartoretti P, Roth AD, Brezault C, Le Charpentier M, et al. Severe hepatic sinusoidal obstruction associated with oxaliplatin-based chemotherapy in patients with metastatic colorectal cancer. Ann Oncol 2004;15:460-6.

189. DeLeve LD, Shulman HM, McDonald GB. Toxic injury to hepatic sinusoids: sinusoidal obstruction syndrome (veno-occlusive disease). Semin Liver Dis 2002;22:27-42.

190. Adam R, Aloia T, Lévi F, Wicherts DA, de Haas RJ, Paule B, et al. Hepatic resection after rescue cetuximab treatment for colorectal liver metastases previously refractory to conventional systemic therapy. J Clin Oncol 2007;25:4593-602.

191. Dixon E, Datta I, Sutherland FR, Vauthey JN. Blood loss in surgical oncology: neglected quality indicator? J Surg Oncol 2009;99:508-12.

192. Stegelmeier BL, Edgar JA, Colegate SM, Gardner DR, Schoch TK, Coulombe RA, et al. Pyrrolizidine alkaloid plants, metabolism and toxicity. J Nat Toxins 1999;8:95-116.

193. Mathew R, Huang J, Shah M, Patel K, Gewitz M, Sehgal PB. Disruption of endothelial-cell caveolin-1alpha/raft scaffolding during development of monocrotaline-induced pulmonary hypertension. Circulation 2004;110:1499-506.

194. Hanumegowda UM, Copple BL, Shibuya M, Malle E, Ganey PE, Roth RA. Basement membrane and matrix metalloproteinases in monocrotaline-induced liver injury. Toxicol Sci 2003;76:237-46.

195. Koutras AK, Makatsoris T, Paliogianni F, Kopsida G, Onyenadum A, Gogos CA, et al. Oxaliplatin-induced acute-onset thrombocytopenia, hemorrhage and hemolysis. Oncology 2004;67:179-82.

196. Narita M, Hatano E, Tamaki N, Yamanaka K, Yanagida A, Nagata H, et al. Dai-kenchu-to attenuates rat sinusoidal obstruction syndrome by inhibiting the accumulation of neutrophils in the liver. J Gastroenterol Hepatol 2009;24:1051-7.

197. Martignoni M, Groothuis GM, de Kanter R. Species differences between mouse, rat, dog, monkey and human CYP-mediated drug metabolism, inhibition and induction. Expert Opin Drug Metab Toxicol 2006;2:875-94.

198. hulman HM, Gooley T, Dudley MD, Kofler T, Feldman R, Dwyer D, et al. Utility of transvenous liver biopsies and wedged hepatic venous pressure measurements in sixty marrow transplant recipients. Transplantation 1995;59:1015-22.

199. Thalheimer U, Leandro G, Samonakis DN, Triantos CK, Patch D, Burroughs AK. Assessment of the agreement between wedge hepatic vein pressure and portal vein pressure in cirrhotic patients. Dig Liver Dis 2008;37:601-8.

200. DeLeve LD, Ito Y, Bethea NW, McCuskey MK, Wang X, McCuskey RS. Embolization by sinusoidal lining cells obstructs the microcirculation in rat sinusoidal obstruction syndrome. Am J Physiol Gastrointest Liver Physiol 2003;284:G1045-52.

201. Hinson JA, Mays JB, Cameron AM. Acetaminophen-induced hepatic glycogen depletion and hyperglycemia in mice. Biochem Pharmacol 1983;32:1979-88.

202. DeLeve LD, Wang X, Kaplowitz N, Shulman HM, Bart JA, van der Hoek A. Sinusoidal endothelial cells as a target for acetaminophen toxicity. Direct action versus requirement for hepatocyte activation in different mouse strains. Biochem Pharmacol 1997;53:1339-45.

203. Youssef SS, Kumar PP. Jaundice secondary to isolated porta hepatis metastasis in colorectal cancer: case report and review of the literature. South Med J 2004;97:287-90.

204. Soubrane O, Brouquet A, Zalinski S, Terris B, Brézault C, Mallet V, et al. Predicting high grade lesions of sinusoidal obstruction syndrome related to oxaliplatin-based chemotherapy for colorectal liver metastases: correlation with post-hepatectomy outcome. Ann Surg 2010;251:454-60.

205. Rubbia-Brandt L, Tauzin S, Brezault C, Delucinge-Vivier C, Descombes P, Dousset B, et al. Gene expression Profiling Provides Insights into Pathways of Oxaliplatin Related Sinusoidal Obstruction Syndrome in Humans. Mol Cancer Ther 2011;10:687-96 .

206. B, Gao. Cytokines, STATs and liver disease. Cell Mol Immunol 2005;2:92-100.

207. Upadhya GA, Strasberg SM. Evidence that actin disassembly is a requirement for matrix metalloproteinase secretion by sinusoidal endothelial cells during cold preservation in the rat. Hepatology 1999;30:169-76.

208. Griffiths MR, Keir S, Burt AD. Basement membrane proteins in the space of Disse: a reappraisal. J Clin Pathol 1991;44:646-8.

209. Deleve LD, Wang X, Tsai J, Kanel G, Strasberg S, Tokes ZA. Sinusoidal obstruction syndrome (veno-occlusive disease) in the rat is prevented by matrix metalloproteinase inhibition. Gastroenterology 2003;125:882-90.

210. Borregaard N, Cowland JB. Granules of the human neutrophilic polymorphonuclear leukocyte. Blood 1997;89:3503-21.

211. ibero D, Wang H, Donadon M, Zorzi D, Thomas MB, Eng C, et al. Bevacizumab improves pathologic response and protects against hepatic injury in patients treated with oxaliplatin-based chemotherapy for colorectal liver metastases. Cancer 2007;110:2761-7.

212. Iguchi A, Kobayashi R, Yoshida M, Kobayashi K, Matsuo K, Kitajima I, et al. Vascular endothelial growth factor (VEGF) is one of the cytokines causative and predictive of hepatic veno-occlusive disease (VOD) in stem cell transplantation. Bone Marrow Transplant 2001;27:1173-80.

213. Corpechot C, Barbu V, Wendum D, Kinnman N, Rey C, Poupon R, et al. Hypoxia-induced VEGF and collagen I expressions are associated with angiogenesis and fibrogenesis in experimental cirrhosis. Hepatology 2002;35:1010-21.

214. Cursiefen C, Chen L, Borges LP, Jackson D, Cao J, Radziejewski C, et al. VEGF-A stimulates lymphangiogenesis and hemangiogenesis in inflammatory neovascularization via macrophage recruitment. J Clin Invest 2004;113:1040-50.

215. Bock F, Onderka J, Dietrich T, Bachmann B, Kruse FE, Paschke M, et al. Bevacizumab as a potent inhibitor of inflammatory corneal angiogenesis and lymphangiogenesis. Invest Ophthalmol Vis Sci 2007;48:2545-52.

216. Tamandl D, Klinger M, Eipeldauer S, Herberger B, Kaczirek K, Gruenberger B, et al. Sinusoidal obstruction syndrome impairs long-term outcome of colorectal liver metastases treated with resection after neoadjuvant chemotherapy. Ann Surg Oncol 2011;18:421-30.

217. Attal M, Huguet F, Rubie H, Huynh A, Charlet JP, Payen JL, et al. Prevention of hepatic veno-occlusive disease after bone marrow transplantation by continuous infusion of low-dose heparin: a prospective, randomized trial. Blood 1992;79:2834-40.

218. Deleve LD, Wang X, Tsai J, Kanel G, Strasberg S, Tokes ZA. Sinusoidal obstruction syndrome (veno-occlusive disease) in the rat is prevented by matrix metalloproteinase inhibition. Gastroenterology 2003;125:882-90.

219. Bast A, Haenen GR, Bruynzeel AM, Van der Vijgh WJ. Protection by flavonoids against anthracycline cardiotoxicity: from chemistry to clinical trials. Cardiovasc Toxicol 2007;7:154-9.

220. van Acker SA, Kramer K, Grimbergen JA, van den Berg DJ, van der Vijgh WJ, Bast A. Monohydroxyethylrutoside as protector against chronic doxorubicin-induced cardiotoxicity. Br J Pharmacol 1995;115:1260-4.

221. van Acker SA, Boven E, Kuiper K, van den Berg DJ, Grimbergen JA, Kramer K, et al. Monohydroxyethylrutoside, a dose-dependent cardioprotective agent, does not affect the antitumor activity of doxorubicin. Clin Cancer Res 1997;3:1747-54.

222. Willems AM, Bruynzeel AM, Kedde MA, van Groeningen CJ, Bast A, van der Vijgh WJ. A phase I study of monohydroxyethylrutoside in healthy volunteers. Cancer Chemother Pharmacol 2006;57:678-84.

223. Bruynzeel AM, Niessen HW, Bronzwaer JG, van der Hoeven JJ, Berkhof J, Bast A, et al. The effect of monohydroxyethylrutoside on doxorubicin-induced cardiotoxicity in patients treated for metastatic cancer in a phase II study. Br J Cancer 2007;97:1084-9.

224. Dhar DK, Wang TC, Tabara H, Tonomoto Y, Maruyama R, Tachibana M, et al. Expression of trefoil factor family members correlates with patient prognosis and neoangiogenesis. Clin Cancer Res 2005;11:6472-8.

225. Wadworth AN, Faulds D. Hydroxyethylrutosides. A review of its pharmacology, and therapeutic efficacy in venous insufficiency and related disorders. Drugs 1992;44:1013-32.

226. Cesarone MR, Belcaro G, Pellegrini L, Ledda A, Vinciguerra G, Ricci A, et al. Circulating endothelial cells in venous blood as a marker of endothelial damage in chronic venous insufficiency: improvement with venoruton. J Cardiovasc Pharmacol Ther 2006;11:93-8.

227. Abou El Hassan MA, Verheul HM, Jorna AS, Schalkwijk C, van Bezu J, van der Vijgh WJ, et al. The new cardioprotector Monohydroxyethylrutoside protects against doxorubicin-induced inflammatory effects in vitro. Br J Cancer 2003;89:357-62.

228. Chun YS, Laurent A, Maru D, Vauthey JN. Management of chemotherapy-associated hepatotoxicity in colorectal liver metastases. Lancet Oncol 2009:10:278-86.

229. oots AW, Li H, Schins RP, Duffin R, Heemskerk JW, Bast A, et al. The quercetin paradox. BHaenen GR. Toxicol Appl Pharmacol 2007;222:89-96.

230. Jacobs H, van der Vijgh WJ, Koek GH, Draaisma GJ, Moalin M, van Strijdonck GP, et al. Characterization of the glutathione conjugate of the semisynthetic flavonoid monoHER. Free Radic Biol Med 2009;46:1567-73.

231. acobs H, Moalin M, Bast A, van der Vijgh WJ, Haenen GR. An essential difference between the flavonoids monoHER and quercetin in their interplay with the endogenous antioxidant network. PLoS One 2010;5:e13880.

232. Clark CJ, Boswell F, Greer IA, Lyall F. Treatment of endothelial cells with serum from women with preeclampsia: effect on neutrophil adhesion. J Soc Gynecol Investig 1997;4:27-33.

233. Nieminen AL, Byrne AM, Herman B, Lemasters JJ. Mitochondrial permeability transition in hepatocytes induced by t-BuOOH: NAD(P)H and reactive oxygen species. Am J Physiol 1997;272:C1286-94.

234. Borregaard N, Cowland JB. Granules of the human neutrophilic polymorphonuclear leukocyte. Blood 1997;89:3503-21.

235. Upadhya AG, Harvey RP, Howard TK, Lowell JA, Shenoy S, Strasberg SM. Evidence of a role for matrix metalloproteinases in cold preservation injury of the liver in humans and in the rat. Hepatology 1997;26:922-8.

236. DeLeve LD, Valla DC, Garcia-Tsao G and Diseases, American Association for the Study Liver. Vascular disorders of the liver. Hepatology 2009;49:1729-64.

237. Bearman SI, Lee JL, Barón AE, McDonald GB. Treatment of hepatic venocclusive disease with recombinant human tissue plasminogen activator and heparin in 42 marrow transplant patients. Blood 1997;89:1501-6.

238. Richardson PG, Elias AD, Krishnan A, Wheeler C, Nath R, Hoppensteadt D, et al. Treatment of severe veno-occlusive disease with defibrotide: compassionate use results in response without significant toxicity in a high-risk population. Blood 1998;92:737-44.

239. Richardson PG, Murakami C, Jin Z, Warren D, Momtaz P, Hoppensteadt D, et al. Multi-institutional use of defibrotide in 88 patients after stem cell transplantation with severe veno-occlusive disease and multisystem organ failure: response without significant toxicity in a high-risk population and factors predictive of outcome. Blood 2002;100:4337-43.

240. Narita M, Hatano E, Ikai I, Miyagawa-Hayashino A, Yanagida A, Nagata H, et al. A phosphodiesterase III inhibitor protects rat liver from sinusoidal obstruction syndrome through heme oxygenase-1 induction. Ann Surg 2009;249:806-13.

241. The cardioprotector monoHER does not interfere with the pharmacokinetics or the metabolism of the cardiotoxic agent doxorubicin in mice. 4, 2003, Cancer Chemother Pharmacol, Vol. 51, pp. 306-10.

242. Abou El Hassan MA, Kedde MA, Zwiers UT, Bast A, van der Vijgh WJ. Bioactivation of monocrotaline by P-450 3A in rat liver. J Cardiovasc Pharmacol 1997;30:124-9.

243. Molteni A, Ward WF, Ts'ao CH, Solliday NH. Monocrotaline pneumotoxicity in mice. Virchows Arch B Cell Pathol Incl Mol Pathol 1989;57:149-55.

244. Ito Y, Bethea NW, Abril ER, McCuskey RS. Early hepatic microvascular injury in response to acetaminophen toxicity. Microcirculation 2003;10:391-400.

245. Walker RM, Racz WJ, McElligott TF. Scanning electron microscopic examination of acetaminophen-induced hepatotoxicity and congestion in mice. Am J Pathol, Vol 1983;113:321-30.

246. Ito Y, Abril ER, Bethea NW, McCuskey RS. Inhibition of matrix metalloproteinases minimizes hepatic microvascular injury in response to acetaminophen in mice. Toxicol Sci 2005;83:190-6.

247. Liu ZC, Chang TM. Transdifferentiation of bioencapsulated bone marrow cells into hepatocyte-like cells in the 90% hepatectomized rat model. Liver Transpl 2006;12:566-572.

248. Gao Y, Mu N, Xu XP, Wang Y. Porcine acute liver failure model established by two-phase surgery and treated with hollow fiber bioartificial liver support system. World J Gastroenterol 2005;, Vol. 11, pp. 5468-5474.

249. Soloviev V, Hassan AN, Akatov V, Lezhnev E, Ghaffar TY, Ghaffar YA. A novel bioartificial liver containing small tissue fragments: efficiency in the treatment of acute hepatic failure induced by carbon tetrachloride in rats. Int J Artif Organs 2003;26:735-42.

250. Mark AL, Sun Z, Warren DS, Lonze BE, Knabel MK, Melville Williams GM, Locke JE, et al. Stem cell mobilization is life saving in an animal model of acute liver failure. Ann Surg 2010;252:591-6.

251. Tuñón MJ, Alvarez M, Culebras JM, González-Gallego J. An overview of animal models for investigating the pathogenesis and therapeutic strategies in acute hepatic failure. World J Gastroenterol 2009;15:3086-98.

252. Gehling UM, Willems M, Dandri M, Petersen J, Berna M, Thill M, et al. Partial hepatectomy induces mobilization of a unique population of haematopoietic progenitor cells in human healthy liver donors. J Hepatol 2005;43:845-53.

253. Eisenblätter M, Ehrchen J, Varga G, Sunderkötter C, Heindel W, Roth J, et al. In vivo optical imaging of cellular inflammatory response in granuloma formation using fluorescence-labeled macrophages. J Nucl Med 2009;50:1676-82.

254. R, Weissleder. A clearer vision for in vivo imaging.Nat Biotechnol 2001;19:327-31.

255. Choi MS, Catana AM, Wu J, Kim YS, Yoon SJ, Borowsky AD, et al. Use of bioluminescent imaging to assay the transplantation of immortalized human fetal hepatocytes into mice. Cell Transplant 2008;17:899-909.

256. Gupta S, Rajvanshi P, Sokhi R, Slehria S, Yam A, Kerr A, et al. Entry and integration of transplanted hepatocytes in rat liver plates occur by disruption of hepatic sinusoidal endothelium. Novikoff PM. Hepatology 1999;29:509-19.

257. van Poll D, Parekkadan B, Cho CH, Berthiaume F, Nahmias Y, Tilles AW, et al. Mesenchymal stem cell-derived molecules directly modulate hepatocellular death and regeneration in vitro and in vivo. Hepatology 2008;47:1634-43.

258. LaFramboise WA, Petrosko P, Krill-Burger JM, Morris DR, McCoy AR, Scalise D, et al. Proteins secreted by embryonic stem cells activate cardiomyocytes through ligand binding pathways. J Proteomics 2010;73:992-1003.

259. Moriya K, Yoshikawa M, Ouji Y, Saito K, Nishiofuku M, Matsuda R, et al. Embryonic stem cells reduce liver fibrosis in CCl4-treated mice. Int J Exp Pathol 2008;89:401-9.

260. Imamura T, Cui L, Teng R, Johkura K, Okouchi Y, Asanuma K, et al. Embryonic stem cell-derived embryoid bodies in three-dimensional culture system form hepatocyte-like cells in vitro and in vivo. iwara N, Sasaki K. Tissue Eng 2004;10:1716-24.

261. Novik EI, Barminko J, Maguire TJ, Sharma N, Wallenstein EJ, Schloss RS, et al. Augmentation of EB-directed hepatocyte-specific function via collagen sandwich and SNAP. Biotechnol Prog 2008;24:1132-41.

262. Min J, Shang CZ, Chen YJ, Zhang L, Liu L, Deng XG, et al. Selective enrichment of hepatocytes from mouse embryonic stem cells with a culture system containing cholestatic serum. Acta Pharmacol Sin 2007;28:1931-7.

263. Rubbia-Brandt L, Audard V, Sartoretti P, Roth AD, Brezault C, Le Charpentier M, et al. Severe hepatic sinusoidal obstruction associated with oxaliplatin-based chemotherapy in patients with metastatic colorectal cancer. Ann Oncol 2004;15:460-6.

264. Harris TA, Yamakuchi M, Ferlito M, Mendell JT, Lowenstein CJ. MicroRNA-126 regulates endothelial expression of vascular cell adhesion molecule 1. Proc Natl Acad Sci U S A 2008;105:1516-21.

265. to Y, Bethea NW, Abril ER, McCuskey RS. Early hepatic microvascular injury in response to acetaminophen toxicity. Microcirculation 2003;10:391-400.

266. Hay DC, Zhao D, Ross A, Mandalam R, Lebkowski J, Cui W. Direct differentiation of human embryonic stem cells to hepatocyte-like cells exhibiting functional activities. Cloning Stem Cells 2007;9:51-62.

267. Yamada T, Yoshikawa M, Kanda S, Kato Y, Nakajima Y, Ishizaka S, et al. In vitro differentiation of embryonic stem cells into hepatocyte-like cells identified by cellular uptake of indocyanine green. Stem Cells 2002;20:146-54.

268. Fatma S, Selby DE, Singla RD, Singla DK. Factors Released from Embryonic Stem Cells Stimulate c-kit-FLK-1(+ve) Progenitor Cells and Enhance Neovascularization. Antioxid Redox Signal 2010;13:1857-65.

269. Nussbaum J, Minami E, Laflamme MA, Virag JA, Ware CB, Masino A, et al. Transplantation of undifferentiated murine embryonic stem cells in the heart: teratoma formation and immune response. FASEB J 2007;21:1345-57.

270. Irie T, Asahina K, Shimizu-Saito K, Teramoto K, Arii S, Teraoka H. Hepatic progenitor cells in the mouse extrahepatic bile duct after a bile duct ligation. Stem Cells Dev 2007;16:979-87.

271. Ren M, Yan L, Shang CZ, Cao J, Lu LH, Min J, Cheng H. Effects of sodium butyrate on the differentiation of pancreatic and hepatic progenitor cells from mouse embryonic stem cells. J Cell Biochem 2010;109:236-44.

272. Teratani T, Yamamoto H, Aoyagi K, Sasaki H, Asari A, Quinn G, et al. Direct hepatic fate specification from mouse embryonic stem cells. Hepatology 2005;41:836-46.

273. Asahina K, Teramoto K, Teraoka H. Embryonic stem cells: hepatic differentiation and regenerative medicine for the treatment of liver disease. Curr Stem Cell Res Ther 2006;1:139-56.

274. Garcia-Pagan JC, De Gottardi A, Bosch J. Review article: the modern management of portal hypertension--primary and secondary prophylaxis of variceal bleeding in cirrhotic patients. Aliment Pharmacol Ther 2008;28:178-86.

275. Kauffman CR, Mahvash A, Kopetz S, Wolff RA, Ensor J, Wallace MJ. Partial splenic embolization for cancer patients with thrombocytopenia requiring systemic chemotherapy. Cancer 2008;112:2283-8.

276. Fried MW, Connaghan DG, Sharma S, Martin LG, Devine S, Holland K, et al. Transjugular intrahepatic portosystemic shunt for the management of severe venoocclusive disease following bone marrow transplantation. Hepatology 1996;24:588-91.

277. Rapoport AP, Doyle HR, Starzl T, Rowe JM, Doeblin T, DiPersio JF. Orthotopic liver transplantation for life-threatening veno-occlusive disease of the liver after allogeneic bone marrow transplant. Bone Marrow Transplant 1991;8:421-4.

Appendix-1

Micro RNA-126 as a diagnostic marker for SOS

MicroRNA (miRNA) isolation (Applied Biosystems, Warrington, UK)

Sample disruption and organic extraction

1- Homogenization of frozen live samples and addition of 600µ of lysis buffer
2- The mixture was then vortexed and 1/10 volume of miRNA Homogenate was added to the homogenate, vortexed and the mixture left on ice for 10 minutes
3- Addition of Acid-Phenol: Chloroform that is equal to the lysate volume before addition of the miRNA Homogenate Additive and vortexed for 30-60 sec to mix
4- Centrifugation for 5 min at maximum speed (10,000 x g) at room temperature to separate the aqueous and organic phases resulting in a compact interphase
5- The aqueous (upper) phase was carefully removed without disturbing the lower phase, and transferred it to a fresh tube

Final miRNA isolation

1- Addition of 1.25 volumes of room temperature 100% ethanol to the aqueous phase
2- Pipetting of the lysate/ethanol mixture onto the filter cartridge and centrifuged to maximum speed and repeat till all of the lysate/ethanol mixture was drained through the filter
3- Application of 700 µL miRNA wash solution 1 (working solution mixed with ethanol) to the filter cartridge and centrifuge for approximately 5–10 sec
4- Application of 500 µL Wash Solution 2/3 (working solution mixed with ethanol)

5- Repeated with a second 500 µL aliquot of Wash Solution 2/3
6- After discarding the flow-through from the last wash, the filter cartridge was replaced in the same collection tube and the assembly spinned for 1 min to remove residual fluid from the filter
7- The filter cartridge then was transferred into a fresh collection tube. Application of 100 µL of pre-heated (95°C) nuclease-free water to the center of the filter, and the cap closed and spinned for ~20–30 sec at maximum speed to recover the RNA.
8- The eluate was then collected (which contains the RNA) and stored at –20°C

RNA quantification

We used the Nanodrop 2000 spectrophotometer (Wilmington, USA) to calculate the concentration of miRNA in the solution.

Reverse transcription (RT) (TaqMan MicroRNA Reverse Transcription Kit) (Applied Biosystems, Warrington, UK)

1- The kit components were thawed on ice
2- In a polypropylene tube, the RT master mix was prepared. RNA was diluted to reach a final concentration of 10ng/15 µL of RT reaction. Each 15 µL of RT reaction consisted of 7µL master mix, 3 µL primer, and 5 µL RNA sample
3- The tubes were sealed and mixed gently to bring the solution to the bottom of the tube
4- The tubes were incubated on ice for 5 min and kept till ready to load the thermal cycler (Quanta Biotech 2, Surrey, UK)

PCR amplification

1- For preparation of the PCR reaction plate, a master mix volume of 20 µL/reaction was prepared containing Taqman 2X Universal PCR Master Mix (10 µL), Taqman miRNA assay (1 µL) and nuclease free water (5 µL). The c-DNA was then added to each well to make a total of (20 µL)
2- The target primer used was miRNA-126 and the endogenous control u-87
3- The microamp plates were sealed and loaded to the 7500 fast real time PCR (Applied Biosystems, Warrington, UK) and an amplification plot was performed (Fig.46)

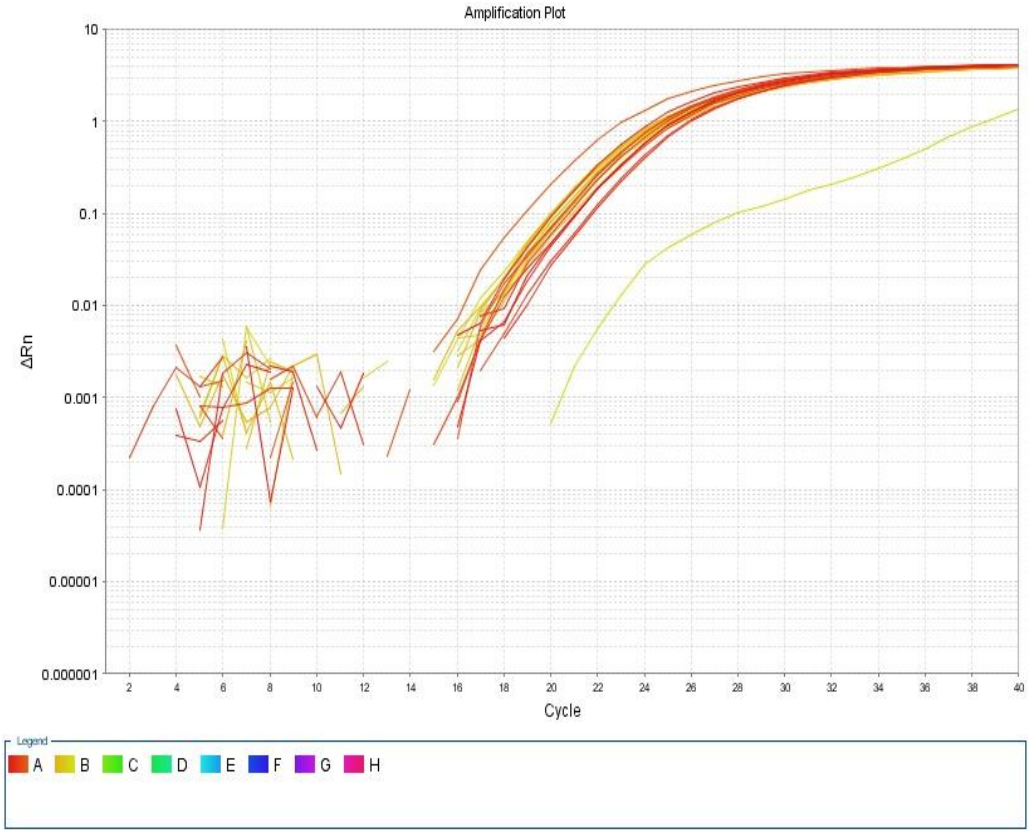

Figure 46 The amplification plot following the PCR reaction.

4- The fold difference in gene expression was calculated plotted in a graph

Appendix-2

Establishing a primary cell culture of bile duct epithelial cells in rats

We studied the possibility of using bile duct epithelial cells which have been shown to be the primary source of hepatic stem cells (84). We performed Bile duct ligation (BDL) in order to increase the number of cells that would make it possible to establish a primary cell culture of BDL cells

Surgical technique for bile duct ligation in rats

Under general anaesthesia, the hair of the anterior abdominal wall was shaved with a clipper and the animal was placed in a supine position on the operating table. The skin was prepared with povidone iodine 10% and draped using sterile towels.

An upper midline skin incision was made followed by incision of the anterior abdominal wall musculature and peritoneum. Care was taken in this step not to injure any bowel which might be very superficial. Also, the left lobes of the liver are almost very close to the anterior abdominal wall and care was taken not to cut through the liver which might lead to uncontrollable bleeding.

Once the peritoneal cavity was open, the liver lobes were gently pushed upwards by the means of sterile cotton balls. Using cotton buds, the duodenum was retracted downwards to expose the portal vein and the bile duct. The bile duct was then carefully separated from the portal vein by sharp dissection using very fine forceps and a silk suture 4/0 was passed to ligate the lower end of the duct immediately above the duodenum. It is important not to include the duodenum in the ligature or this would lead to bowel obstruction. The silk suture was left long to assist in the

downward pull exposing the upper part of the bile duct which was ligated twice. The bile duct was divided between the two ligatures without injuring the closely related portal vein.

Haemostasis was checked and any bleeding points were cauterized using a hand held cautery device. The cotton ball was removed and the liver was replaced back in position. The peritoneum and the anterior abdominal wall musculature were closed using 4/0 continuous Vicryl suture. The skin was closed using interrupted 4/0 silk with the ties cut close to the knot to avoid other animals from biting on it leading to abdominal dehiscence.

The wound were then sprayed with opsite and animals were kept in recovery under observation till they were fully active.

Killing of the animals and collection of the ligated bile ducts and gall bladders

At the designated time points (1, 2 and 4 weeks) the animals were killed under general anaesthesia by means of exsanguination. Retrieval of the dilated bile duct was performed carefully due to multiple adhesions between the bowel and the dilated duct. Also the bile duct needed to be carefully dissected from within the liver lobes. It was important not to puncture it as the plane of dissection would be lost making the procedure very difficult.

Once the dilated bile duct was excised, it was washed with cold sterile PBS 5X and then placed in a 50 ml tube containing Hanks Balanced Saline Solution. The tube was kept on ice and taken immediately to the lab.

Rats unlike mice lack a gallbladder and hence in order to achieve a considerable number of cells that might be used for purposeful transplantation, we performed BDL. We sacrificed the rats at different time points following BDL and we performed a primary cell culture at each time point. The one week time point was the most appropriate in terms of the highest number of cell, least adhesions intra-operatively and least number of fibroblasts when cultured on collagen coated plates. It was possible to achieve a primary cell culture from bile duct cells following scraping of mucosal surface. After 10 days, we could see a configuration similar to the bile duct with polygonal/polyhedral cells surrounding a lumen and surrounded by some fibroblasts (Fig.47). We performed Immunocytochemistry (ICC) using CD-133 marker which is a stem cell marker and were able to detect very few positive cells within the cultured BDL cells. This did not occur without BDL (Fig.48).

After 10 days in culture, the polygonal cells could not maintain their architecture and were converted into fibroblasts with very few numbers of polygonal cells.

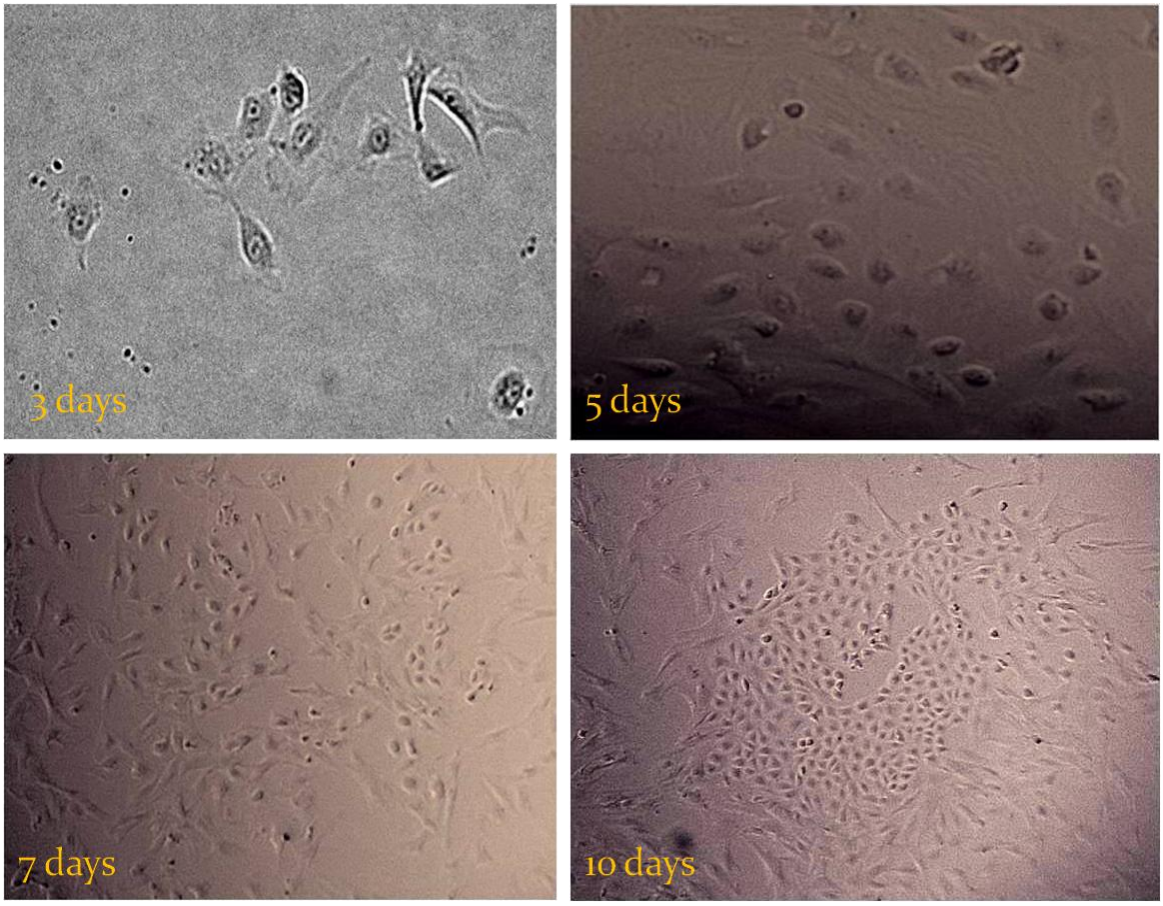

Figure 47 Primary cell culture of ligated bile duct epithelial cells showing organization of the cells at different time points. At day 10 the cells form a structure resembling a bile duct with a lumen and surrounded by polyhedral and rounded cells with another layer of fibroblasts and mesenchymal cells.

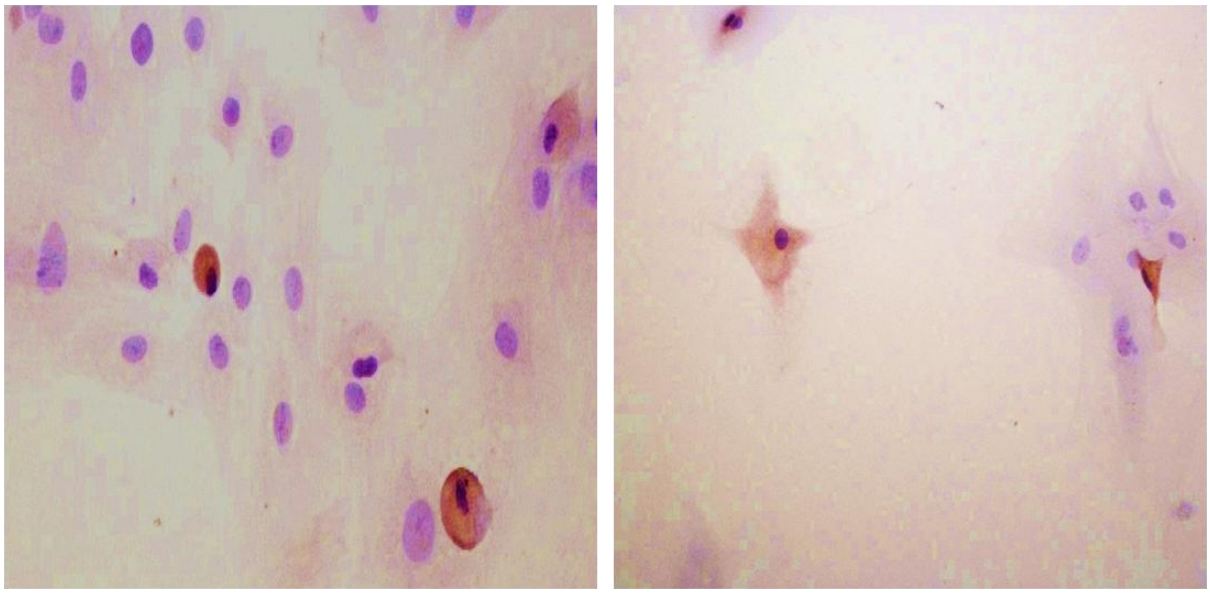

Figure 48 A primary cell culture of bile duct epithelial cells with some cells of variable morphology expressing CD 133.

Protocol for Immunocytochemistry (ICC)

ICC was performed in order to assess the presence of a certain antigen expressed by cells within cell culture flasks following similar principles of IHC. We used ICC to detect the presence of CD-133 cells within a cell culture of bile duct and gall bladder epithelial cells.

Procedure:

1- In order to achieve this, an 18 x22 mm cell culture tested coverslip (VWR, UK) was placed using sterile forceps in each well of a 6-well cell culture flask. The wells with the coverslips were then coated with rat tail collagen (Invitrogen, UK) and incubated for one hour at room temperature.

2-Excess collagen was aspirated immediately before cell culture and the wells were rinsed well using PBS.

3-The cells were then plated with confirmation that the cells were also covering the coverslips by visualization under the inverted microscope and then placed into the CO2 incubator.

4-After culturing for the appropriate duration, the media was aspirated and the coverslips side by side on the coverslip-basket that soaked in the 37ºC-warmed medium.

5-The coverslips were then incubated at 37 degrees for more than 30 minutes (recovery culture).

6-The fix solution was prepared (4% paraformaldehyde in PBS) and the coverslips were placed into the 37 degree pre-warmed fix-solution and incubated at room temperature for more than 20 minutes. This was followed by PBS wash (4 min × 3 times).

7- The coverslips were then soaked in 0.1% Triton-X100 in PBS at room temperature for 20 min to ensure permeabilization of plasma membranes which is required for the easy access of antibody molecules to the target molecules in the cell. This was followed by PBS wash (4 min × 3 times).

8-Drops of the primary antibody CD 133 (1:500, Abcam, UK) were then placed on a parafilm (50-100ML) and the coverslips were transferred on the drops of the primary antibody with the cellular surface down. After incubation for one hour, the coverslips were transferred to the wells with the cell surface up and washed with PBS x3.

9-Drops of the secondary antibody were then placed on fresh parafilm and the coverslips places cell surface down and incubated for 30 minutes. This was followed by PBS wash (4 min × 3 times).

10- Steps 14-18 as in IHC (Chapter 3)

Appendix-3

Embryoid body formation

Mouse C57BL/6 GFP+ ESCs (Millipore, Co Durham, UK) were used for EB formation.

Mouse ES cells were grown in proper cell culture conditions for at least three passages before attempting to form embryoid bodies.

1. The medium used to culture mouse ESCs was carefully removed from the tissue culture flasks and the plates were washed twice with 1X PBS.
2. 5 mL Accutase (Millipore, Co Durham, UK) was applied to the cells and incubated in a 37°C incubator for 3-5 minutes.
3. The flasks were carefully inspected to ensure the complete detachment of cells by gently tapping the side of the flask with the palm of the hand.
4. 5 mL of EB formation medium (Millipore, Co Durham, UK) pre-warmed to 37°C was applied to each flask.
5. The cells were then pipette into a conical tube and centrifuge t at 300 xg for 2-3 minutes to

pellet the cells.

6. The supernatant was discarded and 2mmL EB formation medium was added to the conical tube to resuspend the cells thoroughly without vortexing.
7. The number of cells were counted using a haemocytometer.
8. 3 x 10^6 cells were aliquoted in 10 ml EB formation medium and placed in a sterile 10-cm
9. Aliquot 2 to cells in 10mL Embryoid Body Formation Medium and place in a ultra low attachment Petri dish (VWR, Leicestershire, UK)

10. Cells were then incubated at 37°C, 5% CO_2 incubator for two days.

11. The cells were carefully collected using a 10 mL serological pipette, (both aggregated EBs and non aggregated cells) into a 15 mL conical tube and allowed to settle by gravity for 15 minutes.

12. The supernatant was then carefully removed and the cells resuspended 10 mL fresh EB Formation Medium.

13. The cell suspention was then transferred to a fresh sterile 10-cm low attachment plate and incubate at 37°C in a 5% CO_2 incubator for 2 days.